



CHPM2030 DELIVERABLE D 6.2 APPENDIX 6.2.4

REPORT ON PILOTS: THE KRISTINEBERG AND NAUTANEN MINING AREAS IN NORTHERN SWEDEN

Summary:

This report provides a brief overview of two study areas in northern Sweden around the Kristineberg and the abandoned Nautanen mine, where the CHPM technique can be suitable to be applied. It includes description of the geological settings, and on-going efforts in geophysics increasing resolution for detecting mineralised zones at even larger depth. The report also is attempting to estimate the low enthalpy geothermal potential of these areas.

Authors:

Gerhard Schwarz, Geological Survey of Sweden, Geophysicist
Benno Kathol, Geological Survey of Sweden, Geologist
Magnus Ripa, Geological Survey of Sweden, Geologist
Bo Thunholm, Geological Survey of Sweden, Hydrogeologist
Edward P. Lynch, Geological Survey of Sweden, Geologist
Johan Jönberger, Geological Survey of Sweden, Geophysicist

This project has received funding from the European Union's Horizon 2020 research and innovation programme under grant agreement n° 654100.



TABLE OF CONTENTS

TABLE OF CONTENTS	i
LIST OF FIGURES	iii
LIST OF TABLES	v
EXECUTIVE SUMMARY	1
1. INTRODUCTION AND OUTLINE OF WORK	3
1.1. Country and site specific issues	3
1.2. Goals	3
2. GEOLOGY AND GEOPHYSICS OF THE PROSPECTIVE AREAS	6
2.1. The Kristineberg mine in the Skellefte district	6
2.1.1. Skellefte district	6
2.1.2. Regional geology	6
2.1.3. The Kristineberg area	8
2.1.4. The Kristineberg mine	11
2.1.5. Geochemical analyses	14
2.1.6. Drill holes	14
2.1.7. Geophysics in the Kristineberg area	18
2.1.8. Electrical resistivity studies	18
2.1.9. Modelling	22
2.1.10. Combining seismic and magnetotelluric results	22
2.1.11. Natural seismicity	24
2.2. The Nautanen deposit in the Northern Norrbotten ore province	25
2.2.1. Regional geology	25
2.2.2. Local geology	28
2.2.3. Stratigraphy and correlations with regional successions	29
2.2.4. The Nautanen deformation zone and related iron oxide-copper-gold mineralisation	29
2.2.5. Lithologies in the Muorjevaara group	32
2.2.6. Structures in the eastern volcanosedimentary domain	33
2.2.7. Structures in the Nautanen deformation zone	34
2.2.8. Structures in the western volcanosedimentary domain	34
2.2.9. Geophysics in the Nautanen area	35
2.2.10. Nautanen – three-dimensional modelling of shallow structures	36
2.2.11. Three-dimensional geophysical modelling of magnetite-banded rocks in the NDZ	38
2.2.12. Natural seismicity	39

3. EGS GEOTHERMAL POTENTIAL.....	41
3.1. Temperature gradient and heat flow density	41
3.2. Heat production	42
3.3. Hydraulic properties, deep fluid flow.....	43
3.4. Fluid composition	44
3.5. Mineral stability.....	46
3.6. A case study in short: The st1 project	46
4. CONCLUDING REMARKS.....	48
ACKNOWLEDGEMENTS	48
REFERENCES	49
APPENDIX	63
Abbreviations	63
List of databases.....	63

LIST OF FIGURES

Figure 1: Bedrock geology of Sweden (SGU data), where major ore districts, potential sites for nuclear waste disposal (<i>SKB test site</i>) and sites of deep drill holes (<i>COSC, Siljan, DGE-1</i>) are noted.....	4
Figure 2. Mines and mineralisations in Sweden, state of activity from 2017. The currently active, major ore provinces of Northern Norrbotten, Skellefte district and Bergslagen are marked with dark green shading. The Nautanen and the Kristineberg mining areas are marked by red boxes.	5
Figure 3. Simplified bedrock map of the Skellefte district and surrounding areas, modified from Kathol & Weihed (2005). The metallogenetic area of the Skellefte district is roughly outlined by a grey, dashed line. Reference grid is the former Swedish National Grid RT90, numbering refers to map sheets of the Swedish land survey.	7
Figure 4. Geological map of the Kristineberg area. Compiled from the SGU databases of maps, mineral resources and bedrock ages. Reference grid SWEREF 99 TM.....	9
Figure 5. Total magnetic field anomaly map (no field values assigned) of the Kristineberg area. Reference grid is SWEREF 99 TM.	10
Figure 6. Kristineberg mine with the head frames. Photo: Benno Kathol.	11
Figure 7. Cross section through the Kristineberg deposit. From Årebäck et al. (2005).....	12
Figure 8. Three-dimensional model (unscaled) of the bedrock around the Kristineberg mine, showing sample sites for chemical analyses at distance of more than 500 m (a) and 1000 m (b) from the ore bodies. View towards the north-northwest. By courtesy of Boliden Mines.	15
Figure 9. Drill hole maps from the area of the Kristineberg deposit. A. Horizontal projection of almost all drill holes around the Kristineberg deposit, view from above. The positions of drill holes KRC 4317 and KRC4407 are marked with red lines. B. Vertical projection of drill holes in a narrow, roughly north-south striking section around drill hole KRC4407, the latter marked with a red line. C. Vertical projection of drill holes in a 100 m wide north-south striking section around drill hole KRC4317, the latter marked with a red line. By courtesy of Boliden Mines.	16
Figure 10. Photos of drill core sections from drill cores KRC4317 and KRC4407. Fractured cores are giving indications of the present and past stress regime in the crust. A. Crushed drill core of cordierite quartzite and sericite quartzite, 281,10–286,70 m, drill core KRC4407. B. Massive drill core of cordierite quartzite, 389,90–395,75 m, drill core KRC4407. C. Crushed drill core of chlorite schist, 23,90–29,90 m, drill core KRC4317. D. Massive drill core of chlorite quartzite, 302,00–307,80 m, drill core KRC4317. Photos by courtesy from Boliden Mines.	17
Figure 11. Geological map of the Kristineberg area where, e.g., reflection seismic and magnetotelluric investigations of the upper crust were done. Profiles 1, 2, 5 and HR are shown as black lines with common depth points indicated (Dehgannejad et al. 2012a).	19
Figure 12. Seismic cross sections with migrated profiles 1, 2 and the HR profile, and mineralisation surfaces from borehole data in the Kristineberg mine (after Ehsan et al. 2012). Reflection K1 correlates with the mineralization horizon (dark blue, green, light blue), belonging to the Rävliiden massive sulphide deposits. Section depth is 3800 m, no exaggeration. a) View towards the northwest. B) View towards the northeast.	20
Figure 13. 3D electrical resistivity model of the Kristineberg area, cut into slices (Hübert et al. 2013). On surface, outline of geological structures and position of MT measuring sites (triangles). Coordinate system <i>Swedish Grid RT90</i> (in km). Resistors associated with, RIa, RIb: Revsund granite; RII: Viterliiden intrusion; RIII:	

Mafic dykes within the metasedimentary rocks; Conductors related to CI: Skellefte crustal conductivity anomaly; CII: black shales at the base of the metasedimentary rocks; CIII: alteration or mineralised zones (?) in metavolcanic rocks. 21

Figure 14. Sections through 3D resistivity model (Hübert et al. 2013), together with seismic reflections along profiles 1 (top) and 5 (bottom) (Malehmir et al. 2007). See Figure 11 for locations of the profiles. Thick dashed lines mark interpreted seismic structures. E in section of profile 1 (top) section marks the assumed anticline, hosting Kristineberg mine. RIa, RIb: Revsund granite; RII: Viterliden intrusion; RIII: Mafic dykes within the metasedimentary rocks; Conductors related to CI: Skellefte crustal conductivity anomaly; CII: black shales at the base of the metasedimentary rocks; CII: alteration or mineralised zones (?) in metavolcanic rocks. 23

Figure 15. Kristineberg mining area - 3D views showing stages of the geological interpretation (Malehmir et al. 2009b). a) Early interpretation of seismic reflection data (Rodriguez-Tablante et al. 2007); b) Predicted 3D model for major structures obtained from five 2D geologic cross sections (see Malehmir et al. 2007); c, d) Final geological model for metal potential from 3D inverse and forward gravity modelling, all data available combined for targeting new prospecting areas. Horizontal to vertical scale 1:1. 24

Figure 16. Simplified bedrock map of northern Norrbotten County, modified from Bergman et al. (2001). KNDZ = Kiruna–Naimakka deformation zone, KADZ = Karesuando–Arjeplog deformation zone, NDZ = Nautanen deformation zone, PDB = Pajala deformation belt. Inset map: Sk = Svecokarelian orogen, Sn = Sveconorwegian orogen, Ca = Caledonian orogen, Pl = Platformal sedimentary cover rocks, A (green ornament) = Archaean rocks in part reworked in the Palaeoproterozoic, K (grey ornament) = Karelian rocks, S (without ornament) = Svecofennian supracrustal rocks and Svecokarelian intrusive rocks; thick lines are major deformation zones. The abandoned Nautanen mine (67° 11' 30" N, 20° 52' 49" E) is close to Gällivare at the lower edge of map. 26

Figure 17. Geology of the Nautanen area (Lynch et al. 2018a). Abbreviations: EVD = eastern volcanosedimentary domain; NDZ = Nautanen deformation zone (domain); WVD = western volcanosedimentary domain. Geochronology abbreviations and sources: U-Pb S zr = U-Pb SIMS zircon dating (Sarlus 2016, and this study = highlighted bold text in NDZ), U-Pb T zr = U-Pb TIMS zircon dating (Wanhainen et al. 2006), Re-Os T mol = Re-Os TIMS molybdenite dating (Wanhainen et al. 2005), U-Pb T ti = U-Pb TIMS titanite dating (Wanhainen et al. 2005), U-Pb LA ti + al = U-Pb laser ablation-inductively coupled-mass spectrometry titanite and allanite dating (Smith et al. 2009). Nautanen is situated in the upper third of the map. Coordinate system is SWEREF 99 TM. 30

Figure 18. Magnetic anomaly map of the Nautanen area, combined of airborne and ground magnetic total field data (after Lynch et al. 2018a). Coordinate system SWEREF 99 TM in km. Red polygons represent study areas where ground magnetic and VLF data were acquired in recent years, divided into three domains, the western- (WVD) and eastern (EVD) volcanosedimentary domain, and the Nautanen deformation zone (NDZ). Numbers 1a, 1b, 2 and 3 mark profiles discussed in text, relating to Figs. 20, 21. Box in dark blue shows the horizontal extent of the 3D magnetic model presented in Figure 22. 36

Figure 19. Residual gravity field in the Nautanen area. Black dots show the location of measuring points. . 37

Figure 20. Three cross-sections of magnetic susceptibility of shallow sub-surface structures, taken from 3D inversion models based on ground magnetic data for profiles 1a, 1b and 2 (see fig. 18). The profiles are disposed along the north-northwest–south-southeastern strike of the Nautanen deformation zone, here indicated by the dashed grey line. Profile length in metre, vertical extend in m above sea level. For better orientation, eastern longitude in m according to SWEREF 99 TM annotated. 39

Figure 21. Resistivity cross-section derived by inverting electromagnetic data from VLF measurements along profile 3 in Figure 18. View to the northeast. 40

Figure 22. Three-dimensional magnetic susceptibility model for the Nautanen deformation zone (outline marked by dark blue rectangle in Fig. 18). Two isosurfaces coloured in cyan and grey are shown. Total

magnetic anomaly field is indicated at the surface (no scale given). View from southeast to northwest. XY-coordinates refer to SWEREF 99 TM, Z is height a.s.l., all in metres.	40
Figure 23. Measured temperature ($^{\circ}\text{C}$) as a function of borehole depth (in m below ground surface) in the Kristineberg area (left) and in five drill holes located in the Kiruna mining district (right), at about 60 km north of the Nautanen area. Three of the boreholes were measured in the Kiruna iron ore mine at about 1200 m depth. Note different depth and temperature scales in both figures.	41
Figure 24. Map with corrected surface heat flow density in Fennoscandia (Balling 2013), based on measurements at more than 250 sites, marked by black dots. K : Kristineberg area, N : Nautanen area.	42
Figure 25. Heat production calculated from airborne radiometric data related to outcrops over northern Sweden (except of the mountain areas), in $\mu\text{W}/\text{m}^3$ (after Schwarz et al. 2010). K : Kristineberg area, N : Nautanen area. Coordinate system is SWEREF 99 TM in m.	43
Figure 26. Estimated trends in hydraulic conductivity vs depth in a borehole, meant to represent the Kristineberg area (purple line). The dark blue line indicates hydraulic conductivity at depth close to Oskarshamn in southern Sweden (Ericsson et al. 2006).	44
Figure 27. Estimated water flow Q_w (in l/s) as a function of hydraulic conductivity (in m/s) (top) and heat extraction Q_H (in MW) as function of water flow (in l/s) (lower).	45
Figure 28. Sketch of the first deep Enhanced Geothermal System (EGS) under construction in southern Finland, at Espoo, close to Helsinki, planned for urban heating (Kwiatek et al. 2019). Drilling of the production borehole was finished in 2018. The bedrock was hydraulically stimulated at depth between 5500 to 6100 m. Induced seismicity was surveyed by a network of 38 geophones installed either in boreholes or on surface (Saarno 2019). The insert shows the location of stimulation stages S1 to S5 into the bottom open hole section and basic stimulation parameters. Note: Geologically, southern Finland and most of northern Sweden belong to the Svecokarelian orogen, i.e., crustal structures and conditions are comparable, and analogies may be drawn for the bedrock in the Kristineberg and Nautanen areas.	47

LIST OF TABLES

Table 1. Production tonnage and grades of the VMS deposits in the Kristineberg area. From Kathol & Weihed (2005).	13
Table 2. Increased metal content in surrounding formations being of crucial importance for a CHPM system: Chemical data from rock volumes 500 m (a) and 1000 m (b) away from the modelled ore bodies at Kristineberg. Data by courtesy of Boliden Mines.	13
Table 3. Metal content in surrounding formations being of crucial importance for a CHPM system: Chemical background values of the bedrock in the Nautanen area (see text). Data courtesy of Boliden Mines.	31
Table 4. Petrophysical properties, i.e., density, magnetic susceptibility and Königsberger ratio Q of different rocks in the Nautanen area. Total number of samples is 267.	38

EXECUTIVE SUMMARY

There are four major ore provinces in Sweden, i.e., Bergslagen, the Skellefte district, the Northern Norrbotten ore province and the Caledonian orogen. In these, we have chosen the areas around the Kristineberg mine in the Skellefte district and the abandoned Nautanen mine in Northern Norrbotten for further screening the applicability of the CHPM technology there.

The Kristineberg area in the southwestern part of the Skellefte district is known for its volcanogenic massive sulphide deposits (VMS). Based on their age and geological history of rock sequences, the bedrock in the Skellefte district and surrounding areas in northern Västerbotten and southern Norrbotten counties can be divided and assigned to three major lithotectonic units. These are the Svecokarelian orogen, the Ediacaran to Cambrian sedimentary cover sequence and the Caledonian orogen. The Skellefte district *sensu stricto* belongs entirely to the Svecokarelian orogen.

The bedrock in the Skellefte district was formed or reworked by Svecokarelian orogenic processes, which lasted from about 1.96 to 1.75 Ga. This time interval includes subduction-related processes, collision, and extension-related collapse of the thickened crust. The peak of Svecokarelian deformation and metamorphism occurred between 1.85 and 1.80 Ga, but earlier phases of deformation at 1.89 – 1.87 Ga have been reported under the last decade. The Svecokarelian orogen comprises Svecokarelian intrusive rocks, formed by orogenic processes and Svecofennian supracrustal rocks, i.e. early orogenic sedimentary and volcanic rocks, the latter hosting the VMS deposits of the Skellefte district and thus the Kristineberg mine.

The Kristineberg mine is the oldest and largest massive sulphide mine in the Skellefte district and in continuous operation until today. Mining began in the year 1940 at the ore body outcropping at surface. Since then, production has reached down to around 1 200 m making Kristineberg to one of the deepest mines in Sweden. The ore is a complex massive sulphide with zinc being the main metal, although in some areas copper-gold ores are mined. Until year 2017, 31 million tons have been mined, reserves are 5 million tons and resources about 13 million tons. The combined grades of mined ore, reserves and resources are 3.9 % zinc, 0.7 g/t gold, 44 g/t silver, 0.9 % copper and 0.4 % lead.

The rocks surrounding the Kristineberg deposit have been strongly hydrothermally altered and are multiphase folded and strongly sheared. The schistose rocks are now dominated by quartz–muscovite–chlorite–pyrite in varying proportions, and exhibit marked sodium depletion and co-enrichment of magnesium and potassium. Cordierite, phlogopite and andalusite occur in considerable amounts. Kyanite has rarely been observed, mainly associated with quartz veins. In general, the iron–magnesium alteration minerals are magnesium-rich, and the modal chlorite content increases towards the Kristineberg ore horizon, which is surrounded by a halo of more muscovite-rich rocks.

The Geological Survey of Sweden has a long-standing tradition in geological mapping of the country with the support from airborne geophysics, motivated by the low degree of bedrock exposures. Magnetic properties, electrical resistivity and gamma radiation of shallow crustal rocks were thus studied in the Skellefte district and the Nautanen area, completed by ground surveys on these rock properties and on gravity.

During the last two decades, reflection seismic investigations were introduced in Sweden in larger extent by academia in cooperation with the mining industry for prospecting after minerals and ores in the Earth's uppermost crust. The Kristineberg area in the western Skellefte district was studied at depth down to 12 km by seismic methods, complimented by drillhole data down to ca 1400 m below surface. High resolution reflection seismic data provided detailed images of an VMS ore body and associated structures. But, the seismic experiments have also shown that considerable efforts need to be undertaken in geologically complex areas to properly acquire data, i.e., preferably by 3D instead of 2D surveys.

The Nautanen deposit is situated in the Northern Norrbotten ore province in northernmost Sweden. At this historical mining location, intermittent exploration has been carried out for over 100 years. Approximately 72 000 tonnes of copper and iron ore were extracted between 1902 and 1907. Further exploration in the 1970s and 80s produced a pre-regulatory total resource estimate for the “old” Nautanen deposit of approximately 2.94 Mt grading 0.78% Cu and 0.52 ppm Au. Present-day exploration by Boliden Mines AB has resulted in the discovery of an additional copper-gold mineralisation approximately 1.6 km north-northwest of the old Nautanen mine along the trend of the Nautanen deformation zone (NDZ). This “Nautanen North” deposit has an indicated resource of 9.6 Mt grading 1.7% Cu, 0.8 ppm Au, 5.5 ppm Ag and 73 ppm Mo, with an additional inferred resource of 6.4 Mt grading 1.0% Cu, 0.4 ppm Au, 4.6 ppm Ag and 41 ppm Mo.

The bedrock in Northern Norrbotten is part of the 2.0–1.8 Ga old Svecokarelian orogen. The orogen comprises both pre-orogenic rocks formed in the Archaean and early Palaeoproterozoic, as well as rocks formed during the orogeny itself. The bedrock in the Nautanen area consists of a partly conformable succession of syn-orogenic, Palaeoproterozoic volcano-sedimentary rocks. This supracrustal sequence is generally of calc-alkaline, basaltic andesite to andesite composition and has undergone extensive deformation, metamorphism, recrystallisation and hydrothermal alteration. Intrusive rocks, including deformed gabbroic, syenitic and dioritic bodies and younger, deformed to massive granitic and gabbroic-doleritic plutons and dykes, occur in the area.

The mineralisations at Nautanen are part of several hydrothermal copper-gold occurrences assigned to the iron oxide-copper-gold (IOCG) mineral deposit class which occur within the regional approximately north-northwest-trending Nautanen deformation zone (NDZ). The NDZ represents the most conspicuous structural feature in the area and is clearly delineated on magnetic anomaly maps as a somewhat dilational, linear zone of sub-parallel and tightly banded magnetic susceptibility anomalies. The coupling of high-strain deformation and magnetic banding reflects episodic metasomatic-hydrothermal fluid flow, probably enhanced by increased permeability associated with protracted and focused deformation. Two general styles of mineralisation are recognised in the area: (1) an inferred older phase of disseminated to semi-massive (replacement-style) sulphide mineralisation forming sub-vertical lenses and linear zones mainly within the NDZ; and (2) mineralisation associated with quartz \pm tourmaline \pm amphibole veins occurring mainly east of the NDZ or as a late-stage brittle overprint within the high-strain zone.

Geophysical surveys, mostly using potential field and electrical methods in the Nautanen area were concentrated on the shallow sub-surface down to some hundred metres depth, being of economic interest. No investigations are known in the surroundings of Nautanen that are covering deeper seated structures and formations.

Our understanding of deep-seated fluids in the crystalline bedrock is still rudimentary. Hydraulic conductivity decreases with depth at a high degree of variability. Investigations in boreholes indicate that hydraulic conductivity below 650 m depth varies between 10^{-7} and 10^{-12} m/s. Data on the composition of fluids indicate that brines (> 5 % TDS/l) occur far inland at several 1000 metres depth. Their residence time was estimated at the order of some hundred million of years by the analysis of He-isotopes. Corrected geothermal heat flow density is about 50 mW/m². Data on heat production do not show large differences between rock types related to their content in radioactive elements.

The generally low geothermal gradient of less than 20 °C/km in the crystalline basement of the Fennoscandian Shield was verified by sensing temperature in deep boreholes in the Skellefte district and adjacent to the Nautanen mine. The temperature gradient measured here to about 16 °C/km should allow for low- to mid-enthalpy geothermal systems as part of a possible CHPM unit.

1. INTRODUCTION AND OUTLINE OF WORK

1.1. Country and site specific issues

Available data on the bedrock geology of Sweden (Fig. 1) derive mainly from observations at the Earth's surface. The overall low degree of bedrock exposure (on average < 10 % due to Quaternary till and sediment cover) in the country means that bedrock maps in unexposed areas are based on results from geophysical investigations, e.g., airborne geophysical measurements. At best, the maps should therefore be considered as probable two-dimensional (2D) models of possible rock configuration and structures. Site specific investigations need further geophysical studies as well as results from drilling. Generally, there is a lack of studies related to upper and mid crustal levels of the Earth.

Large volumes of the bedrock in Sweden have been subject to intense tectonic deformation and subsequent erosion, and rocks, including mineralisations, and structures originally formed at considerable depths in the crust are locally accessible for study at or close to the present surface. In contrast, several mineralisations in Sweden that presently are being mined at and evaluated to some depths were however originally formed at or close to the Earth's surface.

1.2. Goals

In a previous report of the CHPM2030 project (D1.2) we were providing an inventory of three major ore districts in Sweden, namely, Bergslagen in central Sweden, and further north the Skellefte district and the Northern Norrbotten ore province. The present report now informs about two of these areas in more detail, i.e., the area around the Kristineberg mine in the Skellefte district and Nautanen, an abandoned mine in Northern Norrbotten. We have identified both mining areas as being suitable for the challenging future technology, *Combined Heat, Power and Metal extraction from ultra-deep ore formations* (CHPM). The CHPM concept proposes establishing an *Enhanced Geothermal System* (EGS) in a metal-bearing geological formation, that will allow to produce both energy and metals.

Based on geological and geophysical data and borehole records, the work presented here includes subsurface information aiming on the occurrence, composition and location of potential deep mineralised formations in the target districts named above. We also shed some light on spatial variations in crustal heat production, heat flow and temperature and discuss to which extent these parameters may be affected by convection related to groundwater flow. Still, the big challenge is to predict fracture geometry and permeability at depth in crystalline bedrock. Though sub-surface information in the Kristineberg and Nautanen mining fields has increased during the last years, the study of deeper formations still is a tough task as large data gaps exist and some of the information is based on few data points of regional character.

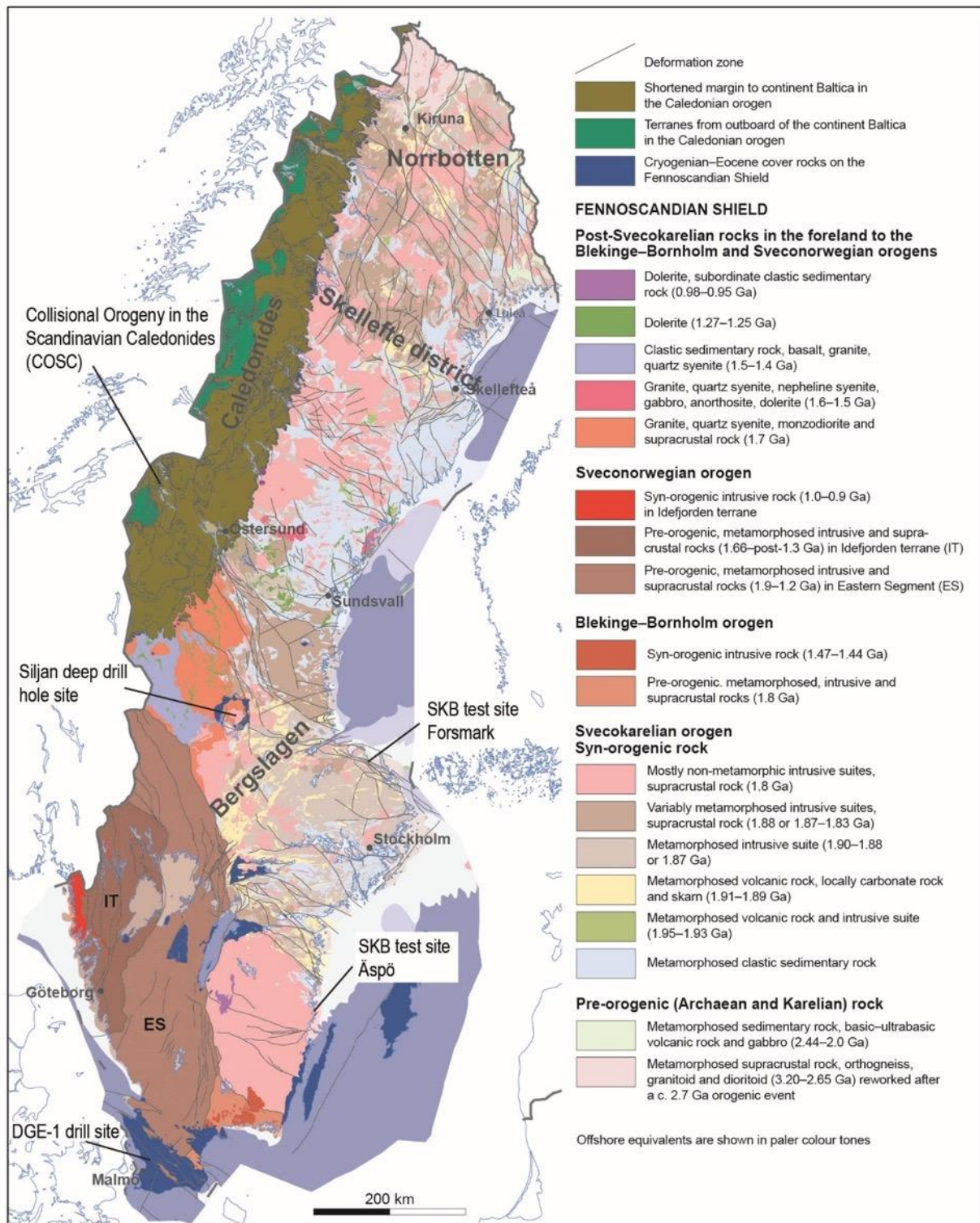


Figure 1: Bedrock geology of Sweden (SGU data), where major ore districts, potential sites for nuclear waste disposal (SKB test site) and sites of deep drill holes (COSC, Siljan, DGE-1) are noted.

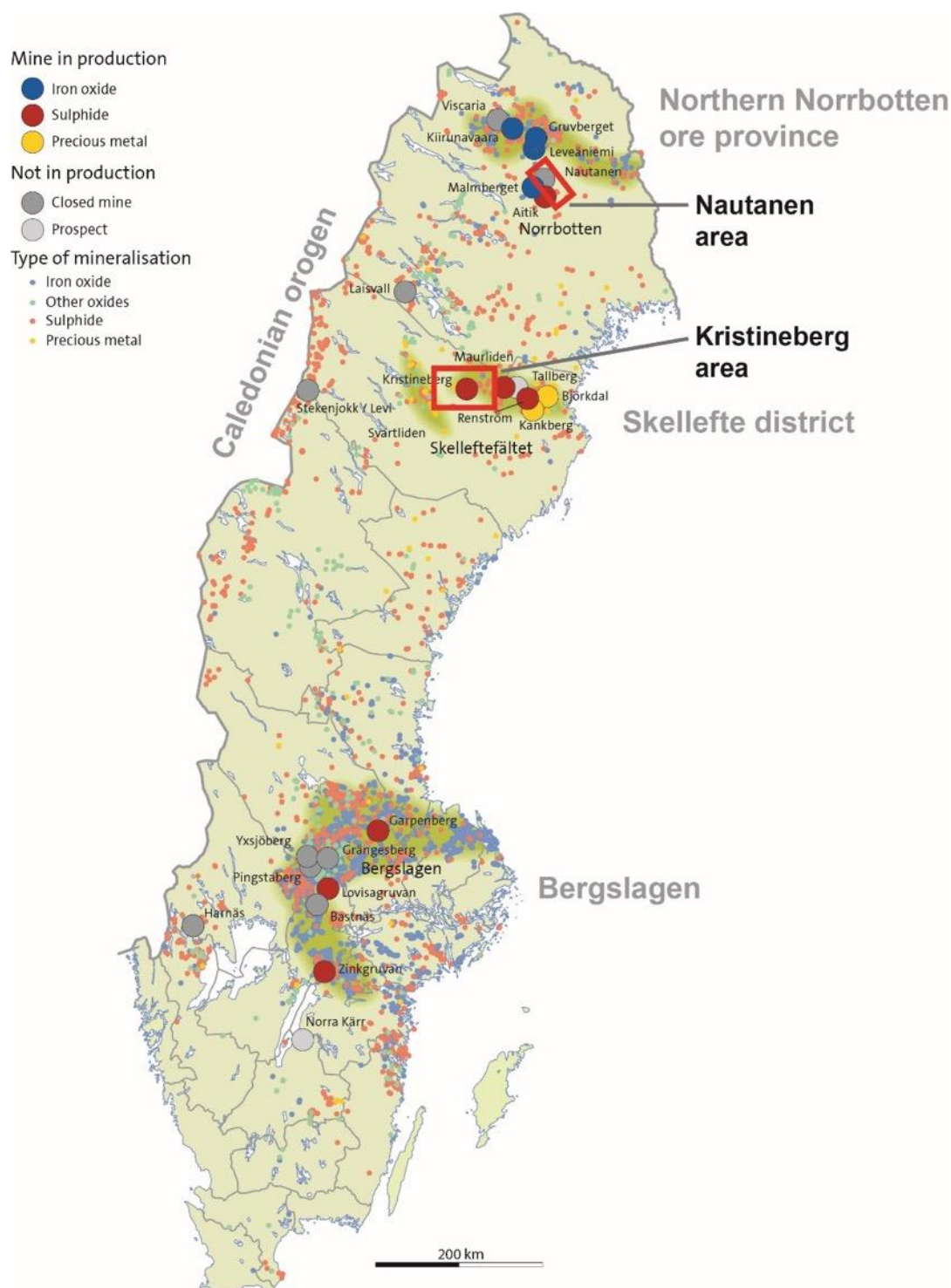


Figure 2. Mines and mineralisations in Sweden, state of activity from 2017. The currently active, major ore provinces of Northern Norrbotten, Skellefte district and Bergslagen are marked with dark green shading. The Nautanen and the Kristineberg mining areas are marked by red boxes.

2. GEOLOGY AND GEOPHYSICS OF THE PROSPECTIVE AREAS

2.1. The Kristineberg mine in the Skellefte district

2.1.1. Skellefte district

The Kristineberg area with the volcanic hosted massive sulphide (VMS) deposit of the Kristineberg mine and other VMS deposits at different stratigraphic levels is situated in the southwestern part of the Skellefte district (Allen et al. 1996; Kathol & Weihed 2005). It is one of four major ore-provinces, of which three are currently ore-producing in Sweden (Fig. 2). The other regions are Bergslagen (Stephens et al. 2009), the Northern Norrbotten ore province (Bergman et al. 2001, Bergman 2018) and the Caledonian orogen. The Skellefte district with surrounding areas is situated in northern Västerbotten and southern Norrbotten counties.

2.1.2. Regional geology

The bedrock in northern Västerbotten and southern Norrbotten counties can, based on the age and geological history of rock sequences be divided and assigned to three major lithotectonic units. These are the Svecokarelian orogen, the Ediacaran to Cambrian sedimentary cover sequence and the Caledonian orogen. Rocks of these three units occur to differing extends in the Skellefte district and surrounding areas (Fig. 3). The Skellefte district *sensu stricto* belongs entirely to the Svecokarelian orogen.

Most of the bedrock in northern Sweden, and thus the Skellefte district, was formed or reworked by Svecokarelian orogenic processes, which lasted from c. 1.96 to 1.75 Ga. This time interval includes subduction-related processes, collision, and extension-related collapse of the thickened crust. The peak of Svecokarelian deformation and metamorphism occurred between 1.85 and 1.80 Ga (Stephens et al. 1997), but earlier phases of deformation at 1.89 – 1.87 Ga have under the last decade been reported by Skyttä et al. (2012).

The Svecokarelian orogen comprises Svecokarelian intrusive rocks, formed by orogenic processes and Svecofennian supracrustal rocks, i.e. early orogenic sedimentary and volcanic rocks, the latter hosting the VMS deposits of the Skellefte district.

The Skellefte district in a wide sense is situated in the transition area between the Bothnian Basin (Hietanen 1975) in the south, and areas consisting mainly of subaqueous marine and subaerial volcanic arc assemblages in the north. Marine, mainly epiclastic supracrustal rocks of the basin are grouped under the name Bothnian supergroup, whereas the volcanic arc assemblages are divided into the subaqueous Skellefte and Vargfors groups and the subaerial Arvidsjaur group. Within the volcanic arc–Bothnian Basin transition zone, epiclastic, commonly turbiditic sedimentary rocks are interpreted to interfinger with subaqueous volcanic rocks of the Skellefte group and sedimentary rocks of the Vargfors group.

Upwards and laterally to the north, the Skellefte group rocks pass into mainly subaerial volcanic sequences of the Arvidsjaur group. The marine equivalent of the Arvidsjaur group is the Vargfors group, which consists mainly of coarse clastic and turbiditic sedimentary rocks and mafic volcanic rocks, deposited on the rocks of the Skellefte and Bothnian groups or the lower parts of the Arvidsjaur group. Differences between the Skellefte, Vargfors, and Bothnian groups are indicated by different geochemical affinities of basic volcanic rocks. However, as these rocks occur only sparsely, especially within the Bothnian supergroup, the boundary between the Skellefte and Vargfors groups on the one hand and the Bothnian supergroup on the other is drawn somewhat arbitrarily on the map (Fig. 3).

This artificial line is generally interpreted as a lateral transition from one group to the other. Rocks of the Skellefte and Vargfors groups have their coeval counterparts within the Bothnian supergroup. In places, the Skellefte/Bothnian groups or Vargfors/Bothnian groups contain laterally equivalent rock associations. In terms of sequence stratigraphy these associations should be considered as one unit, which probably consists of several, individual sequences.

At different stages and at different levels throughout the sedimentary and volcanic evolution within the map area, the supracrustal rocks have been intruded by voluminous amounts of intrusive rocks. On the one hand, these intrusions enable dating of the sedimentary record; on the other hand, they obscure primary relationships between different supracrustal units.

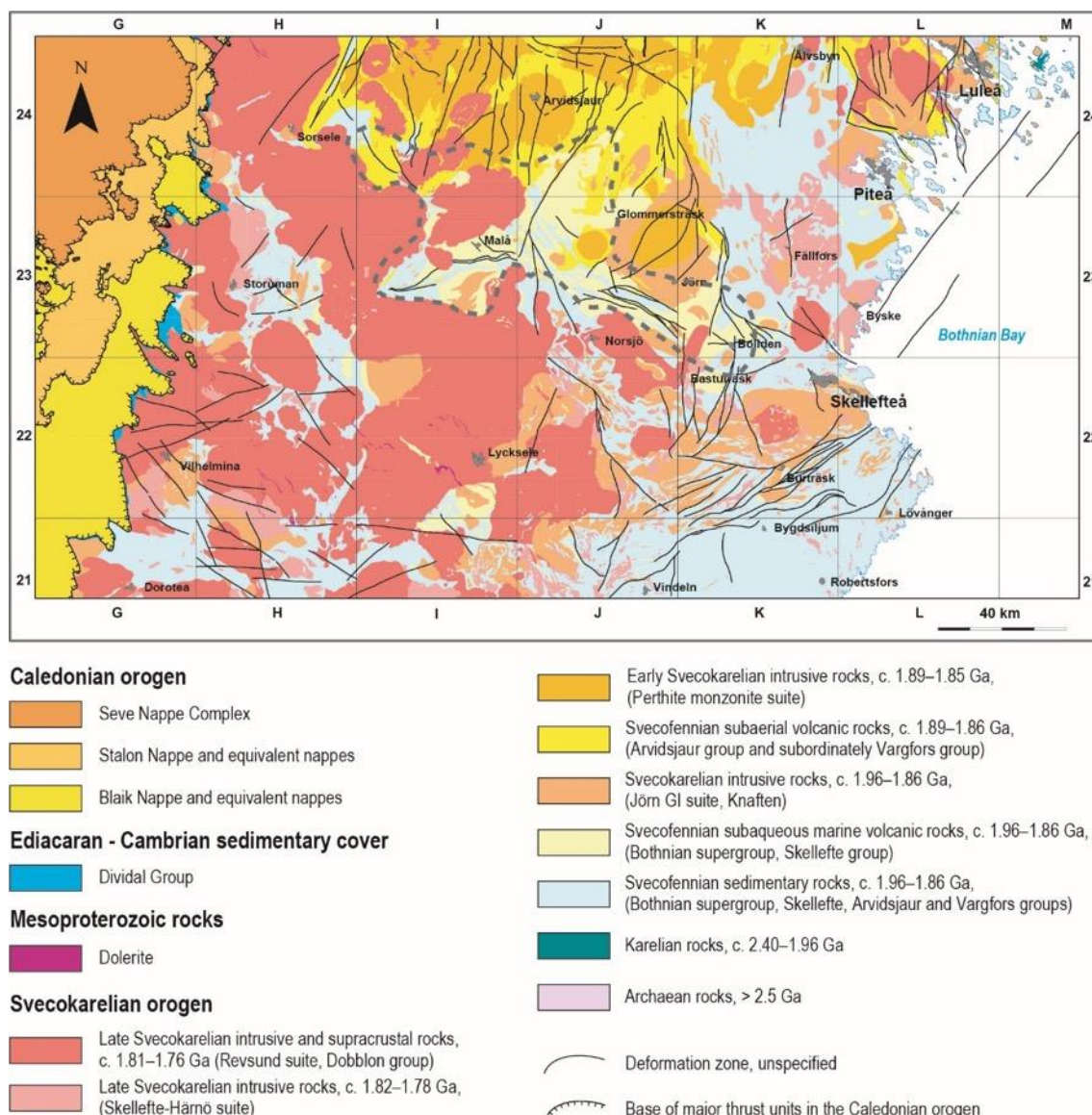


Figure 3. Simplified bedrock map of the Skellefte district and surrounding areas, modified from Kathol & Weihed (2005). The metallogenic area of the Skellefte district is roughly outlined by a grey, dashed line. Reference grid is the former Swedish National Grid RT90, numbering refers to map sheets of the Swedish land survey.

2.1.3. The Kristineberg area

The Kristineberg area constitutes the southwestern part of the Skellefte district, situated in northern Västerbotten County (Fig. 4). Here, Svecofennian supracrustal rocks form two regional scale, southwest–northeast striking antiforms. The larger, southeastern antiform is cored by a tonalite–granodiorite–granite intrusion, belonging to the early Svecokarelian calc–alkaline granitoids (Jörn G1 suite). The northwestern antiform is cored by felsic volcanic rocks (dacites–rhyolite) of the Skellefte group. The antiforms are separated by either a synform (Årebäck et al. 2005) or a large-scale shear zone (Malehmir et al. 2007, Dehghannejad et al. 2010) occurring in the sedimentary rocks of the Vargfors group.

The intrusion, coring the southeastern antiform has been called ‘Kristineberg massive’ and dated with U–Pb method on zircon (TIMS) to 1907 ± 13 Ma by Bergström et al. (1999). The authors interpreted the Kristineberg massive as either a basement to the rocks of the Skellefte group, or stated, when both rock units are taken as coeval, that the volcanic rocks of the Kristineberg area are older than the volcanic rocks in the eastern and central part of the Skellefte district. Bergström & Sträng (1999) considered the Kristineberg massive to be the result of deeply situated magma-chamber, probably related to the Skellefte group volcanism in the area.

The southeastern antiform enclose two individual second-order west-plunging antiforms, both core by tonalitic (Skyttä et al. 2011) or granitic to tonalitic (Bergström & Sträng 1999) intrusive rocks. The Kristineberg and Rävliiden mines and mineralisations are hosted by felsic volcanic rocks of the Skellefte group at the southern limb of the northern second-order antiform.

The intrusion of the ‘Kristineberg massive’ has in the last decade been reinvestigated by Skyttä et al. (2010, 2011, 2013), who also presented new and more reliable age data by the U–Pb method on zircon (SIMS) for intrusive rocks of what they call the ‘Viterliden intrusion’ and adjacent volcanic rocks. Skyttä et al. (2011) dated two samples from a hornblende tonalite and a plagioclase porphyritic tonalite each in the southern part of the intrusion. The obtained ages of 1892 ± 3 Ma and 1891 ± 3 Ma imply that the magmatism in the Kristineberg area was synchronous with the 1.89–1.88 Ga early Svecokarelian intrusions of the Jörn G1-suite (Kathol & Weihed 2005) in the eastern part of the Skellefte district which yielded ages in the interval 1.89–1.88 Ga (Bergström et al. 2003, Gonzàles Roldán 2010).

A quartz-plagioclase porphyritic tonalite is considered as the youngest phase of the Viterliden intrusion and has been dated to 1889 ± 3 Ma by Skyttä et al. (2011). A tentative correlation of this tonalite with the Kristineberg ‘mine porphyry’ suggests that these units are coeval at about 1.89 Ga (Skyttä et al. 2011). According to Kathol & Weihed (2005), a fine-grained, late intrusive facies of the Kristineberg tonalite (‘Viterliden porphyry’ or ‘mine porphyry’) has intruded the ore-bearing rocks close to the ore in the Kristineberg mine. Due to the intrusive nature of this ‘mine porphyry’, the obtained age from the quartz-plagioclase porphyritic tonalite, correlated with the ‘mine porphyry’ gives a minimum age for the Kristineberg ore deposit. Another minimum is constrained by the age of 1883 ± 6 Ma obtained in a felsic volcanic rock in the hanging-wall of the Kristineberg deposit (Skyttä et al. 2011). Finally, based on these relative tight age intervals, the authors conclude that the Viterliden intrusion may equally have intruded into or locally acted as a basement for the ore-hosting volcanic rocks of the Skellefte group.

The age interval of 1.89–1.88 Ga for the intrusive and supracrustal rocks in the Kristineberg area supports also that the Skellefte group defines a laterally continuous volcanic belt throughout the entire Skellefte district (Skyttä et al. 2011).

In the model of Skyttä et al. (2011), the mineralisation in the Kristineberg area was formed at two main horizons in the volcanic pile by syn-extensional volcanism, mineralisation sedimentation and intrusive activity at c. 1.89–1.97 Ga. Subsequent crustal shortening lead to basin inversion and transposition of the mineralised horizons to the present positions.

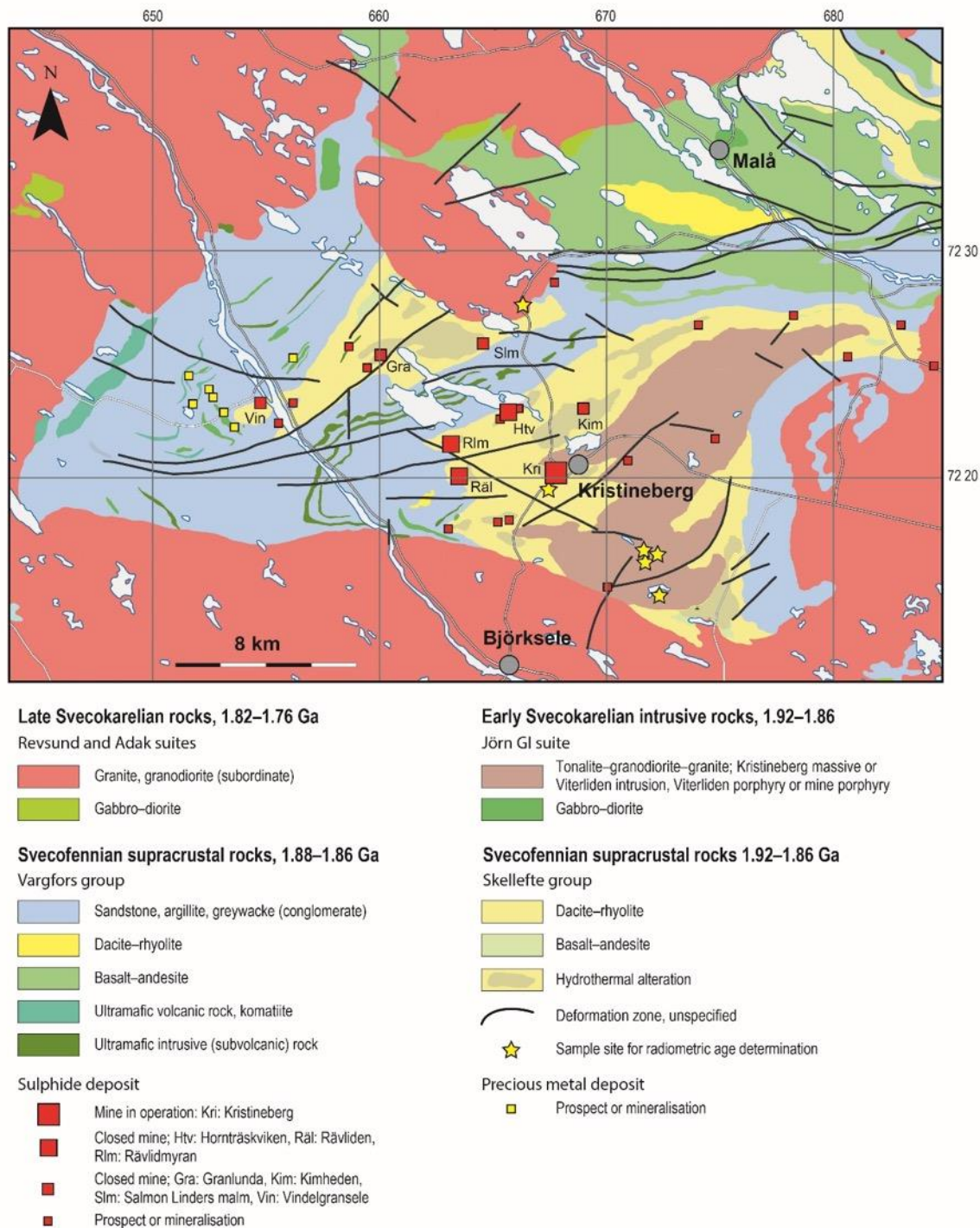


Figure 4. Geological map of the Kristineberg area. Compiled from the SGU databases of maps, mineral resources and bedrock ages. Reference grid SWEREF 99 TM.

Deformation of different intensity has affected the volcanic rocks of the Skellefte group and the sedimentary rocks of the Vargfors group. The deformation intensity is partly a product of the original mica-rich rock, formed by large-scale alteration processes, depending partly on the distance to the important deformation zones separating the bedrock of the Kristineberg area from less deformed rocks to the northwest and north (Kathol & Weihed 2005). These deformation zones are assigned to a major high strain zone which separates deep and shallow crustal domains in the Skellefte district by Skyttä et al. (2012).

The Skellefte group volcanic rocks are mainly rhyolitic subvolcanic intrusions or lava domes and fragment-bearing, locally banded volcanoclastic rocks. Willdén (1986) suggested that the volcanoclastic rocks occupied longitudinal synvolcanic depressions or rifts, formed during extensional phases of the Skellefte group volcanism. The depressions also focused later mafic volcanism, mainly emplaced as subvolcanic sills, and hydrothermal activity. The sericite and chlorite alteration processes affected large volumes of rocks, where original textures can only very rarely be observed. To the south, higher grade metamorphism formed andalusite–cordierite-bearing assemblages in analogous rocks. Magnetite is another important alteration mineral and alteration zones are generally outlined by their magnetic patterns (Fig. 5).

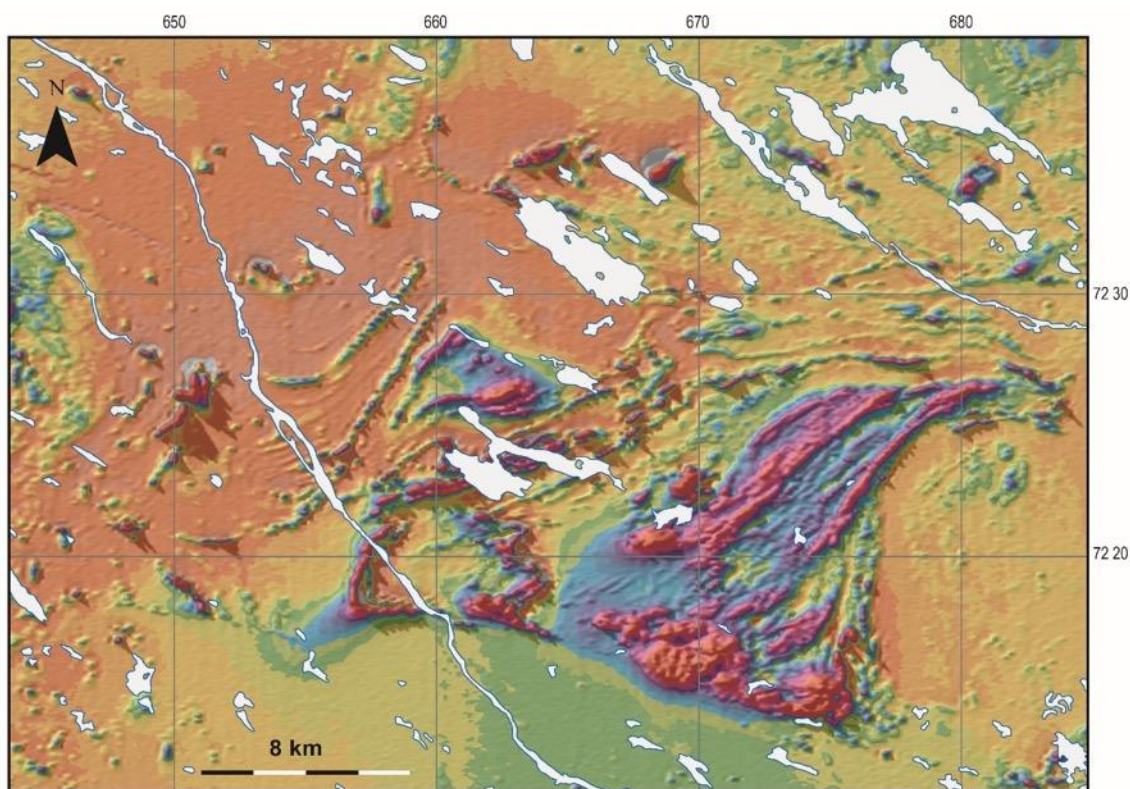


Figure 5. Total magnetic field anomaly map (no field values assigned) of the Kristineberg area. Reference grid is SWEREF 99 TM.

Several ore types are present in the Kristineberg area. The large Kristineberg deposit was a massive pyrite ore body with zinc–copper–gold–silver, which has been deformed into several ore lenses. The Kristineberg deposit was described by Du Rietz (1953), Edelman (1963), Willdén (1986), Vivallo & Willdén (1988) and Årebäck et al. (2005). Further to the north, the massive–disseminated Kimheden pyrite–chalcopyrite deposit occurs at the same structural level as the Kristineberg deposit. Kimheden deposit is hosted by strongly deformed and chlorite-altered volcanic rocks.

In contrast to Kristineberg and Kimheden, the stratigraphic position of the VMS deposits of the Rävliiden area further to the west is somewhat different. There, the ores are strongly stratigraphically controlled and occur along the contact between the volcanic rocks and the overlying Vargfors group sedimentary rocks. The favourable ore horizon in the Rävliiden area is characterized by small sedimentary intercalations hosted by felsic volcanoclastic rocks. The Rävliidenmyran deposit consists of one large pyrite–chalcopyrite ore body and several smaller, zinc–lead-bearing lenses, often associated with strongly deformed argillitic intercalations. In the Hornträskviken deposit, lenses of zinc–lead ore are restricted mainly to small carbonate occurrences. The Rävliiden deposit includes one copper-rich ore lens and one zinc-rich lens, situated adjacent to each other.

Further to the south, the small low-grade Mörkliden ore bodies occur along the same stratigraphic horizon. They are mainly sphalerite–chalcopyrite disseminations with very little ferric oxide. The Nyborg deposit to the north is another example of the similar sphalerite disseminated type. The Vindelgransele area hosts only small VMS mineralisations, for example the high-grade Vindelgransele deposit.

The Kristineberg deposit is one of the largest polymetallic volcanogenic massive sulphide (VMS) occurrences in the Skellefte district. It was discovered in 1918 using electromagnetic survey techniques. Due to logistical issues, related to transportation of the ore through swampy areas and forests, production was only initiated once a 96 km long cable way (“Linbana”) was constructed in 1941. This cable way connected Kristineberg mine to the concentrator plant set up in Boliden after the discovery of the Boliden ore body in 1927. Up until 1987 the cable way was in use but then was replaced by trucks which are still used today for transporting ore to Boliden (Bauer et al. 2013).



Figure 6. Kristineberg mine with the head frames. Photo: Benno Kathol.

2.1.4. The Kristineberg mine

The Kristineberg mine (65° 03' 48" N, 18° 34' 00" E) is the oldest and largest massive sulphide mine in the Skellefte district which has been in continuous operation until today. Mining began in the year 1940 at the orebody which outcrops at surface. Since then production has reached down to around 1 200 m making it one of the deepest mines in Sweden. Some 26.5 million tons of ore were mined at an average grade of 3.56 % zinc, 1.31 g/t gold, 38 g/t silver, 1.05 % copper, 0.24 % lead and 25.6 % sulphur (Bauer et al. 2013). According to the Fennoscandian ore deposit database (see also Eilu et al. 2013), 31 million tons were mined until 2017, reserves are 5 million tons and resources about 13 million tons. The combined grades of mined ore, reserves and resources are 3.9 % zinc, 0.7 g/t gold, 44 g/t silver, 0.9 % copper and 0.4 % lead. The ore is a complex massive sulphide with zinc being the main metal, although in some areas copper-gold ores are mined. The predominant mining method is cut-and-fill with some rill mining. (Bauer et al. 2013).

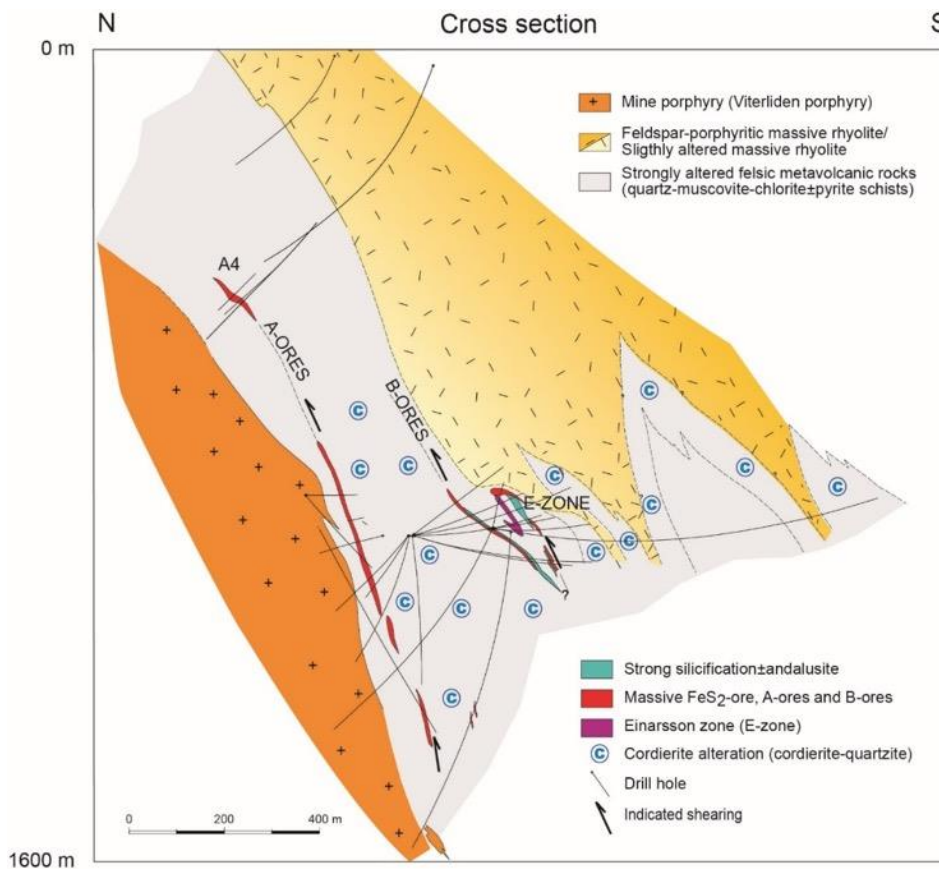


Figure 7. Cross section through the Kristineberg deposit. From Årebäck et al. (2005).

Both, the Kristineberg- and the nearby Kimheden deposit to the north represent an ore horizon which seems to be developed rather deep in the volcanic stratigraphy, compared with many other similar deposits in the Skellefte district. The Rävliiden horizon is developed in the upper part of the volcanic pile and occurs about 3 km west of Kristineberg (Fig. 4). In the latter, abundant calc-silicate assemblages and some marble associations occur which are only locally observed at the Kristineberg–Kimheden horizon. Tonnages and grades in the mined deposits in the Kristineberg area are shown in Table 1.

The rocks surrounding the Kristineberg deposit have been strongly hydrothermally altered and are multiphase folded and strongly sheared. The schistose rocks are now dominated by quartz–muscovite–chlorite–pyrite in varying proportions, and exhibit marked sodium depletion and co-enrichment of magnesium and potassium. Cordierite, phlogopite and andalusite occur in considerable amounts. Kyanite has rarely been observed, mainly associated with quartz veins. In general, the iron–magnesium alteration minerals are magnesium-rich, and the modal chlorite content increases towards the Kristineberg ore horizon, which is surrounded by a halo of more muscovite-rich rocks. Due to the strong alteration, the rocks near the Kristineberg mine are connoted as ‘schists and quartzites’ (see Fig. 10), as it is hard to recognise the nature of the volcanic protoliths.

The bedrock of the Kristineberg deposit is shown in cross-section (Fig. 6). The mine porphyry (Viterliden porphyry) occurs in the footwall of the Kristineberg deposit, and a massive, feldspar-porphyritic rhyolite

Table 1. Production tonnage and grades of the VMS deposits in the Kristineberg area. From Kathol & Weihed (2005).

Mine	In operation (year)	Tonnage (Mt)	Gold g/t	Silver g/t	Copper %	Zinc %	Lead %	Sulphur %
Kristineberg*	1940-	21.1	1.05	36	1.04	3.64	0.24	25.9
Kimheden	1968-1970 1974-1975	0.13	0.44	7	0.95	0.27	-	18.4
Rävlidmyran	1950-1991	7.18	0.79	51	0.95	3.96	0.54	17.8
Rävliden	1941-1950 1966-1988	1.56	0.45	90	1.00	4.23	0.79	16.9
Hornträskviken M.	1981-1991	0.64	0.71	72	1.01	4.90	0.67	11.1
Total	1941-2001	30.3						

* To year end 2001, excluding Einarsson Au-Cu lenses

Table 2. Increased metal content in surrounding formations being of crucial importance for a CHPM system: Chemical data from rock volumes, (a) 500 m and (b) 1000 m away from the modelled ore bodies at Kristineberg. Data by courtesy of Boliden Mines.

a) Metal content 500 m away from ore body 532 samples										
Metal	Ag ppb	Au ppb	Co ppm	Cu ppm	Mo ppm	Ni ppm	Pb ppm	Sn ppm	W ppm	Zn ppm
Min	0	0,05	0,1	0,05	0,05	0,05	0,3	0,4	0,2	0,5
Max	5500	472	379	1081	122	326	1857	14	2386	4386
Average	317,2	13,1	10,1	44,4	3,3	9,0	17,0	1,8	10,1	124,6

b) Metal content 1000 m away from ore body 350 samples										
Metal	Ag ppb	Au ppb	Co ppm	Cu ppm	Mo ppm	Ni ppm	Pb ppm	Sn ppm	W ppm	Zn ppm
Min	50	0,05	0,1	0,05	0,05	0,05	0,3	0,5	0,2	0,5
Max	5100	472	379	1081	122	326	162	14	2386	1805
Average	261,3	15,4	11,7	45,4	3,2	10,8	9,3	1,9	13,7	80,4

forms the hanging wall. Close to the deposit, this rhyolite gradually becomes slightly to moderately muscovite±chlorite-altered. The intervening ore hosting sequence consists of strongly altered and schistose volcanic rocks. The dominating mineral assemblage of this unit is quartz–muscovite–chlorite–phlogopite–pyrite±andalusite±cordierite.

2.1.5. Geochemical analyses

The ore grades of the Kristineberg ore bodies have been described in the chapter “The Kristineberg mine”. Increased metal contents occur also in zoned rock volumes around the ore bodies. These alteration and compositional envelopes interfinger with each other, resulting in larger rock volumes with increased metal contents, which are therefore of interest for a CHPM system.

Figure 8 shows a three-dimensional model over the bedrock hosting the Kristineberg deposit and the sample sites for chemical analyses more than 500 m (a) and 1000 m (b) away from the ore bodies. In the model, the analysed rocks of the ore bearing Skellefte group, mainly dacite–rhyolite and a transition zone, have been omitted to make the sample sites visible. These sites are indicated by light yellow or light grey spheres which represent analyses of dacite–rhyolite and the transition zone, respectively. Most of the samples were taken from drill cores, but some samples stem from surface outcrops or from drill cuttings. Analyses of other rock types were omitted also both from the models in Figure 8 and from Table 2, as they are not relevant for this project. Table 2 shows maximum, average and minimum contents of several metals found in the host rocks.

Similar zonations in metal contents or envelopes have been found at the other VMS-deposits in the Kristineberg area (Kimheden, Rävliiden, Rävliidmyran and Hornträskviken) and can also be expected around deeper situated, at present unknown mineralisations or deposits in the felsic volcanic rocks (dacites–rhyolite) of the area. This means that an increased metal content can be expected in larger rock volumes of the Skellefte group dacites–rhyolites, which occur at levels deeper than the at present known mineralisations. Three-dimensional models and descriptions of volcanic-hosted massive sulphide (VMS) deposits and associated host rocks are found (summarised) in Bauer et al. (2015).

2.1.6. Drill holes

The pattern of drill holes in and around the Kristineberg mine is shown in Figure 9a. Many of the drillings were carried out as diamond drilling. Drill cores are stored in the Boliden archives. By courtesy of Boliden Mines, photos of two entire cores from drill holes KRC4407 and KRC4317 were available for this project (Fig. 9b, c and Fig. 10).

Bore hole KRC4407 was drilled from the southwestern part of the mine at a depth of approximately 1200 m. The direction of this bore hole was almost horizontally to the south (Fig. 9b), which makes it more likely that vertical and subvertical fractures or brittle deformation zones are recorded by the received drill core. Drill hole KRC4317 was drilled from a depth of c. 1000 m with a steeply dipping direction to the north (Fig. 9c). Thus, the drill core from this hole more likely reports the occurrence of flat lying fractures or brittle deformation zones. In Figure 10a-d, a section of crushed drill cores, probably representing a brittle deformation zone and relatively unbroken cores from more massive rock volumes are shown for both drill holes each.

In both drill holes, and so in the Kristineberg area, the degree of alteration of rocks is more critical for the fracture density than differences in the original rock types, as, e.g., coherent volcanic rock or volcanoclastic rock (pers. com. Lena Albrecht, Boliden Mines).

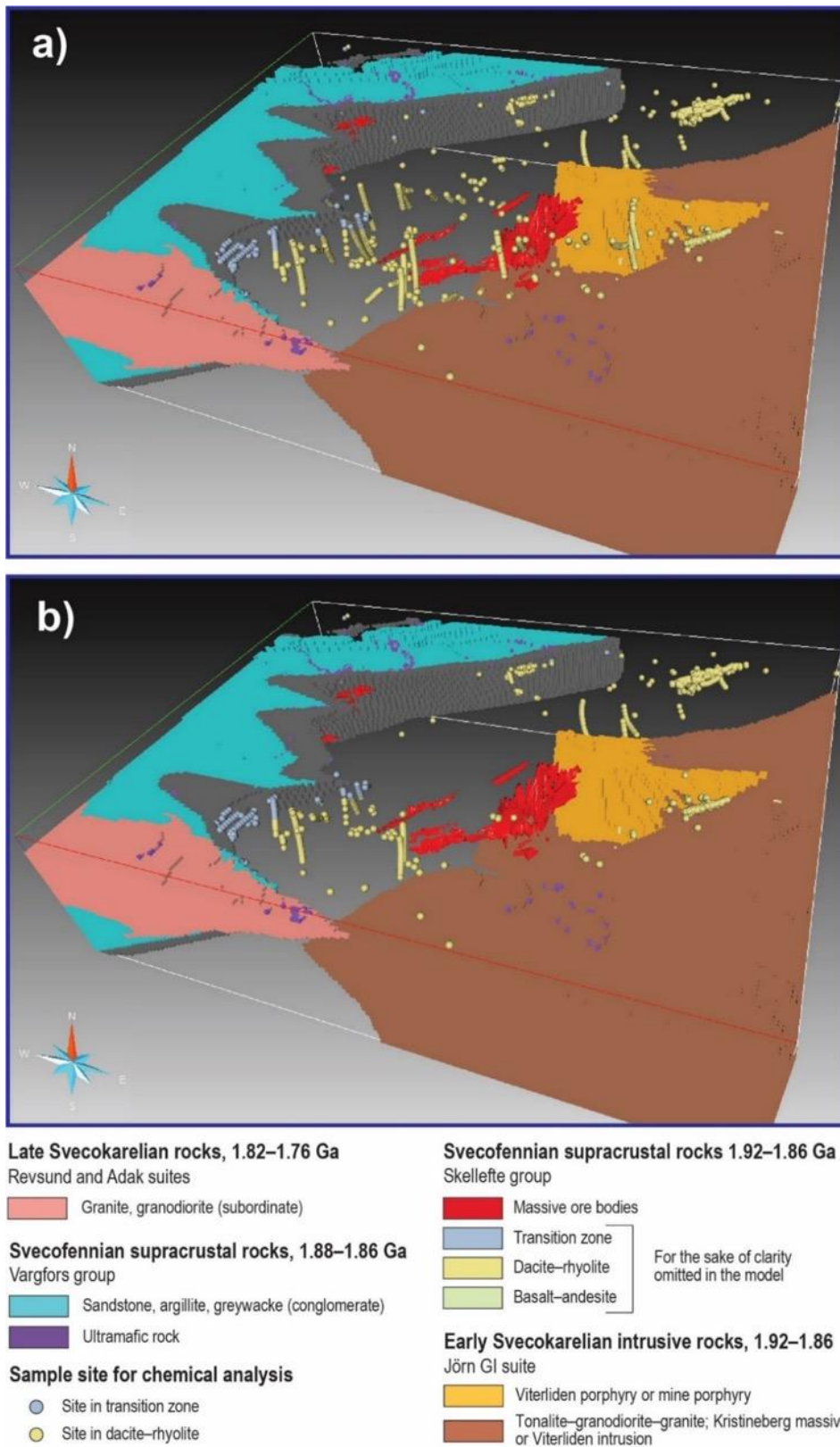


Figure 8. Three-dimensional model (unscaled) of the bedrock around the Kristineberg mine, showing sample sites for chemical analyses at distance of more than 500 m (a) and 1000 m (b) from the ore bodies. View towards the north-northwest. By courtesy of Boliden Mines.

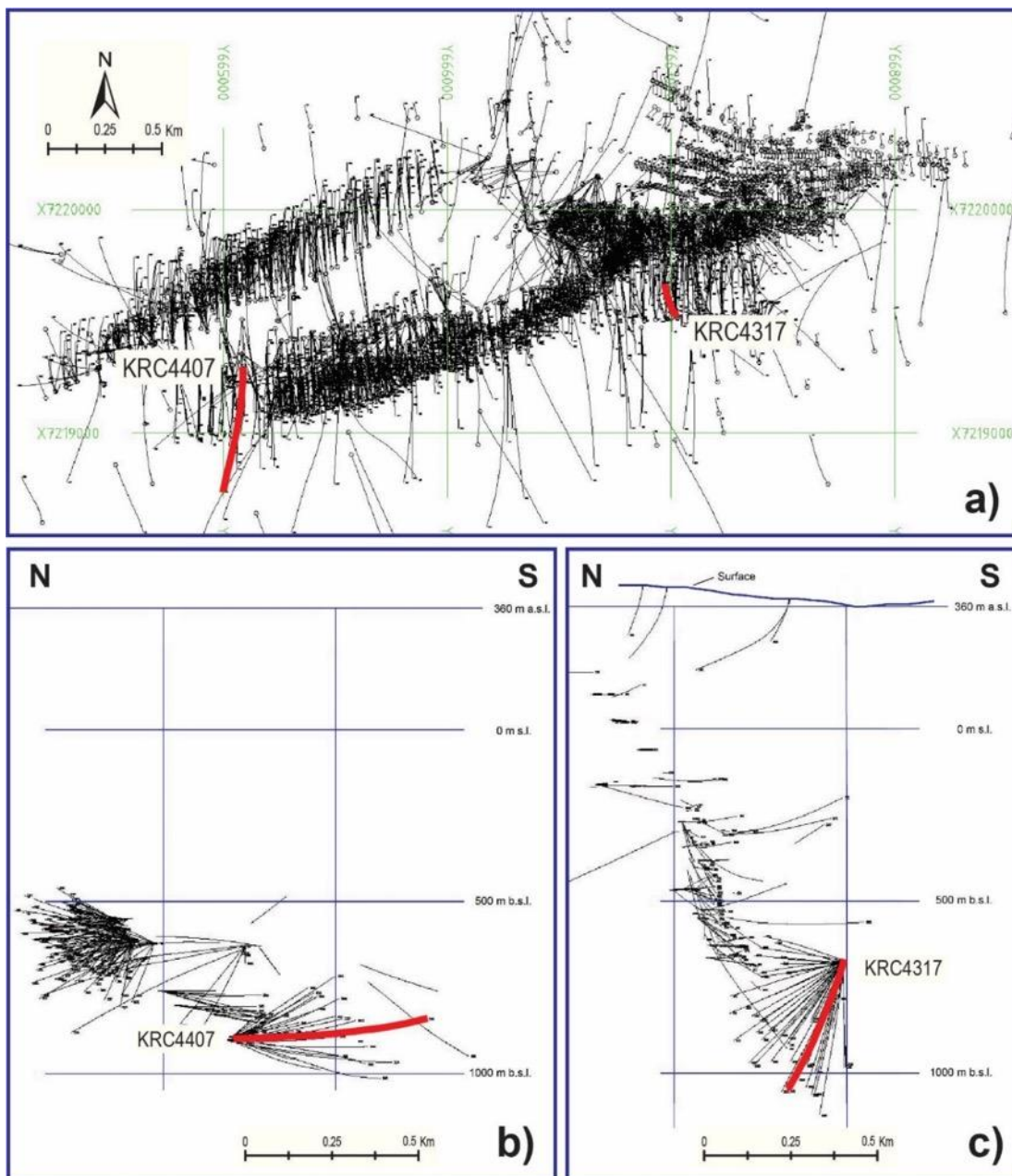


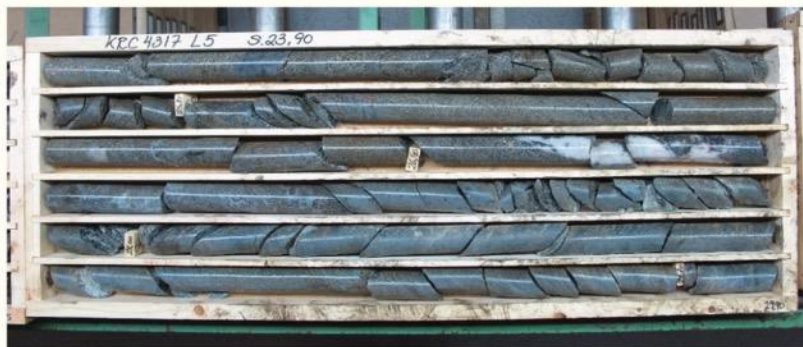
Figure 9. Drill hole maps from the area of the Kristineberg deposit. **A.** Horizontal projection of almost all drill holes around the Kristineberg deposit, view from above. The positions of drill holes KRC 4317 and KRC4407 are marked with red lines. **B.** Vertical projection of drill holes in a narrow, roughly north-south striking section around drill hole KRC4407, the latter marked with a red line. **C.** Vertical projection of drill holes in a 100 m wide north-south striking section around drill hole KRC4317, the latter marked with a red line. By courtesy of Boliden Mines.



a)



b)



c)



d)

Figure 10. Photos of drill core sections from drill cores KRC4317 and KRC4407. Fractured cores are giving indications of the present and past stress regime in the crust. **A.** Crushed drill core of cordierite quartzite and sericite quartzite, 281,10–286,70 m, drill core KRC4407. **B.** Massive drill core of cordierite quartzite, 389,90–395,75 m, drill core KRC4407. **C.** Crushed drill core of chlorite schist, 23,90–29,90 m, drill core KRC4317. **D.** Massive drill core of chlorite quartzite, 302,00–307,80 m, drill core KRC4317. Photos by courtesy from Boliden Mines.

2.1.7. Geophysics in the Kristineberg area

The Geological Survey of Sweden has a long-standing tradition in geological mapping of the country, especially with the support from airborne geophysics, which is necessary due to the low degree of bedrock exposures. These surveys have acquired data on the Earth magnetic field (e.g., in the Skellefte district, Fig. 5), gamma radiation and the VLF electromagnetic field. In addition to these surveys the gravity field of the Earth was measured using ground-based techniques (see also CHPM2030, D 1.2, Schwarz et al. 2016).

Exploring mineral deposits in more detail by geophysical methods was conducted by the mining industry and partly with the help from academia. Potential field and electrical investigations were in the forefront of these studies. In the last two decades, reflection seismic studies became more attractive even in hard rock imaging for prospecting after minerals and ores in the Earth's uppermost crust, owing to their ability in better resolving geological structures (e.g., Malehmir et al. 2012). Tryggvason et al. (2006) and Rodriguez-Tablante et al. (2007) studied the Kristineberg area in the western Skellefte district while Malehmir et al. (2006) extended these investigations further to the east. The western part of the Skellefte district is well documented by boreholes reaching depths greater than 1000 m, high resolution potential field data, i.e., magnetic and gravity, as well as by petrophysical data. Investigations in the Kristineberg area were followed up by employing magnetotellurics (MT) on one of the seismic lines allowing for the joint interpretation of velocity and electrical resistivity data (Hübert et al. 2009). Malehmir (2007) has summarized the outcome of this pilot study: A strong north-dipping reflection in conjunction with higher electrical conductivity is interpreted as the structural basement for the rocks of the Skellefte group (for a map see Fig. 11), though debated. Late Svecokarelian granites were modeled down to various depths between one and five kilometres.

The Kristineberg area was further investigated by using electromagnetic and seismic methods. Between 2002 and 2012, four reflection seismic lines were acquired around the Kristineberg mine (Fig. 11) and further three in the central and eastern Skellefte district, revealing numerous reflections from the top 12 km of the crust. The data also show a series of steeply dipping to sub-horizontal reflections. Some of these reach the surface and allow correlation with geological structures (Dehghannejad 2014).

Figure 12 visualizes seismic reflection data on profiles 1, 2, and HR from the Kristineberg area, where the ore deposits can directly be associated with reflected and diffracted signals. A deeper cluster of reflections describes a high contrast in impedance, but it is unclear whether this is related to some increase in ore content. Dehghannejad (2014) has further analysed the data concluding the mineralisation and associated structures dipping to the south down to at least 2 km in depth. Further re-processing of the seismic data allowed identifying reflections not recognized before. Dehghannejad et al. (2012) suggest this finding to be a target for further mineral exploration in the Kristineberg area, including the contact between the metasedimentary and metavolcanic rocks at depth.

2.1.8. Electrical resistivity studies

Electrical resistivity was studied at larger scales by, e.g., Jones et al. (1983) and Rasmussen et al. (1987). Magnetotelluric investigations within the Fennolara project (Rasmussen et al. 1987) have revealed a crustal zone of higher electrical conductivity. It is extending laterally more than 150 km, centered on the Skellefte district and considered having at least a thickness of 15 km. New magnetotelluric data acquired on a larger scale in north-west Fennoscandia by Cherevatova et al. (2014, 2015a, b) and Korja et al. (2008) confirm the highly conductive belt in the Skellefte district, assigning it a total conductance of more than 1000 Siemens. The anomalous structure is now interpreted as representing shallow graphitic shales of low thickness, embedded in the otherwise resistive crust.

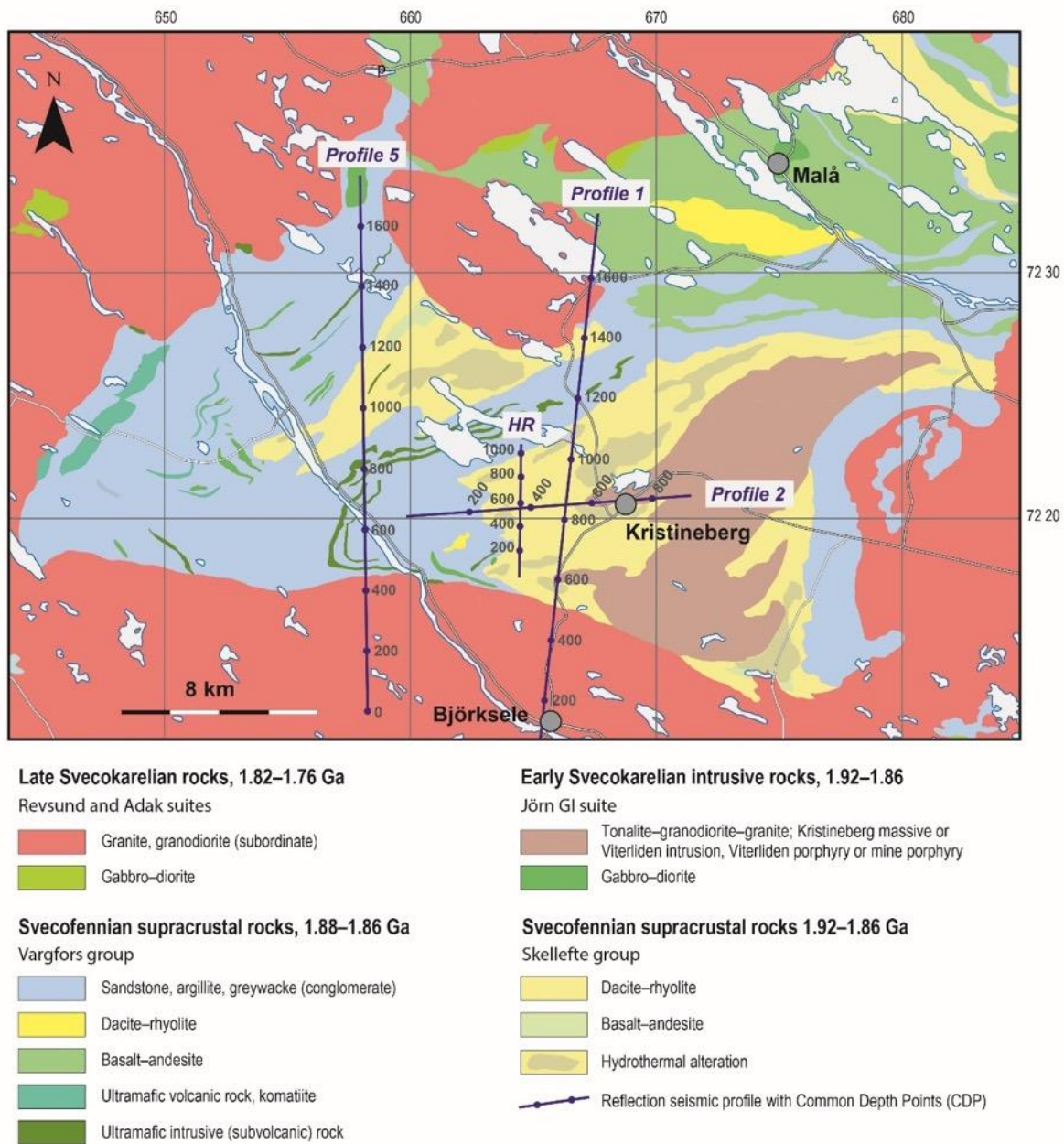


Figure 11. Geological map of the Kristineberg area where, e.g., reflection seismic and magnetotelluric investigations of the upper crust were done. Profiles 1, 2, 5 and HR are shown as black lines with common depth points indicated (Dehgannejad et al. 2012a).

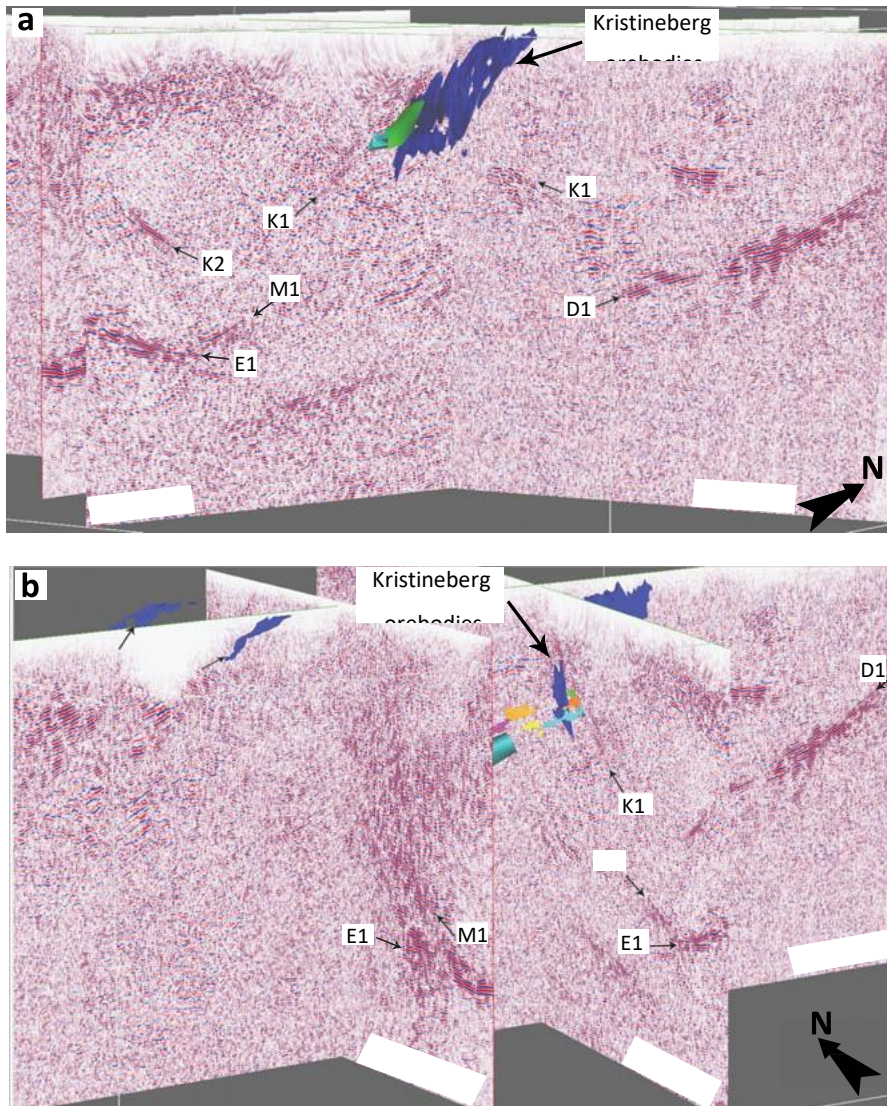


Figure 12. Seismic cross sections with migrated profiles 1, 2 and the HR profile, and mineralisation surfaces from borehole data in the Kristineberg mine (after Ehsan et al. 2012). Reflection K1 correlates with the mineralization horizon (dark blue, green, light blue), belonging to the Rävliiden massive sulphide deposits. Section depth is 3800 m, no exaggeration. a) View towards the northwest. B) View towards the northeast.

Among others, e.g., Hübert (2012), Garcia Juanatey (2012), Bauer et al. (2014) and Tavakoli et al. (2012a, 2012b, 2016a, 2016b) further studied the central Skellefte district, to delineate the structures related to VMS ore deposits and to model lithological contacts down to depths of some hundreds to some thousands of metres. The complexity of data necessitated 3D-modelling, where data of geomagnetic deep soundings (GDS), reflection seismics and geological observations were considered, too.

The model developed by Hübert (2012) and Garcia Juanatey (2012) shows distinct contrasts in electrical resistivity with values from several 1000 Ωm to less than 1 Ωm (Fig. 13). Beside some very shallow good conductors, those ones at larger depths are much more prominent, named CI and CIII in Figure 13. CI is said to correspond with the crustal zone of higher electrical conductivity in the Skellefte district, earlier identified by Rasmussen et al. (1987). It is located at about 4 km depth, a value that is well determined. But,

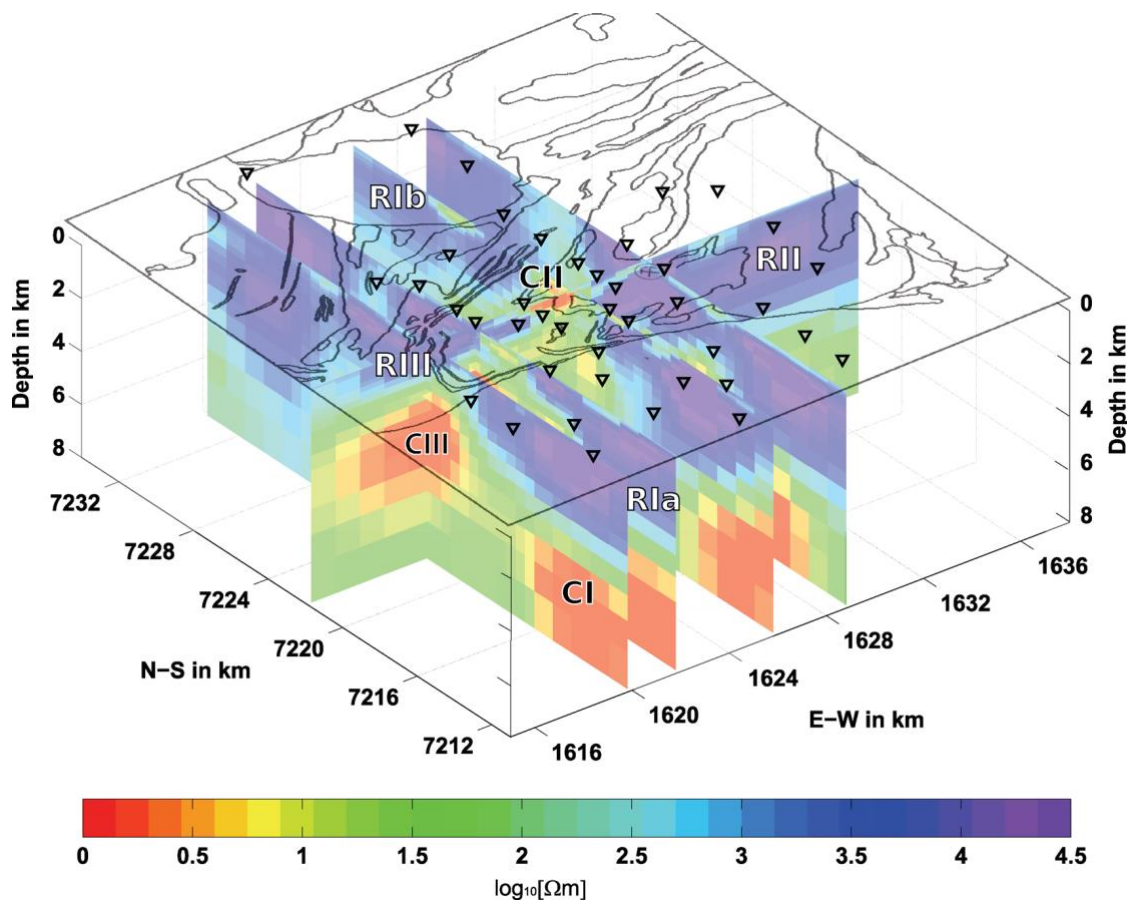


Figure 13. 3D electrical resistivity model of the Kristineberg area, cut into slices (Hübert et al. 2013). On surface, outline of geological structures and position of MT measuring sites (triangles). Coordinate system *Swedish Grid RT90* (in km). Resistors associated with, Rla, Rlb: Revsund granite; RII: Viterliden intrusion; RIII: Mafic dykes within the metasedimentary rocks; Conductors related to CI: Skellefte crustal conductivity anomaly; CII: black shales at the base of the metasedimentary rocks; CIII: alteration or mineralised zones (?) in metavolcanic rocks.

because of limited data extend, thickness constraints are unsecure. CI vanishes towards the north, and likely even towards the east which can be inferred from GDS data. Conductors at intermediate depth, downward from about 2 km, are of unknown origin. Hübert et al. (2013) explain them by alteration zones of increased ore content in the volcanic rocks. The very shallow conductors named CII around Kristineberg are only about 200 m thick. They can be explained with black shales rich in graphite, encountered at the base of the sedimentary rocks of the Vargfors group and confirmed by shallow borehole data (T. Hermansson, pers. comm.). The sedimentary rocks show medium resistivities of 30 to 300 Ωm , while the volcanic rocks of the Skellefte group have no unique resistivity values. Depending partly on their degree of alteration, these rocks are not easily to differentiate from the sedimentary rocks and the Viterliden intrusion.

Apart from the superficial conductors CII, uppermost crustal structures have high electrical resistivity. Most obvious are resistors Rla, Rlb that have several 1000 Ωm (see Figure 13) with maximum thickness in the south of 3 to 4 km, and more than 5 km in the north. Geologically, they can be associated with the Revsund granites. Resistor RII appears sheet-like and in its northern extend it matches with the contact zone of sedimentary and volcanic rocks of the Vargfors and the Skellefte groups, respectively. Well conducting black shales as reported about above, seem to be absent at this contact. The resistive feature RIII extents less than 2 km in depth and might be linked to mafic dykes within the sedimentary rocks and having a distinct magnetic foot print (Malehmir et al. 2007).

2.1.9. Modelling

In geophysical modelling the strategy behind is essential, e.g., 3D modelling is to prefer 2D modelling, independent of the method. The interpretation of structural settings of individual mineralisations or areas of interest is normally based on combinations of surface data, drill core analyses, geophysical data and 3D- and 4D-modelling, the latter including bedrock evolution in geological times. For deeper structures and mineralisations, geophysical data are often the only available means for 3D evaluation unless drilling has been performed. Examples of 3D- (and 4D-) modelling that relate to Swedish bedrock conditions are Bauer (2013), Bauer et al. (2009, 2010, 2011, 2012, 2014), Malehmir et al. (2009), Carranza and Sadeghi (2010), Kampmann (2015), Skyttä et al. (2009, 2012, 2013), Wareing (2011) and Weihed (2014).

The 3D model inversion of electrical resistivity data from Kristineberg compared with 2D modelling, for computational reasons is using a wider grid and less data as input (Hübert 2012, Garcia Juanatey et al. 2011). Therefore, the 3D model is showing less resolution though the depth of conductors CI and CIII is comparable with that one obtained in 2D modelling. But, it indicates differences in extent and values of high conductivity zones. In 2D models, especially the intermediate and deep conductors (CI, CIII) have much larger depth extent. This is regarded as being due to 3D effects, i.e., lateral effects in data observed.

2.1.10. Combining seismic and magnetotelluric results

Hübert et al. (2012) have compared surface geology and seismic reflectors in the upper crust identified on profiles 1 and 5 with slices of their 3D resistivity model, as shown in Figure 14. Profile 1 displays the lower boundary of resistor RIa associated with the southern Revsund granites and coinciding with an increase of reflectivity, while the uppermost crust is much less reflective. The deep conductor below, CI, in its extent does not resemble seismic reflectors, beside its lower bound in south-southwest. Conductor CIII is positioned in a zone of less distinct reflections. The anticline where the Kristineberg mine is established (marked E in Fig. 14) is not specially resolved in the model.

The section along profile 5 (Fig. 14, lower) evinces lateral boundaries of electrical resistivity where even seismic reflectivity is changing. In the southern part, the top of the deep conductors seems to be bound by seismic reflectors dipping to the north. Resistors RIII and RIb are separated from each other by a zone of higher reflectivity which might be related to many mafic dykes within the sedimentary rocks (Hübert et al. 2012).

Malehmir et al. (2009) have composed 2.5- and 3D-models of the Kristineberg area, compiled from potential field-, seismic reflection-, borehole- and geological data (Fig. 15). A transparent seismic reflection zone observed above the zone of north-dipping reflectivity (Fig. 15a) is explained to belong to volcanic rocks of the Skellefte group (Tryggvason et al. 2006). The role of structures below, interpreted by Malehmir et al. (2009) as representing the basement, is debated (e.g., T. Hermansson, pers. comm.). The inversion of gravity data was most effective owing to the high density contrast in lithology, though structures, e.g., dykes, faults and folded and deformed units are rather complex in the area. In the modelling process, seismic data were a key component for providing constraints for geological units. Modelling of magnetic data could have been improved if magnetic properties of rocks should have been available. This should have required rock magnetic measurements on a larger number of samples in the laboratory.

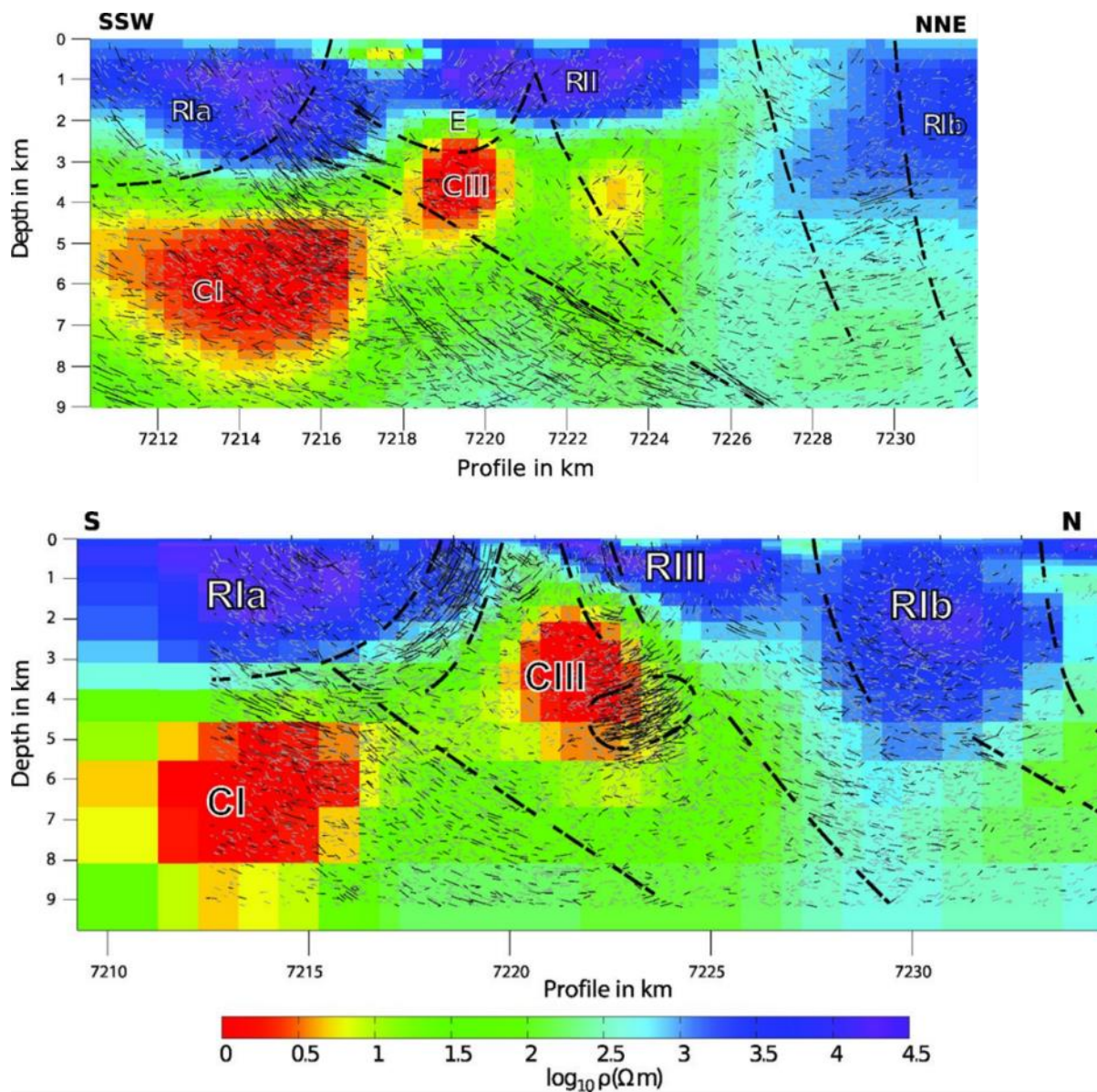


Figure 14. Sections through 3D resistivity model (Hübert et al. 2013), together with seismic reflections along profiles 1 (top) and 5 (bottom) (Malehmir et al. 2007). See Figure 11 for locations of the profiles. Thick dashed lines mark interpreted seismic structures. E in section of profile1 (top) section marks the assumed anticline, hosting Kristineberg mine. Rla, Rlb: Revsund granite; RII: Viterliden intrusion; RIII: Mafic dykes within the metasedimentary rocks; Conductors related to CI: Skellefte crustal conductivity anomaly; CII: black shales at the base of the metasedimentary rocks; CII: alteration or mineralised zones (?) in metavolcanic rocks.

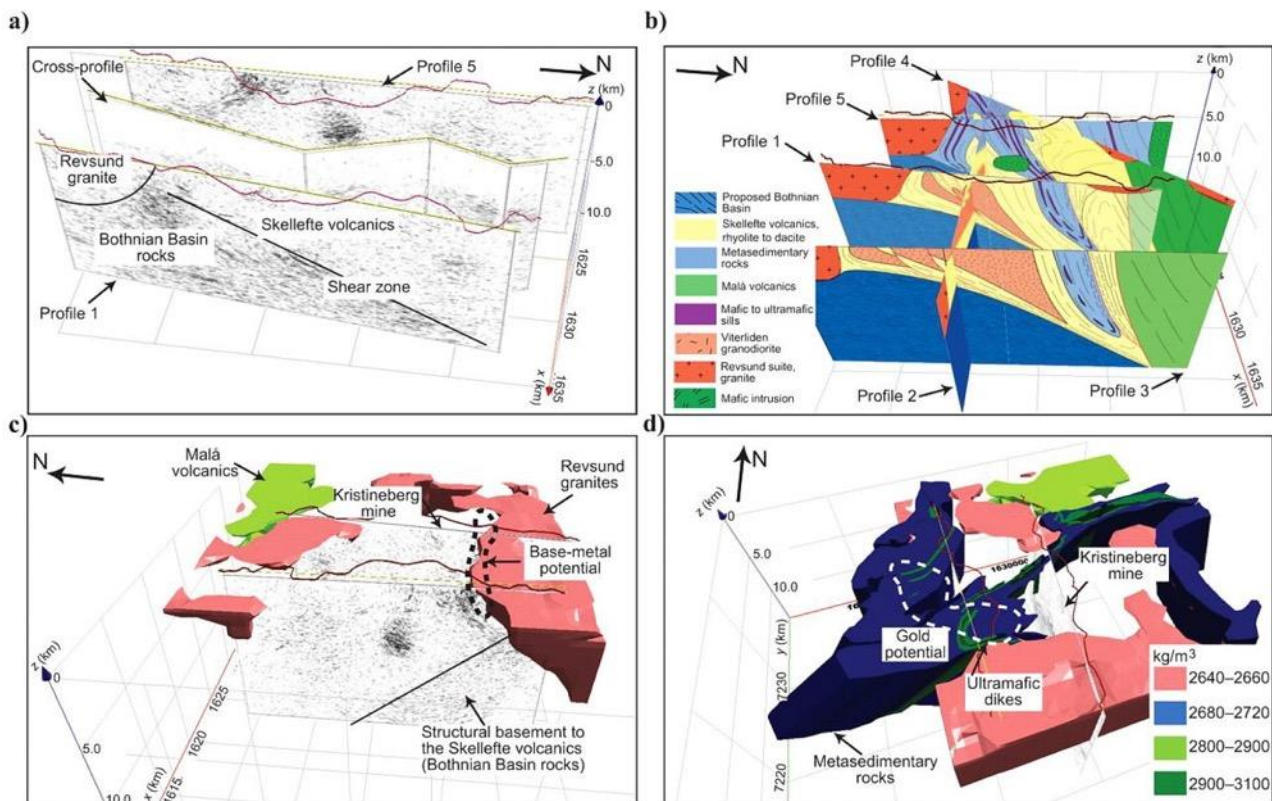


Figure 15. Kristineberg mining area - 3D views showing stages of the geological interpretation (Malehmir et al. 2009b). a) Early interpretation of seismic reflection data (Rodriguez-Tablante et al. 2007); b) Predicted 3D model for major structures obtained from five 2D geologic cross sections (see Malehmir et al. 2007); c, d) Final geological model for metal potential from 3D inverse and forward gravity modelling, all data available combined for targeting new prospecting areas. Horizontal to vertical scale 1:1.

2.1.11. Natural seismicity

The Swedish National Seismic Network (SNSN) started monitoring earthquakes with the installation of a Wiechert seismograph in Uppsala in 1904. The SNSN operates the only permanent, earthquake focused seismic network, consisting of 65 permanent stations in Sweden. The seismic sensors have unusually high gain to facilitate detection of microearthquakes in the regional size network. With an average station spacing of 66 km, the SNSN is complete to magnitude 0.5 (Richter scale) within the network.

Natural seismicity in the Kristineberg area seems to be very low. No local earthquakes were observed in the last two decades, with the observation threshold in magnitude being at about 1.9 on the Richter scale (B. Lund priv.com., SNSN 2019). Thus, seismology does not help to resolve the regional stress regime, and quantitative predictions cannot be done.

2.2. The Nautanen deposit in the Northern Norrbotten ore province

The Nautanen deposit is situated in Northern Norrbotten, the northernmost ore province in Sweden (Figs. 2, 16). The other provinces are Bergslagen, the Skellefte district and the Caledonian orogen. The following description of the regional geology of northernmost Sweden and local geology at Nautanen is modified from Bergman (2018) and Lynch et al. (2018a), respectively. The parts left out are those considered irrelevant to the present CHPM task. The complete reference lists of Bergman (2018) and Lynch et al. (2018a) are however kept.

2.2.1. Regional geology

The Precambrian bedrock in northernmost Sweden is part of the 2.0–1.8 Ga old Svecokarelian orogen. The orogen comprises both pre-orogenic rocks formed in the Archaean and early Palaeoproterozoic, as well as rocks formed during the orogeny itself. All the rocks were deformed and metamorphosed to variable degrees at different stages during the orogenic evolution (Fig. 16).

The oldest rocks were formed in the Archaean (Fig. 16). The main component is gneissic granitoid of mainly tonalitic to granodioritic composition, which shows intrusive relationships with paragneiss, amphibolite and, locally, banded orthogneiss interpreted as metaandesitic to dacitic tuff. Bodies consisting of non-migmatitic metamorphosed granite are locally common. Age determinations suggest crystallisation of granitoids at 2.8–2.7 Ga, and a regional metamorphic event is constrained at 2.7 Ga (Skiöld 1979, Skiöld & Page 1998, cf. Martinsson et al. 1999).

Layered mafic-ultramafic intrusions with an age of 2.5–2.4 Ga occur locally (Fig. 16); more common are mafic dykes and felsic–mafic intrusions related to later events. A metamorphosed volcano-sedimentary sequence, deposited before 2.0 Ga and unconformably overlying the Archaean basement is commonly referred to as Karelian supracrustal rocks (see also Gaál & Gorbatshev 1987). The lowermost Karelian unit in the Kiruna area is the Kovo group, which is composed of a basal clastic sequence of metamorphosed conglomerate and quartzite, overlain by tholeiitic metabasalt and metamorphosed calc-alkaline volcanoclastic rocks of andesitic composition. In the east, the Archaean rocks are overlain by quartzite, along with subordinate metamorphosed conglomerate and phyllite. Locally, metavolcanic rocks of andesitic to dacitic composition occur below the quartzite. Metasandstone, quartzite and quartzo-feldspathic gneiss in the Pajala area and to the south are spatially associated with both Karelian and younger metavolcanic rocks.

In the Kiruna area (Fig. 16), the Kovo group is overlain by the Kiruna greenstone group, which predominantly comprises metamorphosed, tholeiitic basalt lava flows, including pillow lava, less important komatiitic lava, tholeiitic tuff and andesitic to dacitic tuffaceous rocks, and minor conglomerate, black schist and carbonate rock (Martinsson 1997). The Viscaria Cu-rich sulphide deposit is hosted by metamorphosed volcanoclastic and associated sedimentary rocks belonging to the Kiruna greenstone group. The stratigraphic sequence is similar but less complete in the area between Kiruna and Pajala. Mafic pyroclastic deposits are overlain by volcanoclastic rocks interlayered with carbonate rock, graphite schist, skarn-related iron oxide deposits, banded iron formation and chert (Martinsson 1993, Martinsson et al. 2018b, Lynch et al. 2018b). Most of these rocks were deposited before 2.14 Ga.

Svecofennian supracrustal rocks, recording the onset of the Svecokarelian orogeny, unconformably to disconformably overlie the Kiruna greenstone group and related units. The lower part of the sequence is characterised by calc-alkaline metavolcanic rocks of andesitic composition. On a regional scale, these rocks show extensive interlayering, with metamorphosed, siliciclastic sedimentary rocks. Metavolcanic and metasedimentary rocks are traditionally included in the Porphyrite group, defined in the low-grade rocks

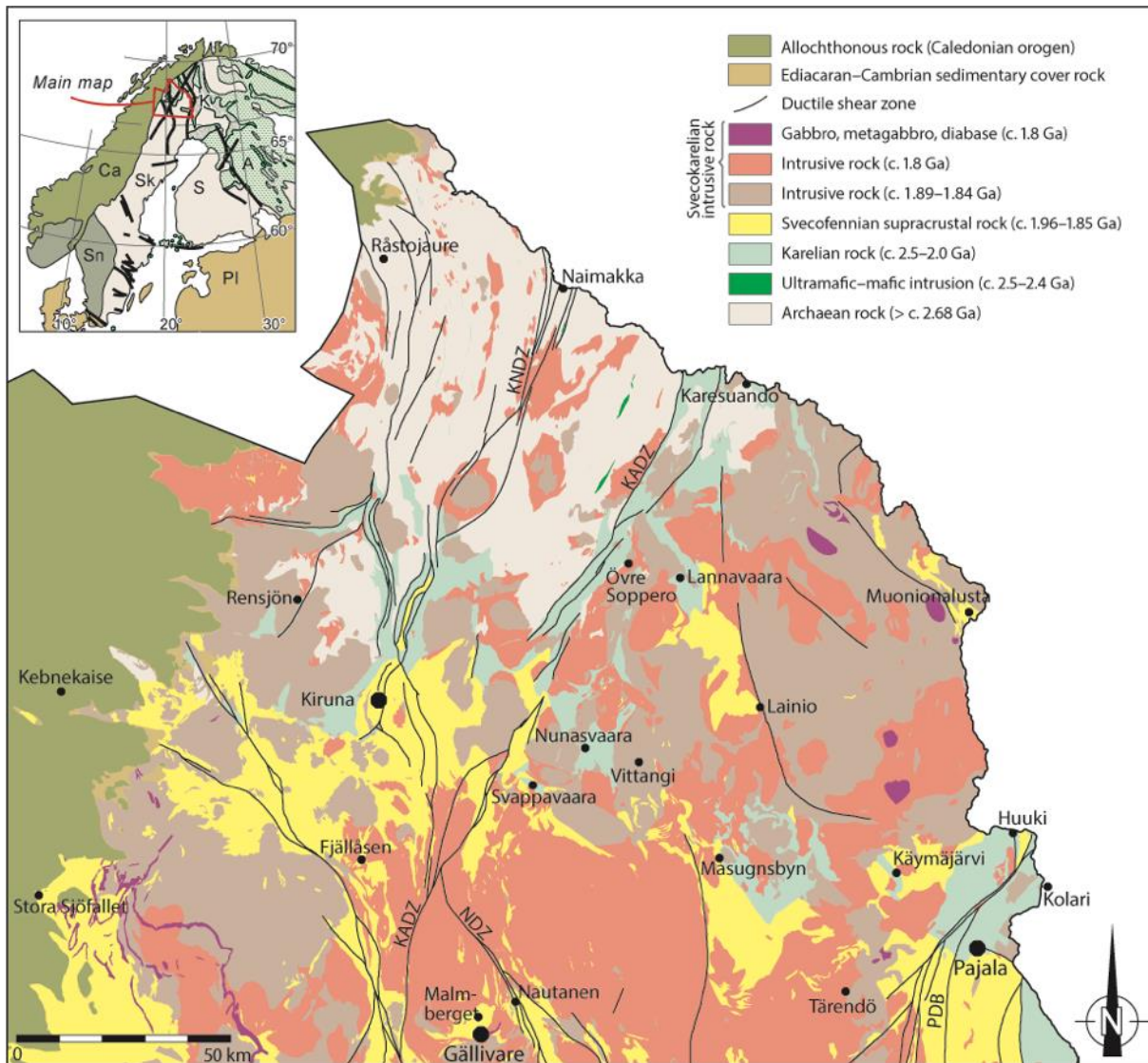


Figure 16. Simplified bedrock map of northern Norrbotten County, modified from Bergman et al. (2001). KNDZ = Kiruna–Naimakka deformation zone, KADZ = Karesuando–Arjeplog deformation zone, NDZ = Nautanen deformation zone, PDB = Pajala deformation belt. Inset map: Sk = Svecokarelian orogen, Sn = Sveconorwegian orogen, Ca = Caledonian orogen, PI = Platformal sedimentary cover rocks, A (green ornament) = Archaean rocks in part reworked in the Palaeoproterozoic, K (grey ornament) = Karelian rocks, S (without ornament) = Svecofennian supracrustal rocks and Svecokarelian intrusive rocks; thick lines are major deformation zones. The abandoned Nautanen mine (67° 11' 30" N, 20° 52' 49" E) is close to Gällivare at the lower edge of map.

southwest of Kiruna. Equivalent units occur in other areas. Available age determinations show crystallisation ages of 1.89–1.88 Ga (Edfelt et al. 2006, Martinsson et al. 2018b, Hellström et al. 2018, Lynch et al. 2018a).

The Kiirunavaara group stratigraphically overlies the Kurravaara conglomerate in the Kiruna area and the Porphyrite group to the southwest of Kiruna (Fig. 16). In Kiruna, metamorphosed andesitic to trachyandesitic lava flows comprise the footwall of the Kiruna apatite iron oxide ore deposit. This deposit is overlain by porphyritic metadacite of pyroclastic origin (Martinsson 2004). The age of the host rocks is 1.89–1.87 Ga, and the ore has been dated at 1.88–1.87 Ga (Westhues et al. 2016). The uppermost unit in the Kiirunavaara group mainly consists of metamorphosed ignimbritic tuff, basalt and siliciclastic sedimentary rock. Southwest of Kiruna a thick sequence of metamorphosed, high-Ti and high-Zr tholeiitic basaltic lava is overlain by a unit

predominantly comprising pyroclastic metadacite. There are subordinate intercalations of metamorphosed andesite, locally ignimbritic rhyolite, conglomerate, sandstone and siltstone (Offerberg 1967, Perdahl & Martinsson 1995, Martinsson 2004).

The youngest supracrustal unit consists of sandstone with subordinate conglomerate and mudstone, and in some areas of basaltic intercalations (Witschard & Zachrisson 1995). Although the contacts are tectonic in most other areas, there is a locality northwest of Vittangi where a metaconglomerate rests unconformably on a metadiorite (Ödman 1939). The metadiorite is 1.88 Ga old, representing the maximum age of the clastic deposition in this area.

The more or less gneissic intrusive rocks in the Haparanda suite are commonly grey and medium-grained, but fine-grained types are also present; porphyritic varieties are uncommon. Magma mingling textures are common in some areas. There is a wide spectrum of rock types, from predominantly gabbroid and dioritoid, through quartz monzonite, tonalite and granodiorite, to subordinate granite (Ödman 1957, Bergman et al. 2001).

The intrusive rocks in the Perthite monzonite suite, formed between 1.88 and 1.86 Ga, mainly occur in the westernmost part of the area (Fig. 16). Quartz-poor rocks, including monzonite, quartz monzonite and quartz monzodiorite, predominate over granite. Many large intrusions of gabbro and diorite, inferred to belong to this suite, are also present. Magmatic layering has been observed in some of these bodies, and several show a concentric, banded magnetic pattern. Ultramafic rocks such as pyroxenite and serpentinite are present in some areas. Perthite-bearing granite is commonly red and medium- to coarse-grained. Enclaves and hybridisation phenomena show that magma mingling and mixing processes were prevalent. The rocks in the Perthite monzonite suite are typically isotropic but there are also areas where a tectonic fabric is prominent. There are geochemical similarities between the Perthite monzonite suite and the Kiirunavaara group (Witschard 1975, 1984), suggesting that the former was emplaced under sub-volcanic conditions. The rock types in the Perthite monzonite suite are similar to those in the Haparanda suite, but have traditionally been considered separate on the basis of several lines of evidence, including field relationships and lithogeochemical characteristics.

A suite of granite and granodiorite has yielded an age of about 1.85 Ga (Fig. 16; Bergman et al. 2006, Hellström & Bergman 2016). The granitoids are spatially associated with pegmatite, and in many places contain biotite-rich seams and partly assimilated remnants of older rocks. The granitoids are porphyritic, have an unequigranular matrix and are weakly foliated.

Large bodies of intrusive rocks belonging to the Lina suite, which formed around 1.8 Ga (Skiöld 1988, Bergman et al. 2002b), are common throughout the area (Fig. 16), and dykes or veins of rocks belonging to this suite commonly cut older rocks. The Lina suite is mainly composed of greyish-red, medium-grained and weakly porphyritic granite; red, fine-grained and equigranular varieties are also common. The granite is usually weakly foliated, associated with pegmatite, and fragments of assimilated country rock are common. Dykes or veins in older rocks consist of granite, pegmatite or aplite. A suite of intrusive rocks consisting of gabbro to granite, with quartz monzonite, monzonite, syenite, quartz monzodiorite and monzodiorite as intermediate members is found in the east of the area (Fig. 16). They have ages close to 1.8 Ga (Romer et al. 1994, Martinsson et al. 2018a).

The Nabrenjarka diabase, west of Gällivare (Fig. 16), is a conspicuous, flat-lying, bowl-shaped and sill-like intrusion with an exposed length of more than 50 km. It intrudes the Lina suite and is 1.8 Ga in age or younger.

Ductile deformation includes several phases of folding and the formation of major crustal-scale shear zones (Fig. 16). The metamorphic grade within the region is variable from greenschist to upper amphibolite facies,

and the intensity of deformation varies from strong penetrative foliation to texturally and structurally well-preserved rocks, both on a regional and local scale. Up to four separate phases of deformation have been identified in the east (Grigull et al. 2018, Lynch et al. 2018b).

An early event of deformation and metamorphism at c. 1.88 Ga, was followed by one at 1.86–1.85 Ga (e.g. Skiöld & Öhlander 1989, Bergman et al. 2001, Hellström 2018, Bergman et al. 2006). From a protracted event or several separate events during the time interval 1.83–1.78 Ga, including movements along the Pajala deformation belt, Bergman et al. 2001, 2006, Lahtinen et al. 2015, Hellström & Bergman 2016 concluded a regime of ductile deformation in the region.

The most important types of mineralisation are stratiform copper deposits, iron formations, Kiruna-type apatite iron ores and epigenetic copper-gold deposits. Age determinations show that major mineralisation events occurred at 1.88–1.86 Ga and 1.79–1.74 Ga, i.e., close in time to major phases of magmatism, deformation and metamorphism.

Hydrothermal alterations are both of regional character and spatially associated with mineralisations. The most characteristic alteration products are scapolite and albite, but skarn, biotite, carbonate, K-feldspar, sericite, tourmaline, epidote and chlorite are also common (e.g. Bergman et al. 2001, Martinsson et al. 2016, Lynch et al. 2018a). The geochemical composition of till overlying the bedrock reflects these alterations as enrichment in e.g. Ba, Ca, Cl, K, Na, Sr, La, Rb and P (Ladenberger et al. 2018). Age determinations show that major mineralisation events occurred at 1.88–1.86 Ga and 1.79–1.74 Ga (Martinsson et al. 2016), i.e., close in time to major phases of magmatism, deformation and metamorphism.

2.2.2. Local geology

The rocks of the Nautanen area form a partly conformable succession of syn-orogenic, Palaeoproterozoic volcanosedimentary rocks (Fig. 17; Witschard 1996). This supracrustal sequence is generally of calc-alkaline, basaltic andesite to andesite composition and has undergone extensive deformation, metamorphism, recrystallisation and hydrothermal alteration (McGimpsey 2010, Waara 2015, Lynch et al. 2015).

A variety of intrusive rocks occur across the area, including deformed gabbroic, syenitic and dioritic bodies and younger, deformed to massive granitic and gabbroic-doleritic plutons and dykes (e.g. Wanhainen et al. 2006, Sarlus 2016). Two large, sub-rounded, mafic-ultramafic intrusions (named the Dundret and Vasaravaara complexes) occur near Gällivare. These rocks exhibit distinct cumulate zones defining a primary magmatic layering consisting of olivine, pyroxene and plagioclase in varying proportions (Sarlus 2016).

Metasupracrustal rocks in the general Gällivare area host the Malmberget iron mine, Sweden's second largest iron resource after the Kiirunavaara deposit in Kiruna, and the Aitik copper-gold-silver deposit, one of Europe's largest copper mines (Fig. 17; e.g., Lund 2009, Wanhainen et al. 2012). Additionally, several hydrothermal copper-gold occurrences assigned to the iron oxide-copper-gold (IOCG) mineral deposit class occur within a regional approximately north-northwest-trending deformation zone termed the Nautanen deformation zone (NDZ; cf. Smith et al. 2013, Drejing-Carroll et al. 2015). Episodic deformation along this zone probably enhanced permeability and hydrothermal fluid flow, resulting in a relatively focused, linear zone of alteration and mineralisation (cf. Witschard 1996).

Metamorphic mineral assemblages and pressure-temperature (*PT*) estimates suggest the area reached middle amphibolite facies conditions during peak regional metamorphism. Bergman et al. (2001) noted a major metamorphic grade boundary in the area, with rocks east of the NDZ having a lower grade than those within the zone and to the west. Pressure-temperature estimates for regional metamorphism range from approximately 550 to 660°C and 2 to 5 kbar (i.e. lower to middle amphibolite facies), for contact metamorphism adjacent to Lina-type granite (forming a sillimanite-biotite-muscovite assemblage) between

approximately 630 and 710°C and 2.0 to 4.4 kbar, and for retrograde conditions between approximately 430 and 570°C, and 3.0 to 3.5 kbar (Tollefsen (2014). Additionally, *PT* estimates of approximately 630–680°C and 6.5 kbars (equivalent to middle amphibolite facies conditions) for metasomatic garnet growth associated with potassic-ferroan alteration and copper-gold mineralisation at the Nautanen deposit have been made by Waara (2015).

2.2.3. Stratigraphy and correlations with regional successions

The supracrustal rocks in the Nautanen area belong to the so-called Muorjevaara group (see Lynch et al. 2015 and references therein) which represents a basal, mainly calc-alkaline volcanosedimentary sequence. This is overlain by the Kiirunavaara group, comprising alkalic (trachytic) intermediate to acidic metavolcanic rocks (Martinsson & Wanhainen 2004). This unit hosts the iron oxide-apatite deposit at Malmberget (e.g. Lund 2009). Local quartzite outliers represent an uppermost stratigraphic unit. In the absence of outcropping transitional contacts, the major stratigraphic units are inferred to be separated by unconformities. The Muorjevaara and Kiirunavaara groups partly correspond to regional *Porphyrite* and *Porphyry groups* (Bergman et al. 2001), respectively. Traditionally, these regional stratigraphic units have been considered broadly coeval and have mainly been divided on the basis of petrographic and geochemical considerations (cf. Perdahl 1995).

2.2.4. The Nautanen deformation zone and related iron oxide-copper-gold mineralisation

The Nautanen deformation zone (NDZ; Witschard 1996) represents the most conspicuous structural feature in the area. It is clearly delineated on magnetic anomaly maps as a somewhat dilational, linear zone of sub-parallel and tightly banded magnetic susceptibility anomalies (see *Geophysical modelling* section). The coupling of high-strain deformation and magnetic banding reflects episodic metasomatic-hydrothermal fluid flow, probably enhanced by increased permeability associated with protracted and focused deformation (e.g. Pitkänen 1997, Smith et al. 2013).

Based on regional structural and magnetic lineament geometries, a dextral-oblique shear sense, with a southwest-side up reverse component has been interpreted (Bergman et al. 2001). Geological mapping and geophysical measurements within the shear zone have also identified several sub-parallel, north-northwest-orientated, moderately plunging folds (e.g. Gustafsson 1986, Pitkänen 1997). Internally, the deformation zone is characterised by moderate to intense shearing, mylonitisation, structural transposition and pervasive metasomatic-hydrothermal alteration.

The supracrustal rocks within and adjacent to the NDZ host several replacement- and vein-related (epigenetic-style) copper and gold deposits and prospects (see reviews by Martinsson & Wanhainen 2004, Martinsson & Wanhainen 2013). Important examples include the Nautanen, Liikavaara and Ferrum prospects (Fig. 17). Two general styles of mineralisation are recognised (e.g. Gustafsson 1985, Martinsson & Wanhainen 2004): (1) an inferred older phase of disseminated to semi-massive (replacement-style) sulphide mineralisation forming sub-vertical, lenses and linear zones mainly within the NDZ; and (2) mineralisation associated with quartz ± tourmaline ± amphibole veins occurring mainly east of the NDZ (e.g. the Ferrum prospect, Gustafsson & Johnsson 1984), or as a late-stage brittle overprint within the high-strain zone.

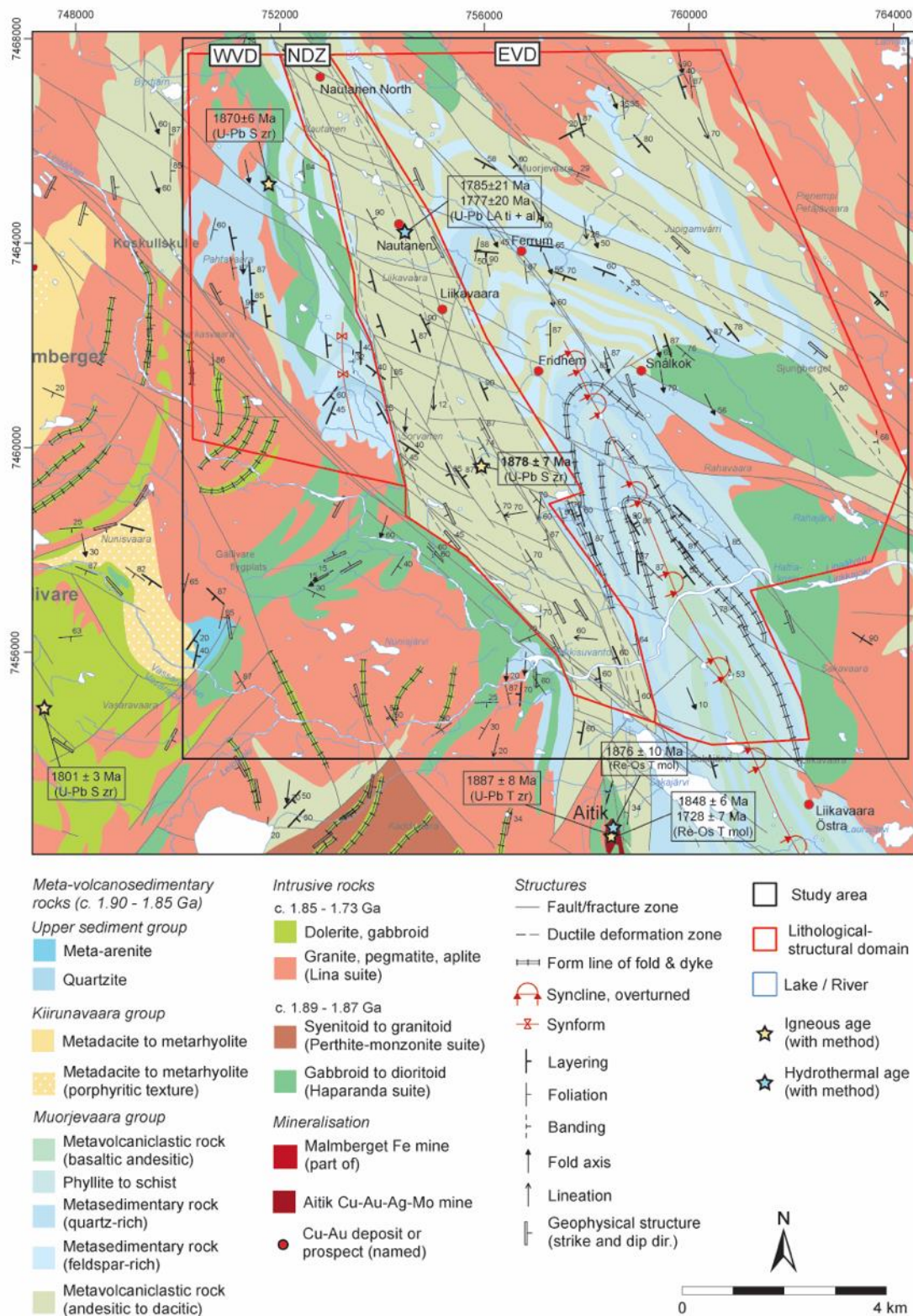


Figure 17. Geology of the Nautanen area (Lynch et al. 2018a). Abbreviations: EVD = eastern volcanosedimentary domain; NDZ = Nautanen deformation zone (domain); WVD = western volcanosedimentary domain. Geochronology abbreviations and sources: U-Pb S zr = U-Pb SIMS zircon dating (Sarlus 2016, and this study = highlighted bold text in

NDZ), U-Pb T zr = U-Pb TIMS zircon dating (Wanhainen et al. 2006), Re-Os T mol = Re-Os TIMS molybdenite dating (Wanhainen et al. 2005), U-Pb T ti = U-Pb TIMS titanite dating (Wanhainen et al. 2005), U-Pb LA ti + al = U-Pb laser ablation-inductively coupled-mass spectrometry titanite and allanite dating (Smith et al. 2009). Nautanen is situated in the upper third of the map. Coordinate system is SWEREF 99 TM.

The area around the Nautanen deposit (67° 11' 30" N, 20° 52' 49" E) in the northern NDZ domain is a historical mining location that has experienced intermittent exploration for over 100 years. Copper mineralisation was first discovered in 1898, and approximately 72 000 tonnes of copper and iron ore were extracted between 1902 and 1907 (Geijer 1918). Further exploration in the 1970s and 80s produced a pre-regulatory total resource estimate for the “old” Nautanen deposit of approximately 2.94 Mt grading 0.78% Cu and 0.52 ppm Au (values derived from Danielson 1985). Present-day exploration by Boliden Mineral AB has resulted in the discovery of an additional copper-gold mineralisation approximately 1.6 km north-northwest of the old Nautanen mine along the trend of the NDZ (Fig. 17). This “Nautanen North” deposit has an indicated resource of 9.6 Mt grading 1.7% Cu, 0.8 ppm Au, 5.5 ppm Ag and 73 ppm Mo, with an additional inferred resource of 6.4 Mt grading 1.0% Cu, 0.4 ppm Au, 4.6 ppm Ag and 41 ppm Mo (New Boliden 2016).

The bedrock in the area, largely enclosed by the red line around Nautanen North, “old” Nautanen, Liikavaara and further about 10 km south-southeast in Figure 17, has been systematically sampled and chemically analysed (n = 836) by Boliden Mines (T. Hermansson, pers. com. 2019). Discarding samples with more than 1,000 ppm Cu, background values for several elements were calculated, and some of these are shown in Table 1. The average values reported in Table 1 are comparable to continental crustal abundances (Taylor 1964) except for silver, tungsten and gold, which are enriched. However, the wide compositional range with high upper values suggest heterogeneity and varying degrees of mineralisation.

Table 3. Metal content in surrounding formations being of crucial importance for a CHPM system: Chemical background values of the bedrock in the Nautanen area (see text). Data courtesy of Boliden Mines.

	Ag	Au	Co	Cu	Li	Mo	Ni	Sn	W	Zn
	ppm	ppb	ppm	ppm	ppm	ppm	ppm	ppm	ppm	ppm
Average	1	7	24,5	71,8	12,9	2	15,0	1,3	3,4	90,0
Max	349	523	92	921,2	160	65	97	12	69	698
Min	0	0	0,5	0	0	0	0	0	0	0

According to criteria presented by Grooves et al. (2010), the geological characteristics of the Nautanen copper-gold deposit are consistent with the restricted definition of a *bona fide* iron oxide-copper-gold (IOCG) system. These include (1) enrichment of copper and gold, with both elements representing potential economic commodities; (2) a spatial and genetic association between the mineralisation and iron silicate and iron oxide gangue minerals (i.e. *not* an iron oxide or iron oxide-apatite deposit with anomalous copper and gold; cf. Williams 2010); (3) hydrothermal mineralisation style (i.e. replacement lenses, zones and veins); (4) sulphur mainly present in the S²⁻ oxidation state; (5) clear structural controls on the mineralisation; and (6) a temporal association with magmatism and deformation, but no obvious causative intrusion.

Pervasive and vein-related potassic-ferroan ± calcic alteration occurs variably in the NDZ domain and adjacent areas and is associated with IOCG and related mineralisation (cf. McGimpsey 2010, Lynch et al.

2015). At the “old” Nautanen deposit (Fig. 17), characteristic almandine porphyroblasts are associated with amphibole + biotite + magnetite + sericite \pm K-feldspar \pm sulphide and tourmaline \pm quartz \pm sulphide banding, patches and veins. Textural relationships suggest garnet growth slightly predated the main-stage alteration and mineralisation event (cf. Waara 2015). Late-stage epidote \pm quartz \pm carbonate alteration also occurs. Chalcopyrite with lesser bornite and chalcocite are the main copper-bearing minerals and are typically associated with pyrite, pyrrhotite, magnetite and tourmaline. Quartz-amphibole \pm tourmaline veins containing pyrite and minor chalcopyrite post-date the main-stage disseminated and micro-fracture type sulphide mineralisation. Gold generally occurs as inclusions and segregations in pyrite, chalcopyrite, bismuth-bearing phases and locally galena (e.g. Sammelin 2011, Bark et al. 2013).

Comparison of “least altered” metavolcanosedimentary rocks from the eastern volcanosedimentary domain with NDZ-hosted, pervasively altered, mylonitic rocks shows that the latter are relatively enriched in copper, silver, gold, iron, molybdenum, barium, manganese and tungsten Cu, Ag, Au, Fe, Mo, Ba, Mn and W. Likewise, the tendency for K/Na ratios to increase when stepping into the NDZ domain reflects the association between potassic alteration and copper-gold-iron enrichment (cf. Lynch et al. 2015). These features are diagnostic of typical geochemical affinities and metal abundance correlations associated with IOCG-style mineralisation, particularly deposits hosted by intermediate to felsic igneous rocks in continental settings (cf. Barton 2014).

Uranium-lead LA-ICP-MS titanite and allanite ages ranging from c. 1.79 to 1.78 Ga for hydrothermal alteration at the Nautanen copper-gold deposit have been reported (Smith et al. 2009). These dates provide a temporal and inferred genetic link between the mineralisation and deformation, fluid mobilisation and late-orogenic granitic magmatism.

2.2.5. Lithologies in the Muorjevaara group

The following petrographic descriptions complement previous accounts by Zweifel (1976), Ros (1980), Monro (1988) and Lynch et al. (2015).

In general, four lithological units are identified in the rocks of the Muorjevaara groups (cf. Fig. 17). They are (1) predominantly intermediate metavolcaniclastic rocks; (2) volcanogenic (epiclastic) metasedimentary rocks; (3) mica schist horizons; and (4) amphibolitic schist (mafic metavolcaniclastic rocks). Units 1 and 2 are the most common units across the Nautanen area.

Units 1, 2 and 3 represent compositionally similar lithologies (mainly basaltic andesitic to andesitic) and are primarily distinguished based on textural, structural and deformation intensity criteria. In the NDZ domain, deformed and altered feldspar-biotite-amphibole schist (locally gneiss) is inferred to represent a composite intermediate metavolcaniclastic unit, probably consisting of a combination of units 1 to 3.

The bedrock in the NDZ domain is affected by relatively intense shearing, transposition and metasomatic-hydrothermal alteration. Thus, primary lithological characteristics are commonly obscured or masked by overprinting processes and remain somewhat equivocal. Nevertheless, local low-strain and “least altered” zones provide some petrographic insights into the primary nature of the rocks in this area and facilitate comparisons with the rocks in the other two lithological-structural domains.

The predominant lithology is a medium to dark grey, fine-to medium-grained, well-sorted and internally laminated, feldspar-biotite \pm amphibole schist to gneiss. Locally, more weakly laminated varieties have a recrystallised, granoblastic appearance and appear more feldspar-rich. Inferred bed forms (although rarely preserved) are approximately 0.1–0.5 m thick and are generally laterally continuous, sub-parallel and planar. In general, anhedral and platy biotite and lesser amphibole grains are aligned parallel to the dominant penetrative cleavage and intergrown with feldspar. Local horizons containing coarser (felsic) clasts (approximately 5–15 mm), elongate and stretched lensoidal patches (remnant clasts?), and composite,

aggregated fragments (lithic clasts?) occur throughout the area. These features are consistent with a possible volcanoclastic derivation. Locally, the schist grades into more quartz-rich sections consisting of fine-grained, granular and anhedral quartz, forming banded zones and aggregated, irregular to sub-rounded, lithic (?) clasts.

Throughout the NDZ domain, the bedrock displays moderate to intense penetrative foliation and shows variable degrees of metasomatic-hydrothermal alteration. Dark to pinkish-red, medium-to coarse-grained garnet porphyroblasts occur locally. These appear to pre-date the main alteration assemblage and copper mineralisation event. Locally, the garnets form quite large crystals up to 10 cm in diameter or aggregated clusters. They are typically of the spessartine-almandine variety, appear to be mainly syn-kinematic, and form disseminated grains or clusters associated with amphibole + biotite + magnetite veins and patches.

The most important belt- to deposit-scale alteration assemblage affecting NDZ rocks is a moderate to intense amphibole + biotite + K-feldspar + magnetite \pm garnet \pm sericite \pm pyrite \pm chalcopyrite assemblage. Typically, it has developed along seams, linear zones and irregular veins trending parallel to the transposed foliation. This inferred “syn-mineralisation” assemblage overprinted an earlier pervasive scapolite \pm albite assemblage. Zones and bands of tourmaline \pm quartz alteration represent a paragenetically later assemblage.

Syn-mineralisation magnetite typically occurs as fine-to medium-grained, anhedral tabular and elongate platy grains within foliation planes. It also forms fracture-filling inclusions and patchy rims around garnet porphyroblasts. Consequently, the bedrock throughout the domain is magnetically anomalous. Locally, feldspar-rich metavolcanoclastic rocks display reddish-pink patches and irregular zones indicative of “red rock”-type hematite staining and iron exsolution affecting alkali feldspar. A late-stage epidote \pm quartz \pm carbonate alteration assemblage is also present and more typically overprints red rock (K-feldspar-altered) zones. Secondary hematite-goethite commonly replaces magnetite, while chlorite replaces biotite and is associated with epidote.

2.2.6. Structures in the eastern volcanosedimentary domain

The eastern volcanosedimentary domain (EVD, cf. Fig. 17) contains a variety of superimposed ductile and brittle structures recording a protracted, multiphase deformation history. The most commonly observed fabric is a variably intense, planar penetrative foliation, here designated S1. This foliation is generally roughly northwest to north-northwest-aligned, moderate to steeply southwest to west-southwest-dipping, and tends to parallel primary bedding, laminae and compositional banding. S1 has a similar orientation to planar foliations in EVD-hosted dioritic intrusions. The intensity of S1 varies between outcrop and lithology, and where it forms a schistose to gneissic texture, S1 may represent a composite transposed foliation. Locally, S1 is axial planar to tight to isoclinal, asymmetric, intrafolial F1 folds.

The EVD is also characterised by tight to isoclinal folding of primary bedding, compositional banding, alteration banding and foliations. To the immediate east of the NDZ, the predominant structure is a distinct, large-scale, asymmetrical and overturned syncline (cf. Fig. 17). The western limb appears to be truncated roughly north-northwest-trending, shear zones and faults related to the NDZ. Fold vergence is typically eastward, with axial surfaces roughly north to north-northwest-aligned and generally dips steeply towards the west. The fold shapes are non-cylindrical and fold axes are locally curvilinear. The larger-scale fold structures are accompanied by parasitic, asymmetric small-scale folding. In the southern part of the EVD, parasitic fold axes commonly plunge at moderate angles towards the south-southwest, whereas in the north, fold axes have doubly plunging geometries (typically roughly northwest and southeast). Mineral lineations are gently plunging and have variable orientations.

A crenulation cleavage, here designated S2, also occurs in the EVD. It is generally roughly north to north-northeast-aligned, sub-vertical, with axial planar to gentle, upright F2 folds, plunging moderately roughly

south to south-southeast. The S2 cleavage is associated with L2 intersection lineations that typically have a moderate plunge to the south and south-southeast, similar to F2 fold axes. Locally, near the hinge zones of larger-scale folds, fairly intense S2–L2 deformation has developed elongated and stretched L-tectonites, which form mullion-like features along bedding surfaces. In eastern limb areas, local bedding plane surfaces with L2 lineations contain slicken-side notches, indicating top-block reverse movement towards the north and north-northwest.

Brittle deformation in the EVD consists of (1) locally developed spaced cleavage and fracture sets that tend to follow earlier planar structures; (2) numerous roughly north-northwest-and east-aligned, generally sub-vertical, amphibole and quartz vein sets, of which the latter are locally sulphide-bearing; and (3) joint sets developed in intrusive rocks. Additionally, discordant roughly north to north-northeast-aligned brittle deformation zones are inferred from aeromagnetic data (cf. Figs. 17, 18). These crosscutting, locally NDZ-related high-strain zones segment the EVD into several localised blocks.

2.2.7. Structures in the Nautanen deformation zone

The Nautanen deformation zone (NDZ) is characterised by a conspicuous roughly north-northwest to northwest- aligned, steep to locally moderate roughly west-dipping, penetrative foliation (S1), with varying but generally strong intensity. Locally, inferred primary bedding, compositional banding and alteration banding are typically transposed into steep orientations parallel to the dominant foliation, and locally produce a composite fabric that may represent several generations of ductile deformation. The dominant shearing direction strikes roughly north-northwest and shows mainly western-block up reverse kinematics and most commonly oblique dextral and less common sinistral components, recorded by asymmetric foliation deflections around garnet porphyroblasts and local asymmetric kink bands.

The predominant north-northwest-trending reverse shear zones within the NDZ are interconnected by roughly north-trending, sub-vertical high-strain zones with mainly dextral kinematics. In general, these secondary zones are interpreted as Riedel shears that formed in the oblique, dextral-reverse shear zone. Additionally, local tensional features such as quartz-filled tension gashes and en-echelon quartz veins occur along the western margin of the NDZ and are mainly orientated north to north-northeast.

Minor asymmetric folding related to shearing is mainly evident from asymmetrically folded hornblende-, magnetite- and epidote-filled veinlets. To the south of the study area, at the Aitik deposit, the reverse shear zones are more north-south orientated and dip moderately towards the west, with distinct roughly west-plunging mineral lineations. Additionally, a set of sub-vertical, north-northeast-trending high-strain zones is observed.

Mineral lineations in the NDZ are defined by stretching of minerals, and their orientations are variable. In general, lineations plunge moderately towards the south and southwest. Local variations, with gentle to horizontal plunges, were also observed.

2.2.8. Structures in the western volcanosedimentary domain

The western volcanosedimentary domain (WVD) is characterised by alternating layers of metasedimentary and metavolcanosedimentary rocks, with a distinct bedding (S0) and parallel foliation (S1) forming a composite S0-1 fabric. Both bedding and the S1 foliation are folded into inclined to overturned asymmetric folds, with open to close interlimb angles. The predominant large-scale structure in the WVD is a repetition of anticlines and synclines, with non-cylindrical, curvilinear fold axis (see Fig. 17). The overall orientation of fold axes is southward with gentle to moderate plunges. Fold axes in the northwest of the WVD appear to be doubly-plunging.

Typically, an axial planar parallel fabric is not observed across the WVD. Nevertheless, a weak foliation or weak-spaced cleavage, here designated S2, could be observed in several outcrops, especially near the NDZ. This S2 fabric clearly overprints the S0-1 foliation obliquely.

Local crenulation lineations, small-scale fold axes and mineral-stretching lineations are orientated sub-parallel to the larger-scale fold axes.

Brittle deformation in the WVD is dominated by a large-scale, northwest-striking fault zone that divides the foliated and folded metavolcanic and metasedimentary rocks to the north from mainly undeformed granites to the south (Fig. 17). The fault zone is characterised by intense fracturing forming distinct topographic depressions.

2.2.9. Geophysics in the Nautanen area

Since the 1960s until today, geophysical investigations were done in the Nautanen region, mostly in the Nautanen deformation zone (NDZ). They comprise airborne magnetic, electromagnetic and radiometric studies, and the data helped to clarify geological units of the NDZ. In addition, detailed ground measurements were done, like, e.g., magnetic- and regional gravity surveys, radiometric and electromagnetic (slingram and VLF) exploration and petrophysical sampling (cf. Lynch & Jönberger 2014, Lynch et al. 2015, 2018a, and references therein). Other geophysical data, like, e.g., data from seismic reflection surveys that should give structural information at larger depth down to several kilometres, are not known of the area.

The NDZ is a wide deformation zone, characteristically delineated on the magnetic anomaly map (Fig. 18), compiled from airborne and integrated ground magnetic survey data. The map clearly shows the power of denser ground surveys in their much better resolution of magnetic signatures. The western volcanosedimentary domain (WVD) of the Nautanen area is in its magnetical features relatively heterogeneous, showing tight, sub-parallel magnetic bands. Magnetic lows mainly reflect metasedimentary or felsic metavolcaniclastic rocks, while banded highs in the magnetic field are due to mafic to intermediate metavolcaniclastic rocks. Even mafic intrusive rocks are highly magnetised (see Table 4). Gravity data of the area, lowering in value towards the west indicate that granitic intrusions may extent to larger depth (Fig. 19). The NDZ correlates with a broad positive gravity anomaly, implying that more mafic rocks (of higher density) are underlying the NDZ. The positive gravity anomaly extends eastwards from the central NDZ towards Snållkok (cf. Fig. 17) where gabbroic rocks are found.

In the eastern volcanosedimentary domain (EVD), magnetic anomalies resemble the pattern found in the WVD, where high-magnetic bands alternate with lower ones. A synformal fold in the southern part of the EVD is imaged in the magnetic anomaly map (Fig. 18). High-magnetic bands can be associated with mafic metavolcaniclastics, whereas areas of lower magnetisation reflect metasedimentary rocks. North of the EVD, a granitic intrusion correlates well with a zone of low gravity. Further south, alternating metasedimentary and metavolcaniclastic rocks cannot be distinguished in their density, but give a surplus in gravity (Table 4).

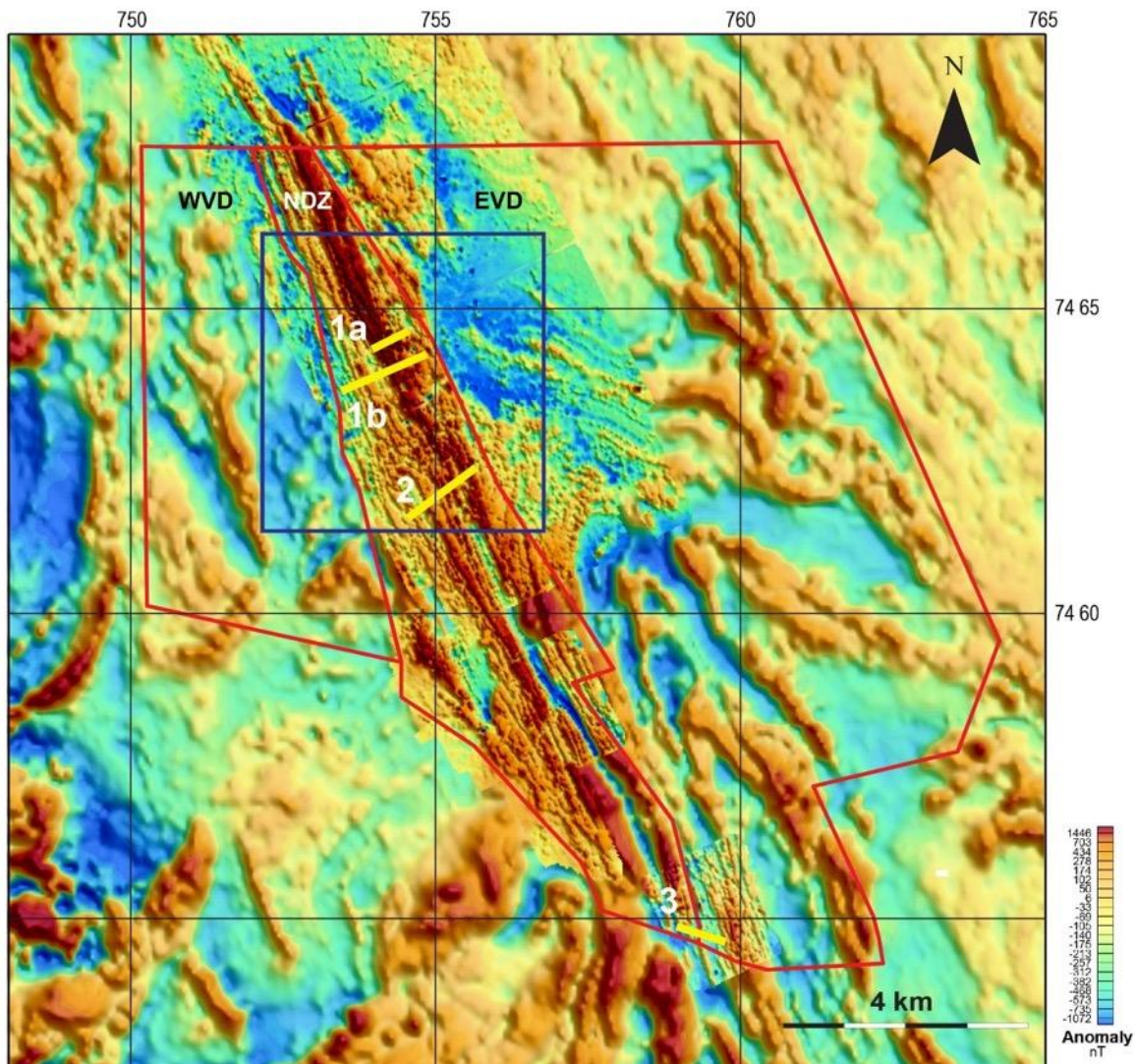


Figure 18. Magnetic anomaly map of the Nautanen area, combined of airborne and ground magnetic total field data (after Lynch et al. 2018a). Coordinate system SWEREF 99 TM in km. Red polygons represent study areas where ground magnetic and VLF data were acquired in recent years, divided into three domains, the western- (WVD) and eastern (EVD) volcanosedimentary domain, and the Nautanen deformation zone (NDZ). Numbers 1a, 1b, 2 and 3 mark profiles discussed in text, relating to Figs. 20, 21. Box in dark blue shows the horizontal extent of the 3D magnetic model presented in Figure 22.

2.2.10. Nautanen – three-dimensional modelling of shallow structures

Three dimensional models of the NDZ were constructed on a smaller scale by inverting ground magnetic data (Lynch et al. 2015, 2018a). The aim was to visualise highly magnetised structures in the sub-surface. Owing to the limited extend of the areas investigated, the magnetic models extend down to a depth of some hundred metres only, which is not the target depth of a CHPM system. But, we present some examples of the modelling attempts here.

The most northerly 3D inversion magnetic model (Fig. 20) was conceived of the Nautanen copper-gold deposit and surrounding area close to profile 1a in Figure 18. Due to the banded highly magnetised structures of the area, susceptibility was constraint to values between 0 and 2 SI units. The cross-section of profile 1b (Fig. 20) shows an overturned, synformal structure in the western part of the profile, with a

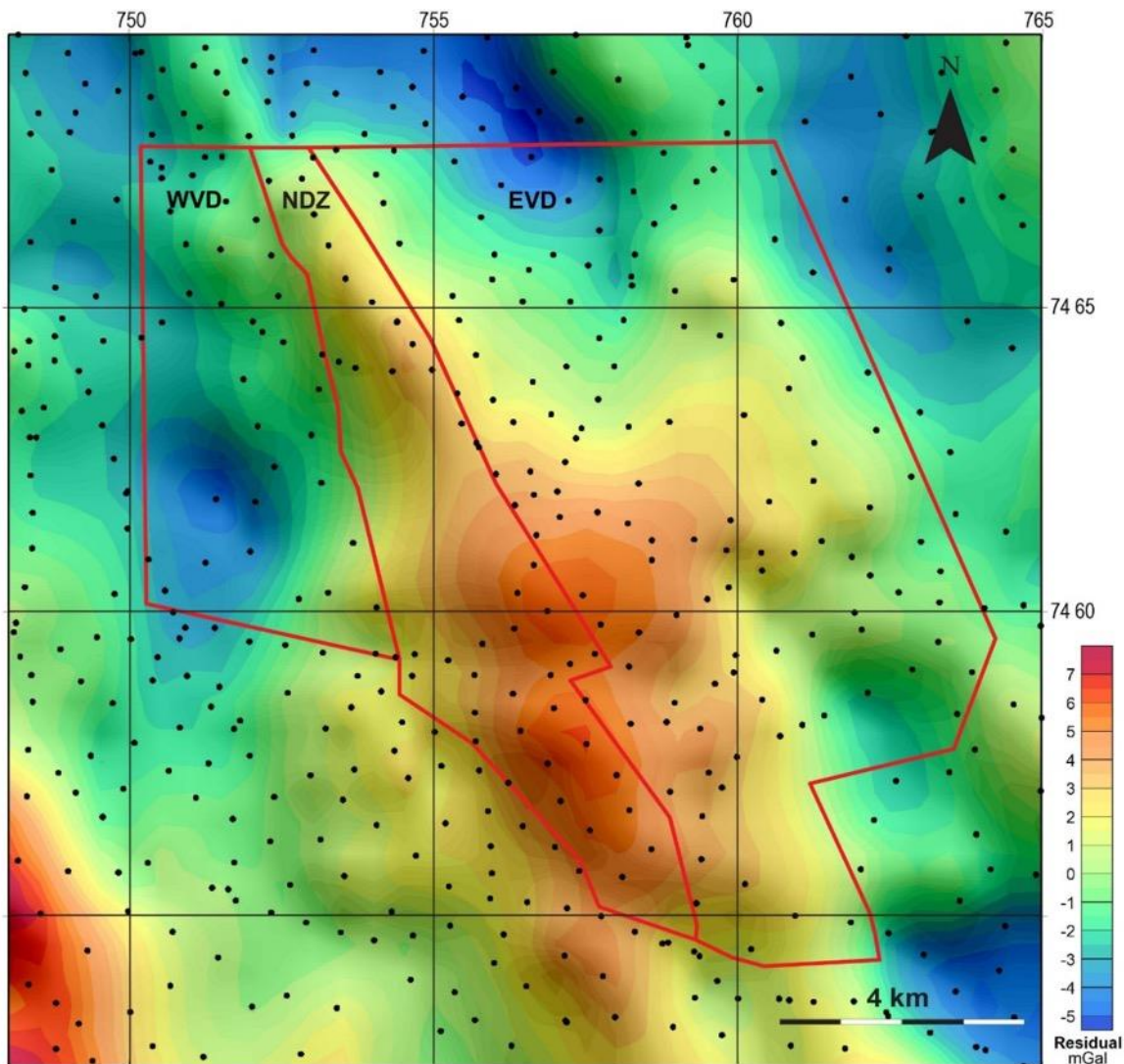


Figure 19. Residual gravity field in the Nautanen area. Black dots show the location of measuring points.

southwesterly dipping axial plane, whereas the magnetic formations on the eastern side dip to the northeast.

Several models were constructed across the NDZ to the south, based on ground magnetic and electrical resistivity (VLF) data. Modelling aimed on visualising the NDZ and bedrock structures (Fig. 20, profiles 1b and 2). However, due to the characteristics of the VLF method, the resolution of resistivity models is limited. Figure 20 shows a cross section (profile 2) through the 3D magnetic susceptibility model, perpendicular to the magnetised structures of the NDZ. Laboratory measurements of rock samples of the area gave a magnetic susceptibility of 0.6 SI units at maximum, but susceptibility of rocks *in-situ* may be higher. Model susceptibility in the inversion was constraint to 0.0001 to 1 SI units. The cross section reveals a magnetic structure in the Southwest, dipping moderately to the southwest. A sudden break in the pattern occurs in the centre of the profile. East of this break, the highest magnetised part of the NDZ can be identified as a synformal pattern continuing towards northeast. From this area, minor magnetite rich structures are likely to extend linearly upwards towards the surface.

Further 8 km south-southeast along the NDZ and predominantly on its eastern side, a broad conductive zone can be seen in the western part of the profile section shown in Figure 21, corresponding to a low in the

magnetic field. In the east, a resistive feature with a relatively shallow south-easterly dip correlates with bands of higher magnetisation as identified in the map of Figure 18.

2.2.11. Three-dimensional geophysical modelling of magnetite-banded rocks in the NDZ

Airborne magnetic data were inverted to a larger 3D model of the deformed and altered bedrock in the NDZ, allowing magnetic susceptibility of the rock to vary (Fig. 22). The model is represented by two surfaces of equal magnetic susceptibility (isosurfaces), highlighting their general 3D form and orientation. Geologically, the isosurfaces can be viewed as proxies for magnetite-alteration and effects of deformation enhanced fluid flow within the NDZ.

In the southern part of the model, the isosurface of lower susceptibility (0.18 SI units, cyan colour) dips to the west-southwest. North of northing grid line 7464000, both the lower and the higher (0.3 SI units, grey colour) isosurfaces tend to have an opposing dip towards the east-northeast. In the aeromagnetic data (Fig. 20, profile 1b), a possible northwest striking deformation zone transects the 7464000 northing grid line. Thus, the lateral change in dip of the isosurface may reflect the primary structural character of the Nautanen deformation zone or later deformational effects that caused a degree of structural re-orientation. Geologically, it cannot be excluded that even deeper levels of the bedrock have a magnetic signature, i.e., magnetic susceptibility is increased.

Table 4. Petrophysical properties, i.e., density, magnetic susceptibility and Königsberger ratio Q of different rocks in the Nautanen area. Total number of samples is 267.

Rock type	No. of samples	Density (SI) Mean	Density (SI) Std. dev.	Susceptibility x 10 ⁻⁵ (SI) min	Susceptibility x 10 ⁻⁵ (SI) max	Susceptibility x 10 ⁻⁵ (SI) median	Q-value min	Q-value max	Q-value median
Granite	13	2 612	17	0	3 691	1 544	0.00	0.87	0.07
Metasedimentary rock	16	2 836	98	18	67 510	784	0.00	89.53	0.16
Gabbro-diorite	22	2 903	50	27	19 781	70	0.00	6.81	0.01
Sandstone	24	2 768	74	12	18 660	1 850	0.00	8.37	0.45
Basalt-andesite	56	2 847	76	44	53 060	5 339	0.00	16.00	0.45
Mica schist	22	2 814	100	44	41 430	1 699	0.00	161.80	0.30
Rhyolite-dacite	18	2 708	34	21	10 933	1 801	0.01	1.76	0.26
Amphibolite	23	2 966	79	60	19 031	7 217	0.00	9.27	1.35
Greywacke	28	2 819	92	39	14 740	2 157	0.00	7.18	0.65
Granodiorite	5	2 714	53	21	3 169	1 975	0.00	1.56	0.16
Argillite	40	2 754	112	234	32 378	2 338	0.03	79.69	0.37

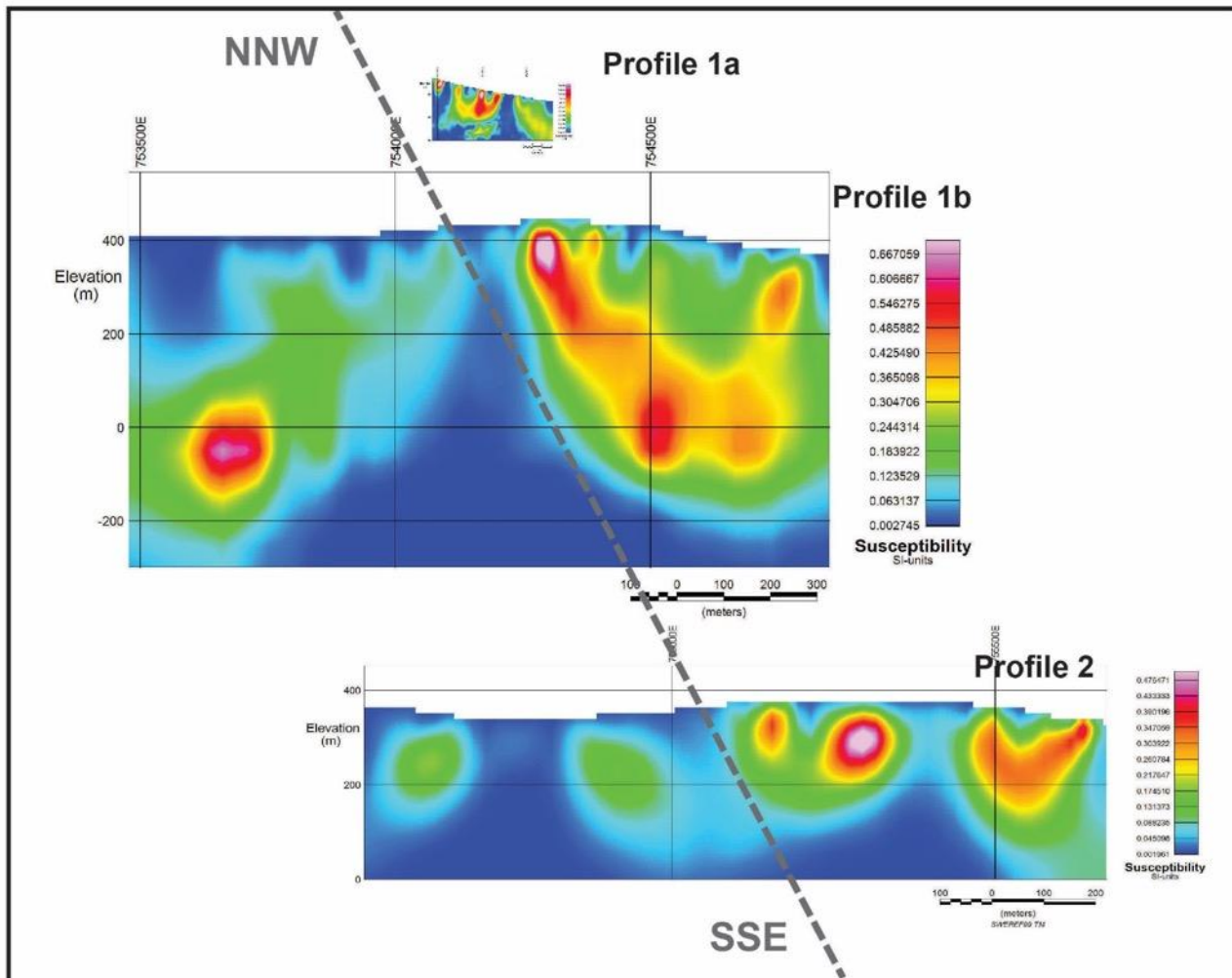


Figure 20. Three cross-sections of magnetic susceptibility of shallow sub-surface structures, taken from 3D inversion models based on ground magnetic data for profiles 1a, 1b and 2 (see fig. 18). The profiles are disposed along the north-northwest–south-southeastern strike of the Nautanen deformation zone, here indicated by the dashed grey line. Profile length in metre, vertical extend in m above sea level. For better orientation, eastern longitude in m according to SWEREF 99 TM annotated.

2.2.12. Natural seismicity

Above, we have introduced the Swedish National Seismic Network (SNSN) and its capabilities. In the last two decades, no local earthquakes were recorded by the network originating from the Nautanen area. But, many blastings from the Malmberget and Aitik mines are found in their archives. As for the Kristineberg area in the Skellefte district, no conclusions can be drawn for the regional stress regime, neither qualitatively nor quantitatively. At the time of writing, owing to an on-going process of legal permitting, we were not able to obtain actual stress data around Nautanen neither from other sources.

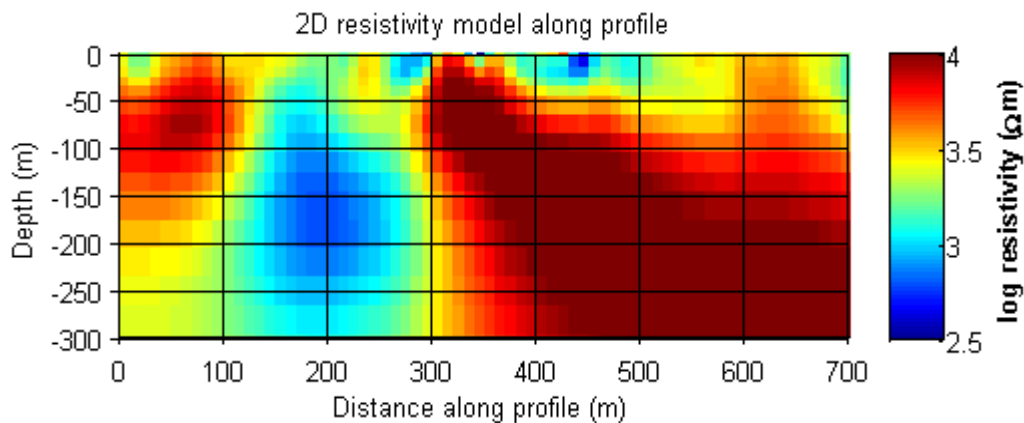


Figure 21. Resistivity cross-section derived by inverting electromagnetic data from VLF measurements along profile 3 in Figure 18. View to the northeast.

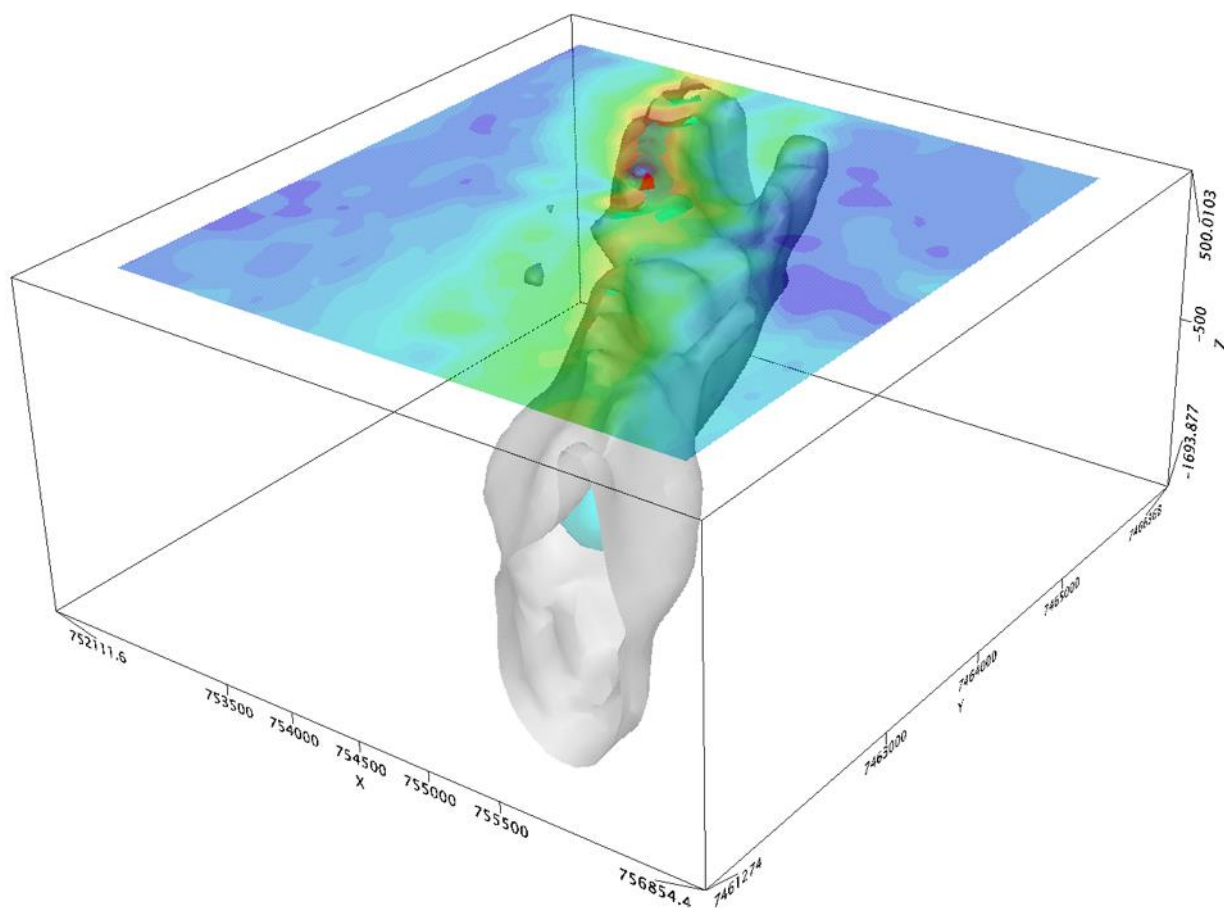


Figure 22. Three-dimensional magnetic susceptibility model for the Nautanen deformation zone (outline marked by dark blue rectangle in Fig. 18). Two isosurfaces coloured in cyan and grey are shown. Total magnetic anomaly field is indicated at the surface (no scale given). View from southeast to northwest. XY-coordinates refer to SWEREF 99 TM, Z is height a.s.l., all in metres.

3. EGS GEOTHERMAL POTENTIAL

3.1. Temperature gradient and heat flow density

Based on temperature measurements in a borehole within the Kristineberg area (Fig. 23, left), the heat flow density was estimated to range between 35 and 50 mW/m². The estimation was based on measured gradients of 0.011 – 0.013 °C/m between 200 and 700 m depth. Parasnis (1975) has estimated corrected heat flow in the Skellefte district at 49 mW/m², based on temperature measurements in boreholes ranging in depth between 365 and 780 m.

Temperature measurements were also made in two boreholes close to the iron ore mine at Kiruna (Fig. 23, right), located about 60 km north of Nautanen. Heat flow density was estimated to range between 35 and 55 mW/m². The estimation was based on measured gradients of 0.013 – 0.014 °C/m for a 500-metre interval. Previous measurements in the iron ore district of Malmberget and Kiruna, with depth ranging from 287 to 1 100 m below ground level, have yielded corrected heat flow density of 51 mW/m² (Parasnis 1981). In addition, measurements have been made in three boreholes inside the iron ore mine at Kiruna (Fig. 23, right). Measurements were made from a level at about 1 200 m below ground surface. The temperature gradients estimated in these boreholes were almost constant at 0.016 – 0.017 °C/m. Heat flow density was calculated to range between 51 and 65 mW/m². Obviously, this estimate indicates a higher geothermal flow compared to the other measurements.

Heat flow density was calculated by using thermal conductivity values between 3.2 and 3.8 W/m K. This interval was assumed to be representative for the bedrock types in the areas. There was no information available to support any correction of the temperature profile.

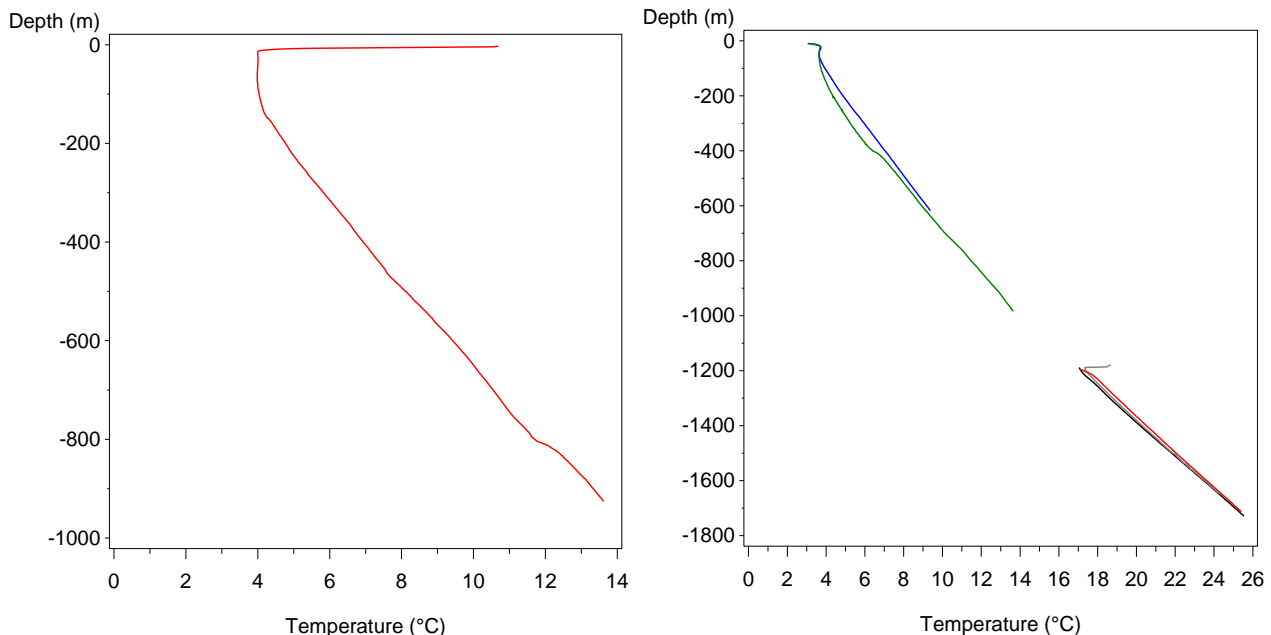


Figure 23. Measured temperature (°C) as a function of borehole depth (in m below ground surface) in the Kristineberg area (left) and in five drill holes located in the Kiruna mining district (right), at about 60 km north of the Nautanen area. Three of the boreholes were measured in the Kiruna iron ore mine at about 1200 m depth. Note different depth and temperature scales in both figures.

When compared with the normal pattern of heat flow density in northern Sweden (Hurter & Haenel 2002), no significant deviation could be found. Estimations of the heat flow, based on the measurement of temperature gradients in the bore holes at Kristineberg and Kiruna could be compared to the map with corrected heat flow density in Scandinavia (Fig. 24, Balling 2013). The map indicates a regional heat flow density of 50 - 60 mW/m².

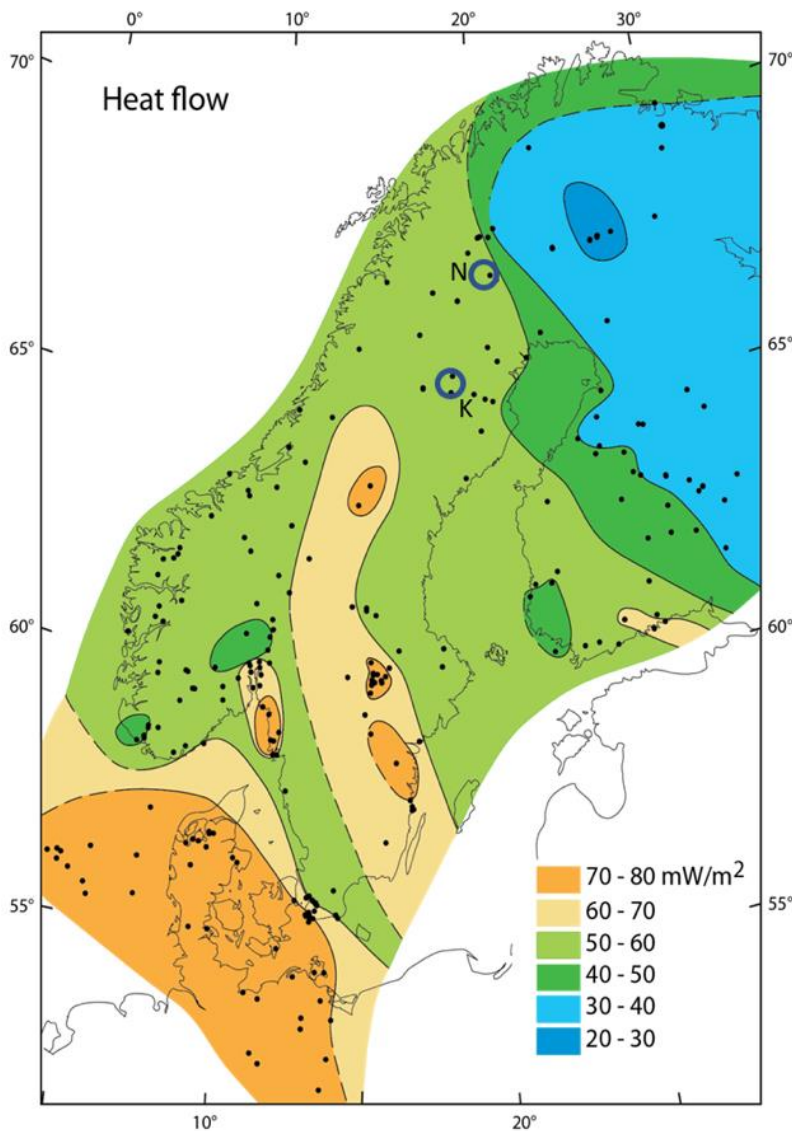


Figure 24. Map with corrected surface heat flow density in Fennoscandia (Balling 2013), based on measurements at more than 250 sites, marked by black dots. K : Kristineberg area, N : Nautanen area.

3.2. Heat production

Heat production of outcrops all over Sweden was estimated using airborne as well as ground based radiometric measurements provided from the gamma radiation database of the Geological Survey of Sweden (Fig. 25, Schwarz et al. 2010). The data from outcrops and site-specific rock types do not indicate any anomalous values in the suggested study areas, Kristineberg and Nautanen. However, in lack of structural

geological data, extrapolation of heat production to deeper levels has not yet been tested. Consequently, heat production at deeper levels could differ considerably when compared to the data from outcrops.

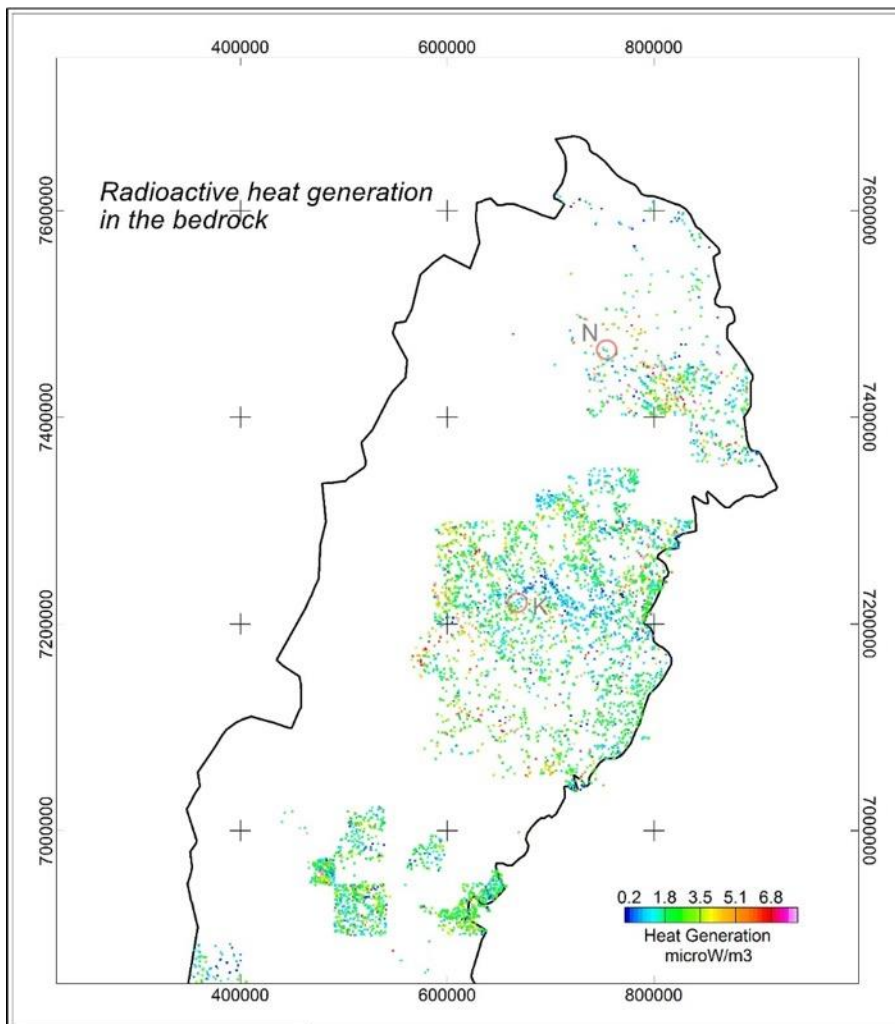


Figure 25. Heat production calculated from airborne radiometric data related to outcrops over northern Sweden (except of the mountain areas), in $\mu\text{W}/\text{m}^3$ (after Schwarz et al. 2010). K : Kristineberg area, N : Nautanen area. Coordinate system is SWEREF 99 TM in m.

3.3. Hydraulic properties, deep fluid flow

There are several reports indicating generally low hydraulic conductivity at deep levels of the Precambrian crystalline bedrock in Sweden. Extensive hydraulic tests were made in several boreholes by the Swedish Nuclear Fuel and Waste Management Company (SKB). In the Äspö area (see Fig. 1), in southern Sweden, the hydraulic conductivity below 650 m depth varies between 10^{-12} and 10^{-7} m/s Sweden (Réhn et al 2008). At deeper levels, about 5 – 10 km, the hydraulic conductivity should be lower, possibly lower than 10^{-8} m/s. These values could probably be used to approximate the hydraulic conductivity at deep levels in the bedrock in Sweden. Trends in hydraulic conductivity down to 2 500 m in the crystalline bedrock have been interpreted by Ericsson et al (2006). At 2 500 m depth the hydraulic conductivity was estimated to about $2 \cdot 10^{-11}$ m/s (Fig. 26). This assessment has been used as a reference for the Kristineberg area (Golder Associates 2017).

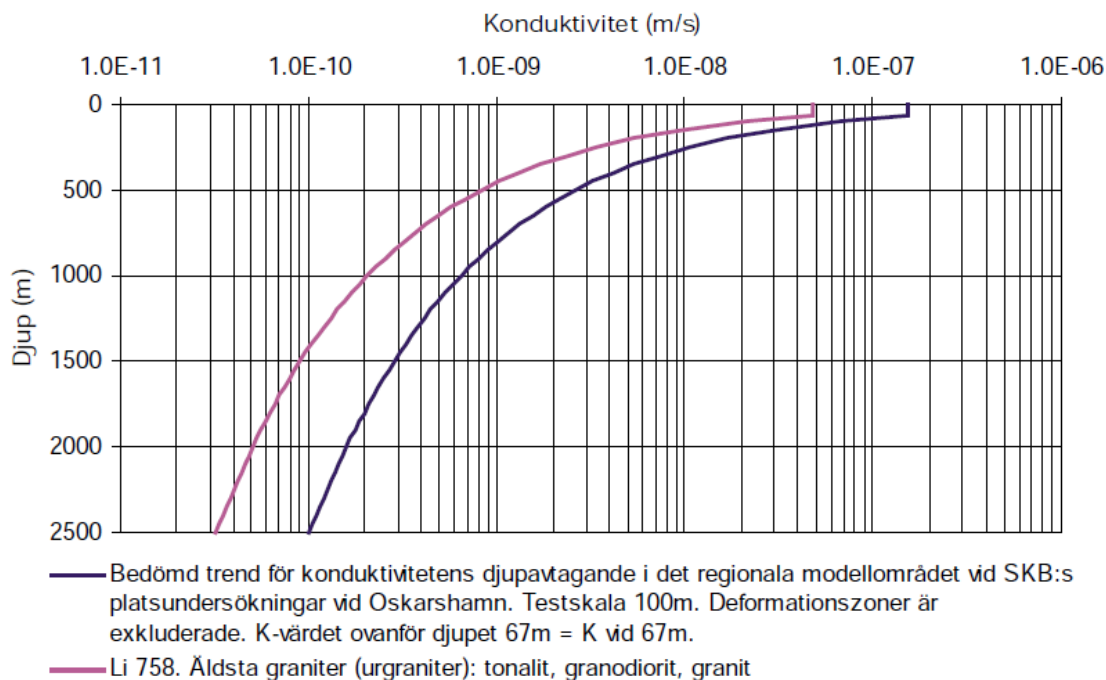


Figure 26. Estimated trends in hydraulic conductivity vs depth in a borehole, meant to represent the Kristineberg area (purple line). The dark blue line indicates hydraulic conductivity at depth close to Oskarshamn in southern Sweden (Ericsson et al. 2006).

About 4 km west of the Kristineberg mine, hydraulic conductivity was measured in 17 boreholes (Golder Associates 2017). A median value of $6.8 \cdot 10^{-8}$ m/s was estimated between the bedrock at surface and an average depth of about 600 m. Extrapolation to depths between 5 and 10 km suggests hydraulic conductivity to decrease to $10^{-10} - 10^{-12}$ m/s. Data from drill core samples from the Kristineberg area indicate a brittle deformation zone which could be important for the interpretation of hydraulic properties.

The fluid flow from deep boreholes could be roughly estimated by using the following assumptions: Considering a hydraulic conductivity between 10^{-12} and 10^{-8} , an estimated open section of 1000 m and a drawdown of the water pile of 300 m, the flow could range from $3 \cdot 10^{-7}$ to $3 \cdot 10^{-3}$ m³/s (Fig. 27). Here, we assume a temperature difference of 100 °C being exploited but considered to be at the very upper limit. With the heat capacity of water of 4.186 MJ/m³, the corresponding extraction of heat from the fluid could be calculated to a minimum value of $1.26 \cdot 10^{-4}$ MW and a maximum of 1.26 MW. This example clearly indicates that the hydraulic conductivity of Precambrian crystalline bedrock at deep levels is a limiting factor for the use of geothermal energy. Moreover, it clearly shows the exigency of hydraulic stimulation of the bedrock to increase fluid flow and to make a CHPM system feasible.

3.4. Fluid composition

Data on fluids, brines and meteoric waters from deep boreholes are generally uncommon, and no available data were found from the Kristineberg and Nautanen areas. For reference purposes, data from the borehole at the Siljan deep drilling site Gravberg (see Fig. 1) could be used to provide an indication of total dissolved solids (TDS) at very large depths. Down to 4 000 m below ground surface, the TDS amount to less than 500 mg/l. Below 4000 m, TDS increase and at about 6000 m a brine with about 150 000 mg/l was found (Juhlin and Sandstedt 1989).

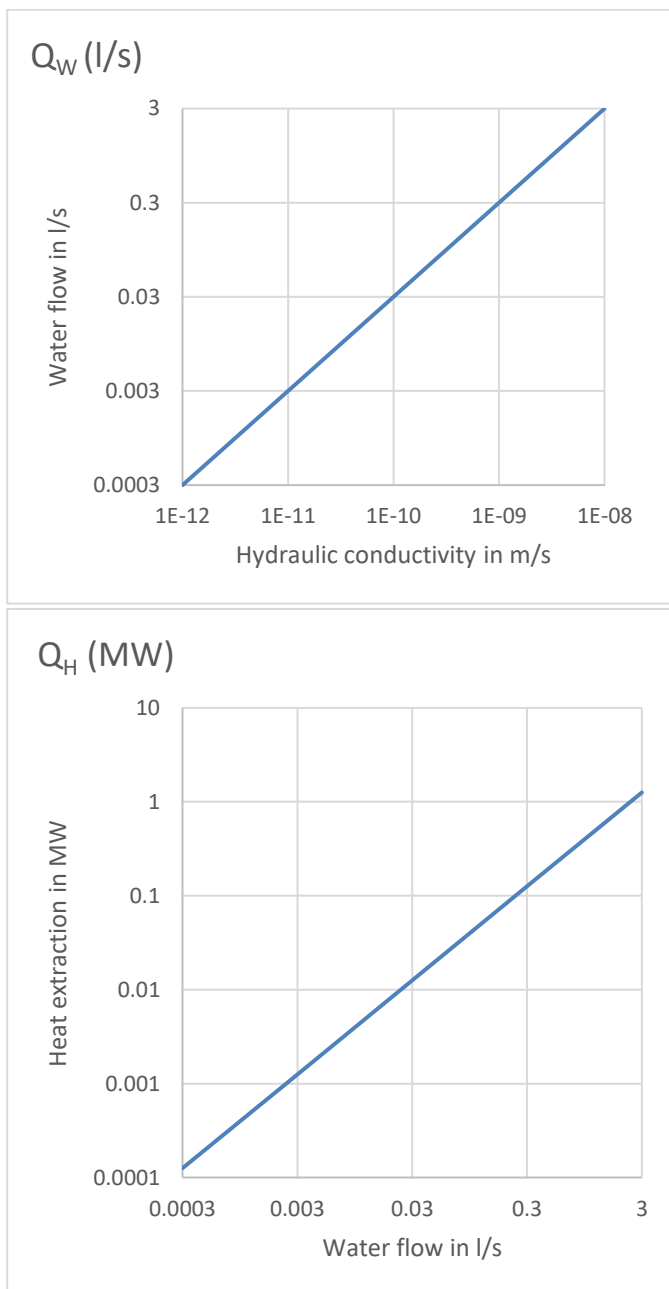


Figure 27. Estimated water flow Q_w (in l/s) as a function of hydraulic conductivity (in m/s) (top) and heat extraction Q_H (in MW) as function of water flow (in l/s) (lower).

Water samples were chemically analysed from nine boreholes nearby the Kristineberg area, representing depths from the ground surface down to about 600 m (Golder associates, 2017). The analysed elements had no exceptional concentrations when compared to regional data of groundwater chemistry in the crystalline bedrock (Geological Survey of Sweden 2013).

3.5. Mineral stability

In this study, we have identified mining areas as being suitable for the challenging future technology, *Combined Heat, Power and Metal extraction from ultra-deep ore formations* (CHPM). The CHPM concept proposes establishing an Enhanced Geothermal System in a metal-bearing geological formation, that will allow the production of energy and metals. The technique under development is meant to be applicable in any crustal environment, given that temperature at depth is not less than 140 °C, metals exist in some form, and the mobility of fluids is enough or can be enhanced.

For the Earth's crust in northern Sweden, temperatures of about 140 °C imply a depth of at least 7 km. Lithostatic pressure at these depths can be assumed to be about 2 kbar. Considering leaching of metals from such depths, one must consider that minerals, as for example copper sulphides, silver sulphides, sulpho salts, antimon phases like stibnite, tellurides and selenites can be altered, replaced or transformed (phase transition).

3.6. A case study in short: The st1 project

In our simple calculations above we have shown, that extracting heat from deeper crystalline rocks by establishing an *Enhanced Geothermal System* (EGS) could be of interest. However, it requires hydraulic conductivity to be improved. Finland, the eastern neighbor country of Sweden, and geologically also part of the Svecokarelian orogen, at the time of writing, is preparing for its first deep EGS in Espoo, close to Helsinki (Saarno 2019, St1, project website). The investigations and drillings there can help to shed some light on the physical properties and the state of the bedrock, which is comparable to the bedrock in the Kristineberg and Nautanen areas. The deep st1 project aims on establishing an EGS only, with the rock volume and temperatures encountered less than those needed for establishing a CHPM system. But, the knowledge already gained and coming lessons to be learned from this project can give valuable information for the further development of the CHPM technique.

The planned geothermal plant for urban district heating will use two boreholes with a maximum (measured) depth of 6 400 m. The deeper one of these holes was drilled already, having a true depth of 6100 m, where bottom hole temperature reaches 120 °C. This wellbore is meant to be the production hole. According to project targets, when completed, the heating plant is estimated to produce about 40 MW_h by extracting hot fluids at a temperature of about 115 °C (Saarno 2019).

During summer of 2018, the first hole was used for stimulation experiments. Water at high pressure of 60 to 90 MPa was injected at an interval of true depth of 5500 to 6100 m, split up into five sections (S1 – S5, see Fig. 28), to increase hydraulic conductivity of the bedrock. The stimulation was injection rate-controlled, with flow rates varying at discrete levels to keep microseismicity at a low level (Leary 2018, Kwiatek et al. 2019). For 49 days, 400 – 800 l/min of water, a total of 18160 m³ was fed into the basement rocks.

As experienced elsewhere (e.g., Diehl et al. 2017), controlling injection-induced seismicity is of utmost importance for public acceptance of energy projects using EGS. Therefore, a year ahead of starting drilling operations, a network of geophones was installed in the area at surface and in boreholes to monitor natural seismicity. When stimulating the bedrock hydraulically, seismic monitoring was performed with a 24-station borehole seismometer network: Additionally, 14 strong-motion seismometers were installed at critical infrastructure sites nearby (Kwiatek et al. 2019). The instruments were recording micro-seismic events due to the influx of water into the bedrock, when opening fissures and fractures. Thus, seismic events recorded during stimulation should allow to monitor connectivity pathways due to the flow of water. The maximum strength of seismic events during stimulation was 1.9 in magnitude on the Richter scale. For security reasons, set by local authorities, the limit for an immediate stop of all operations was set to a magnitude of 2.5 (Saarno 2019). A total of 43882 earthquakes induced were measured during a period covering the time of stimulation

and 1 week after. When the analysis of seismic events recorded will be completed, presumably in late 2019, the second borehole will be drilled down to about 5500 m in depth. Directed into the zone where water flow should be increased, this wellbore will be used for reinjecting the thermal water after heat extraction.

The Espoo on-site experiments can be summarised as follows (Leary 2018): The fluid stimulation of the crystalline rock at 5500 to 6100 m depth did not produce pipe-like flow structures, as implied by spatially-uncorrelated crustal flow properties. Rather, water injection was reactivating fossilised spatially-correlated flow structures, attested by a distribution of low magnitude seismic slip events independent of fluid injection points. An EGS programme of wellbore-centric fluid stimulation appears to be feasible for deep crystalline rock. Leary (2018) analysed the thermal energy to be extracted from a 1000 m wellbore, where crustal temperature is about 100 °C and well- to wellbore distance is about 50 m. The thermal energy output of such a system is determined to about 10 MW_h for a period of about 30 years. This amount of heat extractable is four times less than the value of the official project target (Saarno 2019).

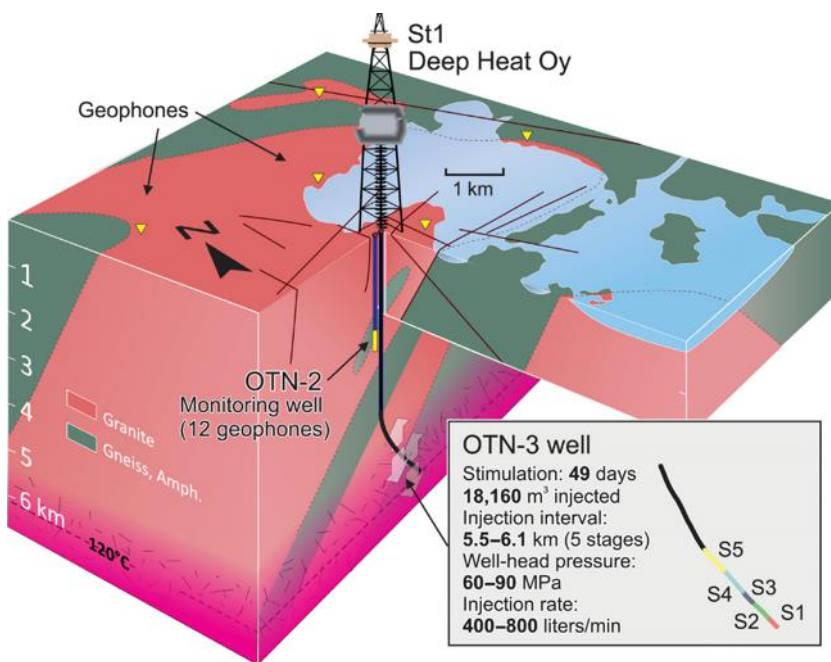


Figure 28. Sketch of the first deep Enhanced Geothermal System (EGS) under construction in southern Finland, at Espoo, close to Helsinki, planned for urban heating (Kwiatk et al. 2019). Drilling of the production borehole was finished in 2018. The bedrock was hydraulically stimulated at depth between 5500 to 6100 m. Induced seismicity was surveyed by a network of 38 geophones installed either in boreholes or on surface (Saarno 2019). The insert shows the location of stimulation stages S1 to S5 into the bottom open hole section and basic stimulation parameters. Note: Geologically, southern Finland and most of northern Sweden belong to the Svecokarelian orogen, i.e., crustal structures and conditions are comparable, and analogies may be drawn for the bedrock in the Kristineberg and Nautanen areas.

4. CONCLUDING REMARKS

The CHPM2030 project requires envisaging structures and lithologies in complex environments at depth down to 7 km. Predicting fracture geometry and permeability at depth in the crystalline bedrock is a crucial point as well and highly challenging. Further intensive multi-disciplinary studies must be considered, e.g., three-dimensional electromagnetic and seismic surveys, as well as better predictions of temperature, heat flow and permeability at depth. The 3D integration of geological and geophysical results will then better allow for planning and conducting of exploration and possibly later-on production drillings.

The ore deposits of Kristineberg and Nautanen originally formed at the Earth's surface or at some depth in the crust have a complex structure. We have identified the mineralised bedrock volumes around these deposits as possible candidates for the challenging future technology, *Combined Heat, Power and Metal extraction from ultra-deep ore formations* (CHPM). The generally low geothermal gradient being of about 16 °C/km in the investigated ore districts will allow for low- to mid-enthalpy enhanced geothermal systems as part of a possible CHPM unit.

ACKNOWLEDGEMENTS

We thank our colleagues at Uppsala and Luleå universities, Boliden Mines and the Geological Survey of Sweden for valuable input to this report. Tobias B. Weisenberger is thanked for reviewing this report.

REFERENCES¹

- Aastrup, M., Thunholm, B., Johnson, J., Berntell, A. & Bertills, U., 1995: Groundwater Chemistry in Sweden. *Swedish EnvironmentAal Protection Agency, Report 4416*, 52 pp.
- Abtahi, S.M., Pedersen, L.B., Kamm, J. & Kalscheuer, T., 2016: Extracting geoelectrical maps from vintage very-low-frequency airborne data, tipper inversion, and interpretation: A case study from northern Sweden. *Geophysics* 81, B135–B147
- Ahl, M., Bergman, S., Bergström, U., Eliasson, T., Ripa, M. & Weihed, P., 2001. Geochemical classification of plutonic rocks in central and northern Sweden. *Sveriges geologiska undersökning, Rapporter och meddelanden* 106, 82 pp.
- Ahlbom, A., Olsson, O. & Sehlstedt, S., 1995: Temperature Conditions in the SKB Study Sites. *SKB Technical report TR-95-16*. 19 pp.
- Ahmadi, O., Juhlin, C., Malehmir, A. & Munck, M., 2013: High-resolution 2D seismic imaging and forward modeling of a polymetallic sulfide deposit at Garpenberg, central Sweden. *Geophysics* 78: B339–B350.
- Albino, B. & Weihed, P., 1997: Au-deposits. In P. Weihed & T. Mäki (eds.): Volcanic hosted massive sulphide deposits and gold deposits in the Skellefte district, Sweden and western Finland. Research and exploration - where do they meet? 4th Biennial SGA meeting, august 11–13, 1997, Turku Finland, excursion guidebook A2. Geologian tutkimuskeskus, Opas - *Geological survey of Finland Guide* 41, 36–42.
- Allen, R. L., Weihed, P. & Svenson, S.-Å., 1996: Setting of Zn-Cu-Au-Ag Massive Sulfide Deposits in the Evolution and Facies Architecture of a 1.9 Ga Marine Volcanic Arc, Skellefte District, Sweden. *Economic Geology* 91, 1022–1053.
- Alm, P.-G. & Bjelm, L., 2006: Proceedings, Thirty-first Workshop on Geothermal Reservoir Engineering, Stanford University, Stanford, CA, 30 January – 1 February 2006. *SGP-TR-179*, 6 pp.
- Årebäck, H., Einarsson, H., Fagerström, P. & Sandström, B., 2000: Nature of recent Cu-Au and Zn discoveries at the Kristineberg Cu-Zn sulfide deposit, Skellefte district, Sweden. Abstract – *The 24th Nordic Geological Winter meeting 2000, Trondheim, Norway*, 182.
- Årebäck, H., Barrett, T.J., Abrahamsson, S. & Fagerström, P., 2005: The Paleoproterozoic Kristineberg VMS deposit, Skellefte district, northern Sweden, part I: Geology. *Mineralium Deposita* 40, 351–367.
- Babel Working Group 1990. Evidence for early Proterozoic plate tectonics from seismic reflection profiles in the Baltic shield. *Nature* 348, 34–38.
- BABEL Working Group, 1993: Integrated seismic studies of the Baltic shield using data in the Gulf of Bothnia region. *Geophys. J. Int.* 112, 305–324.
- Balling, N., 2013: *The Lithosphere Beneath Northern Europe: Structure and Evolution Over Three Billion Years: Contributions from Geophysical Studies*. Doctoral Dissertation, Aarhus University, 191 pp.
- Bark, G., Wanhainen, C. & Pålsson, B.I., 2013: Textural setting of gold and its implications on mineral processing: preliminary results from three gold deposits in northern Sweden. *Proceedings of the 12th SGA Biennial Meeting, Uppsala* 1, 302–305.
- Barton, M.D., 2014: Iron oxide (-Cu-Au-REE-P-Ag-U-Co) systems. In H. Holland & K. Turekian (eds.): *Treatise on Geochemistry*. Elsevier, 2nd edition, volume 13, 515–541.
- Barrett, T.J. & MacLean, W.H., 1999: Volcanic sequences, lithogeochemistry, and hydrothermal alteration in some bimodal volcanic-associated massive sulfide systems. In C.T. Barrie & M.D. Hannington (eds.): Volcanic-associated massive sulfide deposits: processes and examples in modern and ancient environments. *Reviews in Economic Geology* 8, 101–131.
- Bastani, M., Antal Lundin, I., Wang, S. & Bergman, S., 2018: Imaging deeper crustal structures by 2D and 3D modelling of geophysical data. Examples from northern Norrbotten. In S. Bergman (ed.): *Geology of the Northern Norrbotten ore province, northern Sweden. Rapporter och Meddelanden* 141, Sveriges geologiska undersökning, 341–359.
- Båth, M. & Tryggvason, E., 1962: Deep seismic reflection experiments at Kiruna. *Geofisica Pura e Applicata* 51.

¹ With additional literature, not cited in text.

- Bauer, T. 2013: *The crustal architecture of the central Skellefte District, Sweden – structural analysis, setting of VMS deposits and 3D-modelling*. PhD thesis, Luleå University of Technology, Sweden, 142 pp.
- Bauer, T., Skyttä, P., Allen, R.L. & Weihed, P., 2009: 3-D modelling of the Central Skellefte District, Sweden. Smart science for exploration and mining: *Proceedings of the 10th biennial SGA meeting*, Townsville, Australia, 394–396.
- Bauer, T., Tavakoli, S., Dehghannejad, M., Garcia, M. & Weihed, P., 2010: 4-dimensional geological modelling of the Skellefte district, Sweden. *The international archives of the photogrammetry, remote sensing and spatial information sciences*. XXXVIII-4., 93–96.
- Bauer, T.E., Skyttä, P., Tavakoli, S., Dehghannejad, M. & Weihed, P., 2011: *From deposit to regional scale: 4-dimensional geological modeling in the Skellefte Mining District, Sweden*. 3D@GEUS.DK, International workshop on 3D Geological Modeling, Copenhagen, Denmark.
- Bauer, T.E., Skyttä, P., Hermansson, T. & Weihed, P., 2012: *The comparison of ore body shapes and regional deformation patterns as a base for prospectivity mapping in the Skellefte Mining District, Sweden*. Mineral resources potential maps workshop, Nancy, France.
- Bauer, T.E., Paulik, H., Kathol, B. & Pitcairn, I. (eds.), 2013: The Skellefte district, volcanostratigraphy and structures related to Palaeoproterozoic base metal deposits. *Excursion guidebook SWE1, 12th Biennial SGA Meeting, Uppsala*, Sveriges geologiska undersökning, 68 pp.
- Bauer, T.E., Skyttä, P., Hermansson, T., Allen, R.L. & Weihed, P., 2014: Comparison of provenance, ore body shape and regional deformation patterns of VMS deposits for mapping the prospectivity in the Skellefte district, Sweden. *Mineralium Deposita* 19, 555–573.
- Bauer, T.E., Skyttä, P., Hermansson, T., Dehghannejad, M. & Tavakoli, S., 2015: The Skellefte District. In P. Weihed (ed.): *3D, 4D and Predictive Modelling of Major Mineral Belts in Europe*. Mineral Resource Reviews, Springer International Publishing Switzerland, 93–121.
- Berggren, M., 1998: *Hydraulic conductivity in Swedish bedrock estimated by means of geostatistics. A study based on data recorded in the Archive on Wells at the Geological Survey of Sweden*. Royal Institute of Technology, Dept. Civil & Environmental Engineering. Thesis Report, Series 1998:9, 48 pp.
- Bergman Weihed, J., 1997: Regional deformation zones in the Skellefte and Arvidsjaur areas. *Sveriges geologiska undersökning. Final research report of SGU-project 03-862/93*, 39 pp.
- Bergman Weihed, J., 2001. Palaeoproterozoic deformation zones in the Skellefte and Arvidsjaur areas, northern Sweden. In P. Weihed (ed.): *Economic Geology Research 1. Sveriges geologiska undersökning C 833*, 46–68.
- Bergman, S., 2018: Regional geology of northern Norrbotten County. In S. Bergman (ed.): *Geology of the Northern Norrbotten ore province, northern Sweden. Rapporter och Meddelanden 141*, Sveriges geologiska undersökning, 9–17.
- Bergman, S., Kübler, L. & Martinsson, O., 2001: Description of regional geological and geophysical maps of northern Norrbotten County (east of the Caledonian orogen). *Sveriges geologiska undersökning Ba 56*, 110 pp.
- Bergman, S., Martinsson, O. & Persson, P.-O., 2002a: U-Pb zircon age of a metadiorite of the Haparanda suite, northern Sweden. In S. Bergman (ed.): *Radiometric dating results 5. Sveriges geologiska undersökning C 834*, 6–11.
- Bergman, S., Persson, P.-O. & Kübler, L., 2002b: U-Pb titanite and zircon ages of the Lina granite at the type locality NW of Gällivare, northern Sweden. In S. Bergman (ed.): *Radiometric dating results 5. Sveriges geologiska undersökning C 834*, 12–17.
- Bergman, S., Billström, K., Persson, P.-O., Skiöld, T. & Evins, P., 2006: U-Pb age evidence for repeated Palaeoproterozoic metamorphism and deformation near the Pajala shear zone in the northern Fennoscandian Shield. *GFF* 128, 7–20.
- Bergman, S., Weihed, P., Martinsson, O., Eilu, P. & Iljina, M., 2007: Geological and tectonic evolution of the northern part of the Fennoscandian Shield. In V.J. Ojala, P. Weihed, P. Eilu & M. Iljina (eds.): *Metallogeny and tectonic evolution of the Northern Fennoscandian Shield: Field trip guidebook. Geological Survey of Finland, Guide 54*, 6–15.
- Bergman, S., & Stephens, M.B., Anderson, J., Kathol, B. & Bergman T., 2012: Bedrock map of Sweden, scale 1:1 million. *Sveriges geologiska undersökning K 423*.
- Bergström, U., 2001. Geochemistry and tectonic setting of volcanic units in the northern Västerbotten county, northern Sweden. In Weihed P. (ed.). *Economic Geology Research 1. Sveriges geologiska undersökning C 833*, 69–92.
- Bergström, U. & Sträng, T., 1999: Bedrock map 23I Malå NV, NO, SV, SO, scale 1:50 000. *Sveriges geologiska undersökning Ai 114–117*.

- Bergström, U., Billström, K. & Sträng, T., 1999: Age of the Kristineberg pluton, western Skellefte District, northern Sweden. In S. Bergman, (ed.): Radiometric dating results 4. *Sveriges geologiska undersökning C 831*, 7–19.
- Bergström, U., Antal Lundin, I., Winnes, K. & Weihed, P., 2003: Bedrock map 23J Norsjö NV, NO, SV, SO, scale 1:50 000. *Sveriges geologiska undersökning Ai 174–177*.
- Carlson, C.J., 2000: Iron oxide systems and base metal mineralisation in northern Sweden. In T.M. Porter (ed.): *Hydrothermal iron oxide copper–gold and related deposits: a global perspective*. Australian Mining Foundation, Glenside, Australia, 283–296.
- Carranza, E.J.M. & Sadeghi, M., 2010: Predictive mapping of prospectivity and quantitative estimation of undiscovered VMS deposits in Skellefte district (Sweden). *Ore Geology Reviews* 38, 219–241.
- Cassard, D., Bertrand, G., Billa, M., Serrano, J.J., Tourlière, B., Angel, J.M. & Gaál, G., 2015: ProMine Mineral Databases: New Tools to Assess Primary and Secondary Mineral Resources in Europe. In: Weihed, P. (ed.). *3D, 4D and predictive modelling of major mineral belts in Europe*. Springer Int. publishing, 9–59.
- Cherevatova, M., Smirnov, M., Korja, T., Kaikkonen, P., Pedersen, L., Hübert, J., Kamm, J. & Kalscheuer, T., 2014: Crustal structure beneath southern Norway imaged by magnetotellurics. *Tectonophysics* 628, 55–70.
- Cherevatova, M., Smirnov, M.Yu., Jones, A.G., Pedersen, L.B. & MaSca Working Group, 2015a: Magnetotelluric array data analysis from north-west Fennoscandia. *Tectonophysics* 653, 1–19.
- Cherevatova, M., Smirnov, M.Yu., Korja, T., Pedersen, L.B., Ebbing, J., Gradmann, S., Becken, M. & MaSca Working Group, 2015b: Electrical conductivity structure of north-west Fennoscandia from three-dimensional inversion of magnetotelluric data. *Tectonophysics* 653, 20–32.
- Danielsson, S., 1985: Nautanen. Borrhålsprotokoll och analysintyg från 1985-årsarbeten. *Sveriges geologiska undersökning Prap 85090*, 241 pp.
- Dehghannejad, M., 2014: *Reflection seismic investigation in the Skellefte ore district: A basis for 3D/4D geological modeling*. Diss., Uppsala Univ., 68 pp.
- Dehghannejad, M., Juhlin, C., Malehmir, A., Skyttä, P. & Weihed, P., 2010: Reflection seismic imaging of the upper crust in the Kristineberg mining area, northern Sweden. *Journal of Applied Geophysics* 71, 125–136.
- Dehghannejad, M., Bauer, T., Malehmir, A., Juhlin, C. & Weihed, P., 2012a: Crustal geometry of the central Skellefte district, northern Sweden – constraints from reflection seismic investigations. *Tectonophysics* 524, 87–99.
- Dehghannejad, M., Malehmir, A., Juhlin, C. & Skyttä, P., 2012b: 3D constraints and finite-difference modeling of massive sulfide deposits: The Kristineberg seismic lines revisited, northern Sweden. *Geophysics* 77, WC69–WC79.
- Diehl, T., Kraft, T., Kissling, S. & Wiemer, S., 2017: The induced earthquake sequence related to the St. Gallen deep geothermal project (Switzerland): Fault reactivation and fluid interactions imaged by microseismicity. *J. Geophys. Res.* 122, 7272–7290.
- Dreijing-Carroll, D, Bauer, T., Karlsson, P., Coller, D., Nordin, R., Hitzman, M. & Allen, R., 2015: New Insight into the links between major porphyry copper, IOCG, and magnetite-apatite deposits from the Gällivare area, Northern Sweden. Society of Economic Geologists, Annual Conference 2015, Hobart, Tasmania. Program and abstracts.
- Du Rietz, T., 1953: Geology and ores of the Kristineberg deposit, Vesterbotten, Sweden. *Sveriges geologiska undersökning C 524*, 1–89.
- Edelman, N., 1963: Structural studies in the western part of the Skellefte district, northern Sweden. *Geologiska Föreningens i Stockholm Förhandlingar* 85, 185–211.
- Edfelt, Å., Sandrin, A., Evins, P., Jeffries, T., Storey, C., Elming S.-Å. & Martinsson O., 2006: Stratigraphy and tectonic setting of the host rocks to the Tjärrojäkka Fe-oxide Cu-Au deposits, Kiruna area, northern Sweden. *GFF* 128, 221–232.
- Ehsan, S., Malehmir, A. & Dehghannejad, M., 2012: Re-processing and interpretation of 2D seismic data from the Kristineberg mining area, northern Sweden. *Journal of Applied Geophysics* 80, 43–55.
- Eilu, P. (ed.), 2012: Mineral deposits and metallogeny of Fennoscandia. Geological Survey of Finland, *Special Paper* 53, 401 pp.
- Eilu, P., Bergman, T., Bjerkgård, T., Feoktistov, V., Hallberg, A., Korsakova, M., Krasotkin, S., Litvinenko, V., Nurmi, P.A., Often, M., Philippov, N., Sandstad, J.S. and Voytekhovskiy, Y.L. (comp.) 2013. *Metallic Mineral Deposit Map of the Fennoscandian Shield 1:2 000 000. Revised edition*. Geological Survey of Finland, Geological Survey of Norway, Geological Survey of Sweden, The Federal Agency of Use of Mineral Resources of the Ministry of Natural Resources of the Russian Federation.

- Eliasson, T., Eriksson, K.G., Lindquist, G., Malmquist, D. & Parasnis, D., 1991: Sweden. In Hurtig, E., Cermák, V., Haenel, R. & Zui, V. (eds.), *Geothermal Atlas of Europe*, Herman Haack Verlagsgesellschaft, Gotha, p. 78.
- Elming, S.-Å., Thunehed, H., 1991. A seismic reflection investigation in the Skellefte District, northern Sweden. *Geologiska Föreningens i Stockholm Förhandlingar* 113, 258–259.
- Ericsson, L.-O., Holmén, J., Rhén, I. & Blomquist, N., 2008: Storregional grundvattenmodellering –fördjupad analys av flödesförhållanden i östra Småland. Jämförelse av olika konceptuella beskrivningar. *SKB Rapport R-06-64*.
- Eriksson, B. & Hallgren, U., 1975: Beskrivning till berggrundskartbladen Vittangi NV, NO, SV, SO. *Sveriges geologiska undersökning Af 13–16*, 203 pp.
- Eriksson, T., 1954: Pre-Cambrian geology of the Pajala district, northern Sweden. *Sveriges geologiska undersökning C* 522, 38 pp.
- Fennoscandian ore deposit Database: <http://en.gtk.fi/informationsservices/databases/fodd/index.html>.
- Fredholm, K.A., 1886: Öfversigt af Norrbottens geologi inom Pajala, Muonionalusta och Tärändö socknar. *Sveriges geologiska undersökning C* 83, 39 pp.
- Frietsch, R., 1975: Alkali metasomatism in the ore-bearing metavolcanics of central Sweden. *Sveriges geologiska undersökning C* 791, 54 pp.
- Frietsch, R., Tuisku, P., Martinsson, O. & Perdahl, J.-A., 1997: Cu-(Au) and Fe ore deposits associated with Na-Cl metasomatism in early Proterozoic rocks of northern Fennoscandia: A new metallogenic province. *Ore Geology Review* 12, 1–34.
- Gaál, G., & Gorbatshev, R., 1987: An outline of the Precambrian evolution of the Baltic shield. *Precambrian Research* 35, 15–52.
- García Juanatey, M., 2012: *Seismics, 2D and 3D Inversion of Magnetotellurics. Jigsaw pieces in understanding the Skellefte Ore District*. Diss., Uppsala Univ. 55 pp.
- García Juanatey, M., Hübert, J., Tryggvason, A. & Pedersen, L., 2013: Imaging the Kristineberg mining area with two perpendicular magnetotelluric profiles in the Skellefte Ore District, northern Sweden. *Geophysical Prospecting* 61, 200–219.
- Gee, D., Juhlin, C., Pascal, C. & Robinson, P., 2010: Collisional Orogeny in the Scandinavian Caledonides (COSC). *GFF* 132, 29–44.
- Geijer, P., 1918: Nautanenområdet. En malmgeologisk undersökning. *Sveriges geologiska undersökning C* 283, 103 pp.
- Geijer, P., 1931: Berggrunden inom malmtrakten Kiruna–Gällivare–Pajala. *Sveriges geologiska undersökning C* 366, 225 pp.
- Geological Survey of Sweden, 2013: Bedömningsgrunder för grundvatten. *SGU-rapport 2013:01*, Sveriges geologiska undersökning, 125 pp.
- Gharibi, M., 2000: *Electromagnetic Studies of the Continental Crust in Sweden*. Diss., Uppsala Univ., 24 pp.
- Gold, T., 1992: The deep, hot biosphere. *Proc. Natl. Acad. Sci. USA*. Vol 89, 6045–6049.
- Golder Associates, 2017: *Ansökan om bearbetningskoncession. Hydrogeologisk förstudie Rävliiden*. Rapport, unpubl.
- González-Roldán, M. J. 2010: *Mineralogía, petrología y geoquímica de intrusiones sin-volcánicas en el distrito minero de Skellefte, norte Suecia*, unpublished Ph.D. thesis (in Spanish with English summary), University of Huelva, Spain, 273 pp., 2010.
- Grigull, S., Berggren, R., Jönberger, J., Jönsson, C., Hellström, F.A. & Luth, S., 2018: Folding observed in Palaeoproterozoic supracrustal rocks in northern Sweden. In S. Bergman (ed.): *Geology of the Northern Norrbotten ore province, northern Sweden. Rapporter och Meddelanden* 141, Sveriges geologiska undersökning, 205–257.
- Grip, E., 1973: Skelleftefältets sulfidmalmer. In E. Grip & R. Frietsch (eds.): *Malm i Sverige 2, Norra Sverige*. Almqvist & Wiksell, 194–273.
- Grooves, D.I., Bierlein, F.P., Meinert, L.D. & Hitzman, M.W., 2010: Iron oxide copper-gold (IOCG) deposits through Earth history: Implications for origin, lithospheric setting, and distinction from other epigenetic iron oxide deposits. *Economic Geology* 105, 641–654.
- Guggisberg, B., Kaminski, W. & Prodehl, C., 1991: Crustal structure of the Fennoscandian Shield: a traveltimes interpretation of the long-range FENNOLORA seismic refraction profile. *Tectonophysics* 195, 105–137.

- Gustafsson, B., 1985: Fältarbeten 1984 inom delprojektområde Gällivare J Gällivare SV och SO. Slutrapport. *Sveriges geologiska undersökning Prap 85005*, 125 pp.
- Gustafsson, B., 1986: Projekt 5515 Malmberget. Prospekteringsarbeten 1985. Rekommendationer för 1986. Lägesrapport 1986-01-15. *Sveriges geologiska undersökning Prap 86004*, 220 pp.
- Gustafsson, B. & Johansson, L., 1984: Ferrum kopparfyndighet geofysik och geologi 1984. *Sveriges geologiska undersökning Prap 84158*, 18 pp.
- Hanski, E.J., 2012: Evolution of the Palaeoproterozoic (2.50–1.95) non-orogenic magmatism in the eastern part of the Fennoscandian Shield. In V.A. Melezhik, A.R. Prave, E.J. Hanski, A.E. Fallick, A. Lepland, L.R. Kump & H. Strauss (eds.): *Reading the archive of Earth's oxygenation*, Volume 1, Springer, Berlin, 179–245.
- Hanski, E.J. & Huhma, H., 2005: Central Lapland greenstone belt. In R. Lehtinen, P.A. Nurmi, O.T. Rämö (eds.) *Precambrian Geology of Finland – key to the evolution of the Fennoscandian Shield*. Elsevier, Amsterdam, 139–194.
- Heidbach, O., Tingay, M., Barth, A., Reinecker, J., Kurfeß, D. & Müller, B., 2008: The World Stress Map database release 2008.
- Hellström, F.A., 2018: Early Svecokarelian migmatization west of the Pajala Deformation Belt, northeastern Norrbotten Province, northern Sweden. In S. Bergman (ed.): *Geology of the Northern Norrbotten ore province, northern Sweden. Rapporter och Meddelanden 141*, Sveriges geologiska undersökning, 361–379.
- Hellström, F. & Bergman, S., 2016: Is there a 1.85 Ga magmatic event in northern Norrbotten? – U-Pb SIMS zircon dating of the Pingisvaara metagranodiorite and the Jyryjoki granite, northern Sweden, *GFF*, DOI: 10.1080/11035897.2016.1171254.
- Hellström, F.A., Kumpulainen, R., Jönsson, C., Thomsen, T.B., Huhma, H. & Martinsson, O., 2018: Age and lithostratigraphy of Svecofennian volcanosedimentary rocks at Masugnsbyn, northernmost Sweden – host rocks to Zn-Pb-Cu- and Cu ±Au sulphide mineralisations. In S. Bergman (ed.): *Geology of the Northern Norrbotten ore province, northern Sweden. Rapporter och Meddelanden 141*, Sveriges geologiska undersökning, 151–203.
- Hietanen, A. 1975. Generation of potassium-poor magmas in the northern Sierra Nevada and the Svecofennian of Finland. *U.S. Geological Survey Journal of Research* 3, 631–645.
- Högbom, A.G., 1899: Skelleftefältets geologi och bergarter. *Geologiska Föreningens i Stockholm Förhandlingar* 21, 636–638.
- Högdahl, K., Andersson, U.B. & Eklund, O. (eds.), 2004: The Transscandinavian Igneous Belt (TIB) in Sweden: a review of its character and evolution. *Geological Survey of Finland, special paper 37*, 125 pp.
- Holmgren, J. 2013. *Seismic modeling of reflection survey near Kiruna*. BSc thesis, Luleå university, 41 pp.
- Holmqvist, P.J., 1906: Studien über die Granite von Schweden: *Bulletin of the Geological Institution of the University of Upsala VII*, 77–269.
- Hübert J., Malehmir A., Smirnow M., Tryggvason A. & Pedersen L.B., 2009: MT measurements in the western part of the Paleoproterozoic Skellefte Ore District, Northern Sweden: A contribution to an integrated geophysical study. *Tectonophysics* 475, 493–502.
- Hübert, J., 2012: *From 2D to 3D Models of Electrical Conductivity based upon Magnetotelluric Data. Experiences from two Case Studies*. Diss., Uppsala Univ., 55 pp.
- Hübert, J., García Juanatey, M., Malehmir, A., Tryggvason, A. & Pedersen, L., 2013: The upper crustal 3-D resistivity structure of the Kristineberg area, Skellefte district, northern Sweden revealed by magnetotelluric data. *Geophysical Journal International* 192, 500–513
- Hurter, S., & Haenel, R. (eds.), 2002: *Atlas of Geothermal Resources in Europe*, Office for Official Publications of the European Communities, Luxemburg, 91 pp., 89 plates.
- Hurtig, E., Cermak, V., Haenel, R. & Zui, V. (eds.), 1991. *Geothermal Atlas of Europe*. Herman Haack Verlagsgesellschaft, Gotha, 156 pp.
- Isaksson, H., Johansson, R. & Triumf, C.-A., 1994: Förstudie Malå. Geofysisk dokumentation och tolkning. *SKB Djupförvar Projekt Rapport PR 44-94-029*, 1–23.
- Jensen, M., Kashubin, A., Juhlin, C. & Elming, S., 2012: Multidisciplinary study of the hanging wall of the Kiirunavaara iron ore deposit, northern Sweden. *Geophysics* 77, B269–B285.

- Jönberger, J., Jönsson, C. & Luth, S., 2018: Geophysical 2D and 3D modeling in the areas around Nunasvaara and Masugnsbyn, northern Sweden. In S. Bergman (ed.): *Geology of the Northern Norrbotten ore province, northern Sweden. Rapporter och Meddelanden 141*, Sveriges geologiska undersökning, 311–339.
- Jones, A.G., Olafsdottir, B. & Tiikkainen, J., 1983: Geomagnetic induction studies in Scandinavia. III. Magnetotelluric observations. *Journal of Geophysics* 54, 35–50.
- Juhlin, C. & Sandstedt, H., 1989: Storage of nuclear waste in very deep boreholes: Feasibility study and assessment of economic potential. *SKB Technical Report TR-89-39*, 92 pp.
- Juhlin, C., A. A. Aldahan, J. Castano, B. Collini, T. Gorody, & H. Sandstedt, 1991: *Scientific Summary Report for the Deep Gas Drilling Project in the Siljan Ring Impact Structure*. Naturgas. Älvkarleby, Sweden: Vattenfall Research & Development.
- Juhlin C., Wallroth T., Smellie J., Eliasson T., Ljunggren C., Leijon B. & Beswick J., 1998: The Very Deep Hole Concept: Geoscientific appraisal of conditions at great depth. *SKB Technical Report TR 98-05*, 124 pp.
- Juhonjuntti, N., Olsson, S., Bergman, S. & Antal Lundin, I., 2014: Reflexionsseismiska mätningar vid Kiruna – preliminär tolkning, *SGU-rapport 2014:05*, Sveriges geologiska undersökning, 26 pp.
- Kathol, B. & Weihed, P. (eds.), 2005: Description of regional geological and geophysical maps of the Skellefte District and surrounding areas. *Sveriges geologiska undersökning Ba 57*, 197 pp.
- Kathol, B., Weihed, P., Antal Lundin, I., Bark, G., Bergman Weihed, J., Bergström, U., Billström, K., Björk, L., Claesson, L., Daniels, J., Eliasson, T., Frumerie, M., Kero, L., Kumpulainen, R.A., Lundström, H., Lundström, I., Mellqvist, C., Petersson, J., Skiöld, T., Sträng, T., Stølen, L.-K., Söderman, J., Triumf, C.-A., Wikström, A., Wikström, T. & Årebäck, H., 2005: Regional geological and geophysical maps of the Skellefte District and surrounding areas. Bedrock map. *Sveriges geologiska undersökning Ba 57:1*.
- Kautsky, G., 1957: Ein Beitrag zur Stratigraphie und dem Bau des Skelleftefeldes, Nordschweden. *Sveriges geologiska undersökning C 543*, 1–65.
- Koistinen, T., Stephens, M.B., Bogatchev, V., Nordgulen, Ø., Wennerström, M. & Korhonen, J., 2001: Geological map of the Fennoscandian Shield, scale 1 : 2 000 000. *Geological Surveys of Finland, Norway and Sweden and the North-West Department of Natural Resources of Russia*.
- Korja, A., Lahtinen, R. & Nironen, M., 2006: The Svecofennian orogen: a collage of microcontinents and island arcs. In D.G. Gee & R.A. Stephenson (eds.): *European lithosphere dynamics. Geological Society, London, Memoirs 32*, 561–578.
- Kousa, J. & Lundqvist, T., 2000: Svecofennian domain. In Th. Lundqvist & S. Autio (eds): *Description to the Bedrock Map of Central Fennoscandia (Mid-Norden). Geological Survey of Finland, Special Paper 28*, 47–75.
- Kukkonen, I. T., 2007: Outokumpu Deep Drilling Project. Second International Workshop. Geological Survey of Finland, *Report Q10.2/2007/29*, Espoo, 86 pp.
- Kwiatek, G. and 16 others, 2019: Controlling fluid-induced seismicity during a 6.1-km-deep geothermal stimulation in Finland. *SCIENCE ADVANCES*, 01 May 2019, EAAV7224.
- Ladenberger, A., Andersson, M., Smith, C. & Carlsson, M., 2018: Till geochemistry in northern Norrbotten – regional trends and local signature in the key areas. In S. Bergman (ed.): *Geology of the Northern Norrbotten ore province, northern Sweden. Rapporter och Meddelanden 141*, Sveriges geologiska undersökning, 401–428.
- Lagerblad, B. & Gorbatshev, R., 1985: Hydrothermal alteration as a control of regional geochemistry and ore formation in the central Baltic Shield. *Geologische Rundschau* 74, 33–49.
- Lahtinen, R., Korja, A. & Nironen, M., 2005: Paleoproterozoic tectonic evolution. In: M. Lehtinen, P.A. Nurmi & O.T. Rämö (eds.): *Precambrian geology of Finland – key to the evolution of the Fennoscandian Shield*. Elsevier, Amsterdam, 481–532.
- Lahtinen, R., Garde, A.A. & Melezhik, V.A., 2008: Paleoproterozoic evolution of Fennoscandia and Greenland. *Episodes* 31, 1–9.
- Lahtinen, R., Huhma, H., Lahaye, Y., Jonsson, E., Manninen, T., Lauri, L.S., Bergman, S., Hellström, F., Niiranen, T. & Nironen, M., 2015: New geochronological and Sm-Nd constraints across the Pajala shear zone of northern Fennoscandia: Reactivation of a Paleoproterozoic suture. *Precambrian Research* 256, 102–119.
- Lahtinen, R., Korja, A., Nironen, M. & Heikkinen, P., 2009: Paleoproterozoic accretionary processes in Fennoscandia. *Geological Society, London, Special Publications 318*, 237–259.

- Lauri, L.S., Hellström, F., Bergman, S., Huhma, H. & Lepistö, S., 2016: New insights into the geological evolution of the Archean Norrbotten province, Fennoscandian Shield. *Bulletin of the Geological Society of Finland Special Volume 1*, p. 151.
- Leary, P., 2018. Enhanced/Engineered Geothermal Systems (EGS). Uppsala university, Geophysics div., Invited lecture, Uppsala, November 8, 2018.
- Lehnert, O., Meinhold, G., Bergström, S.M., Calner, M., Ebbestad, J.O., Egenhoff, S., Frisk, Å.M., Hannah, J.L., Högstöm, A.E.S., Huff, W.D., Juhlin, C., Maletz, J., Stein, H.J., Sturkell, E. & Vandenbroucke, T.R.A., 2012: New Ordovician-Silurian drill cores from the Siljan impact structure in central Sweden: an integral part of the Swedish Deep Drilling Program. *GFF* 134, 87–98.
- Le Maitre, R.W., 1976: The chemical variability of some common igneous rocks. *Journal of Petrology* 17, 589–637.
- Lorenz, H. 2010. The Swedish deep drilling program: for science and society. *GFF* 132, 25–27.
- Louvat, D., J. L. Michelot, & J. F. Aranyosy, 1999: Origin and residence time of salinity in the Äspö groundwater system. *Applied Geochemistry* 14, 917–925.
- Ludwig, K.R., 2012: User's manual for Isoplot 3.75. A geochronological toolkit for Microsoft Excel. *Berkeley Geochronology Center Special Publication No. 5*, 75 pp.
- Lund, C., 2009: *Mineralogical, chemical and textural properties of the Malmberget iron deposit. A process mineralogically characterisation*. M.Sc. thesis, Luleå University of Technology, Luleå, Sweden, 98 p.
- Lund, C.E., Heikkinen, P. 1987. Reflection measurements along the EGT POLAR-profile, northern Baltic Shield. *Geophys. J. R. Astron. Soc.* 89, 361–364.
- Lundberg, B., 1980: Aspects of the geology of the Skellefte field, northern Sweden. *Geologiska Föreningens i Stockholm Förhandlingar* 102, 156–166.
- Lundberg, E., 2014: 2D and 3D Reflection Seismic Studies over Scandinavian Deformation Zones. Diss., Uppsala Univ., 57 pp.
- Lundbohm, H., 1898: Kirunavara-traktens geologi. *Geologiska Föreningens i Stockholm Förhandlingar* 20, 68–78.
- Lundbohm, H., 1910: Sketch of the geology of the Kiruna district. *Geologiska Föreningens i Stockholm Förhandlingar* 32, 751–788.
- Lundqvist, T., Bøe, R., Kousa, J., Lukkarinen, H., Lutro, O., Roberts, D., Solli, A., Stephens, M. & Weihed, P., 1996a: *Bedrock map of Central Fennoscandia. Scale 1:1 000 000*. Geological Surveys of Finland (Espoo), Norway (Trondheim) and Sweden (Uppsala).
- Lundqvist, T., Bøe, R., Kousa, J., Lukkarinen, H., Lutro, O., Luukas, J., Roberts, D., Solli, A., Stephens, M. & Weihed, P., 1997: *Metamorphic, structural and isotope age map of Central Fennoscandia. Scale 1:1 000 000*. Geological Surveys of Finland (Espoo), Norway (Trondheim) and Sweden (Uppsala).
- Luth, S., Jönberger, J. & Grigull, S., 2018a: The Vakko and Kovo greenstone belts north of Kiruna: Integrating structural geological mapping and geophysical modelling. In S. Bergman (ed.): *Geology of the Northern Norrbotten ore province, northern Sweden. Rapporter och Meddelanden 141*, Sveriges geologiska undersökning, 287–309.
- Luth, S., Jönsson, C., Jönberger, J., Grigull, S., Berggren, R., van Assema, B., Smoor, W. & Djuly, T., 2018b: The Pajala Deformation Belt in northeast Sweden: Structural geological mapping and 3D modelling around Pajala. In S. Bergman (ed.): *Geology of the Northern Norrbotten ore province, northern Sweden. Rapporter och Meddelanden 141*, Sveriges geologiska undersökning, 259–285.
- Luth, S., Jönsson C., Hellström, F., Jönberger J., Djuly, T., van Assema, B. & Smoor, W., 2016: Structural and geochronological studies on the crustal-scale Pajala deformation zone, northern Sweden. *Bulletin of the Geological Society of Finland Special Volume 1*, p. 263.
- Lynch, E.P., Bauer, T.E., Jönberger, J., Sarlus, Z., Morris, G.A. & Persson, P.-O., 2018a: Petrology and deformation of c. 1.88 Ga meta-volcanosedimentary rocks hosting iron oxide-copper-gold and related mineralisation in the Nautanen-Gällivare area, northern Sweden. In S. Bergman (ed.): *Geology of the Northern Norrbotten ore province, northern Sweden. Rapporter och Meddelanden 141*, Sveriges geologiska undersökning, 107–149.
- Lynch, E.P. & Jönberger, J., 2014: Summary report on available geological, geochemical and geophysical information for the Nautanen key area, Norrbotten. *Sveriges geologiska undersökning report 2014:34*, 40 pp.

- Lynch, E.P., Jönberger, J., Bauer, T.E., Sarlus, Z. & Martinsson, O., 2015: Meta-volcanosedimentary rocks in the Nautanen area, Norrbotten: Preliminary lithological and deformation characteristics. *Sveriges geologiska undersökning report 2015:30*, 51 pp.
- Lynch, E.P., Bauer, T.E., Huhma, H., Drejling-Caroll, D., 2018c: Petrogenesis of c. 1.9 Ga meta-volcanosedimentary rocks in the Nautanen-Aitik area, northern Sweden: Geological, lithogeochemical and Sm-Nd isotopic constraints. Proceedings of the 33rd Nordic Geological Winter Meeting, Copenhagen. Program and abstracts.
- Lynch, E.P., Hellström, F.A., Huhma, H., Jönberger, J., Persson, P.-O. & Morris, G.A., 2018b: Geology, lithostratigraphy and petrogenesis of c. 2.14 Ga greenstones in the Nunasvaara and Masugnsbyn areas, northernmost Sweden. In S. Bergman (ed.): *Geology of the Northern Norrbotten ore province, northern Sweden. Rapporter och Meddelanden 141*, Sveriges geologiska undersökning, 19–77.
- Magnusson, N.H., 1970: *Malm i Sverige 1. Mellersta och södra Sverige*. Almqvist & Wiksell, Stockholm, 320 pp.
- Malehmir, A., 2007: *3D Geophysical and Geological Modeling in the Skellefte Ore District: Implications for Targeting Ore Deposits*. Diss., Uppsala Univ., 84 pp.
- Malehmir, A., Tryggvason, A., Juhlin, C., Rodriguez-Tablante, J. & Weihed, P., 2006: Seismic imaging and potential field modeling to delineate structures hosting VHMS deposits in the Skellefte Ore District, northern Sweden. *Tectonophysics* 426, 319–334.
- Malehmir, A., Tryggvason, A., Lickorish, H. & Weihed, P., 2007: Regional structural profiles in the western part of the Palaeoproterozoic Skellefte ore district, northern Sweden. *Precambrian Research* 159, 1–18.
- Malehmir, A., Schmelzbach, C., Bongajum, E., Bellefleur, G., Juhlin, C. & Tryggvason, A., 2009a: 3D constraints on a possible deep > 2.5 km massive sulphide mineralization from 2D crooked-line seismic reflection data in the Kristineberg mining area, northern Sweden. *Tectonophysics* 479, 223–240.
- Malehmir, A., Thunehed, H. & Tryggvason, A., 2009b: The Paleoproterozoic Kristineberg mining area, northern Sweden: Results from integrated 3D geophysical and geologic modeling, and implications for targeting ore deposits. *Geophysics* 74, B9–B22.
- Malehmir, A., Durrheim, R., Bellefleur, G., Urosevic, M., Juhlin, C., White, D.J., Milkereit, B. & Campbell, G., 2012a: Seismic methods in mineral exploration and mine planning: A general overview of past and present case histories and a look into the future. *Geophysics* 77, WC173–WC190.
- Malehmir, A., Urosevic, M., Bellefleur, G., Juhlin, C. & Milkereit, B., 2012b: Seismic methods in mineral exploration and mine planning - Introduction. *Geophysics* 77, WC1–WC2.
- Malehmir, A., Andersson, M., Lebedev, M., Urosevic, M. & Mikhaltsevitch, V., 2013: Experimental estimation of velocities and anisotropy of a series of Swedish crystalline rocks and ores. *Geophysical Prospecting* 61, 153–167.
- Malehmir, A., Wang, S., Lamminen, J., Brodic, B. & Bastani, M. et al., 2015: Delineating structures controlling sandstone-hosted base-metal deposits using high-resolution multicomponent seismic and radio-magnetotelluric methods: a case study from Northern Sweden. *Geophysical Prospecting* 63, 774–797.
- Malin, P.E., 2016: Drilling 5 km to Boiling: The St1 Helsinki District-Heating Gamble. Presentation at the SMU Power Plays Conf., 26 April 2016. https://www.smu.edu/-/media/Site/Dedman/Academics/Programs/Geothermal-Lab/Conference/PastPresentations/2016/Malin_SMUPowerPlays_2016.pdf?la=en
- Marsic, N. & Grundfelt, B., 2013: Review of geoscientific data of relevance to disposal of spent nuclear fuel in deep boreholes in crystalline rock. *SKB report P-13-12*, 31 pp.
- Martinsson, O., 1993: Stratigraphy of greenstones in the eastern part of northern Norrbotten. In O. Martinsson, J.-A. Perdahl & J. Bergman: *Greenstone and porphyry hosted ore deposits in northern Norrbotten, NUTEK Project nr 92-00752P*, 1–5.
- Martinsson, O., 1995: Greenstone and porphyry hosted ore deposits in northern Norrbotten. *PIM/NUTEK report #3*, 58 pp.
- Martinsson, O., 1997a: *Tectonic Setting and Metallogeny of the Kiruna Greenstones*. Ph.D. thesis, Luleå University of Technology, Luleå, Sweden.
- Martinsson, O., 1997b: Paleoproterozoic greenstones at Kiruna in northern Sweden: a product of continental rifting and associated mafic-ultramafic volcanism. In O. Martinsson: *Tectonic setting and metallogeny of the Kiruna greenstones. Doctoral thesis 1997:19, Paper I*, 1–49. Luleå University of Technology.
- Martinsson, O., 1999a: Berggrundskartan 30J Rensjön SO, skala 1:50 000. *Sveriges geologiska undersökning Ai 133*.

- Martinsson, O., 1999b: Berggrundskartan 31J Råstojaure SV/SO, skala 1:50 000. *Sveriges geologiska undersökning Ai 135*.
- Martinsson, O., 2004: Geology and Metallogeny of the Northern Norrbotten Fe-Cu-Au Province. In R.L. Allen, O. Martinsson & P. Weihed (eds.): Svecofennian Ore-Forming Environments: Volcanic-Associated Zn-Cu-Au-Ag, Intrusion-Associated Cu-Au, Sediment-Hosted Pb-Zn, and Magnetite-Apatite Deposits of Northern Sweden. *Society of Economic Geologists, Guidebook Series 33*, 131–148.
- Martinsson, O. & Wanhainen, C., 2004: Character of Cu-Au mineralisation and related hydrothermal alteration along the Nautanen deformation zone, Gällivare area, northern Sweden. In R.L. Allen, O. Martinsson & P. Weihed (eds.): Svecofennian ore-forming environments of northern Sweden – volcanic-associated Zn-Cu-Au-Ag, intrusion-associated Cu-Au, sediment-hosted Pb-Zn, and magnetite-apatite deposits in northern Sweden. *Society of Economic Geologists, guidebook series 33*, 149–160.
- Martinsson, O. & Wanhainen, C. (eds.), 2013a: Fe oxide and Cu-Au deposits in the northern Norrbotten ore district. *Excursion guidebook SWE5, 12th Biennial SGA Meeting, Uppsala, Sveriges geologiska undersökning*, 70 pp.
- Martinsson, O. & Wanhainen, C., 2013b: The Northern Norrbotten ore district. In O. Martinsson & C. Wanhainen (eds.): Fe oxide and Cu-Au deposits in the northern Norrbotten ore district. *Excursion guidebook SWE5, 12th Biennial SGA Meeting, Uppsala, Sweden*, 19–28.
- Martinsson, O., Vaasjoki, M. & Persson, P.-O., 1999: U-Pb ages of Archaean to Palaeoproterozoic granitoids in the Torneträsk-Råstojaure area, northern Sweden. In S. Bergman (ed.): Radiometric dating results 4. *Sveriges geologiska undersökning C 831*, 70–90.
- Martinsson, O., Billström, K., Broman, C., Weihed, P. & Wanhainen, C., 2016: Metallogeny of the Northern Norrbotten Ore Province, northern Fennoscandian Shield with emphasis on IOCG and apatite-iron ore deposits. *Ore Geology Reviews 78*, 447–492.
- Martinsson, O., Bergman, S., Persson, P.-O. & Hellström, F.A., 2018a: Age and character of late-Svecokarelian monzonitic intrusions in north-eastern Norrbotten, northern Sweden. In S. Bergman (ed.): *Geology of the Northern Norrbotten ore province, northern Sweden. Rapporter och Meddelanden 141*, Sveriges geologiska undersökning, 381–399.
- Martinsson, O., Bergman, S., Persson, P.-O., Schöberg, H., Billström, K. & Shumlyanskyy, L., 2018b: Stratigraphy and ages of Palaeoproterozoic metavolcanic and metasedimentary rocks at Käymäjärvi, northern Sweden. In S. Bergman (ed.): *Geology of the Northern Norrbotten ore province, northern Sweden. Rapporter och Meddelanden 141*, Sveriges geologiska undersökning, 79–105.
- Martinsson, O., Billström, K., Broman, C., Weihed, P. & Wanhainen, C., 2016: Metallogeny of the Northern Norrbotten ore province, northern Fennoscandian Shield with emphasis on IOCG and apatite-iron ore deposits. *Ore Geology Reviews 78*, 447–492.
- McGimpsey, I., 2010: *Petrology and lithogeochemistry of the host rocks to the Nautanen Cu-Au deposit, Gällivare area, northern Sweden*. M.Sc. thesis, Lund University, Lund, Sweden, 82 pp.
- McPhie, J., Doyle, M. & Allen, R., 1993: *Volcanic textures: A guide to the interpretation of volcanic textures in volcanic rocks*. CODES Key Centre, University of Tasmania, 198 pp.
- Melezhik, V.A. & Fallick, A.E., 2010: On the Lomagundi-Jatuli carbon isotopic event: The evidence from the Kalix Greenstone Belt, Sweden. *Precambrian Research 179*, 165–190.
- Melezhik, V.A. & Hanski, E.J., 2012: The early Paleoproterozoic of Fennoscandia: Geological and tectonic settings. In V.A. Melezhik, A.R. Prave, E.J. Hanski, A.E. Fallick, A. Lepland, L.R. Kump & H. Strauss (eds.): *Reading the archive of Earth's oxygenation*, Volume 1, Springer, Berlin. 33–38.
- Melezhik, V.A., Kump, L.R., Hanski, E.J., Fallick, A.E. & Prave, A.R., 2012. Tectonic evolution and major global Earth-surface palaeoenvironmental events in the Palaeoproterozoic. In V.A. Melezhik, A.R. Prave, E.J. Hanski, A.E. Fallick, A. Lepland, L.R. Kump & H. Strauss (eds.): *Reading the archive of Earth's oxygenation*, Volume 1, Springer, Berlin, 3–21.
- Mellqvist, C., Öhlander, B., Skiöld, T. & Wickström, A., 1999: The Archean-Proterozoic paleoboundary in the Luleå area, northern Sweden: field and isotope geochemical evidence for a sharp terrane boundary. *Precambrian Research 96*, 225–243.
- Monro, D., 1988: *The geology and genesis of the Aitik Cu-Au deposit, arctic Sweden*. Ph.D. thesis, University College Cardiff, UK, 386 pp.
- Muhamad, H., Juhlin, C., Lehnert, O., Meinhold, G. & Andersson, M., et al. 2015: Analysis of borehole geophysical data from the Mora area of the Siljan Ring impact structure, central Sweden. *Journal of Applied Geophysics 115*, 183–196.

- New Boliden, 2016. *Nautanen copper-mineralization in northern Sweden*. Company press release, 05-02-2016. <www.boliden.com>
- Nironen, M., 1997: The Svecofennian orogen: a tectonic model. *Precambrian Research* 86, 21–44.
- Ödman, O. H., 1939: Urbergsgeologiska undersökningar inom Norrbottens län. *Sveriges geologiska undersökning C 426*, 100 pp.
- Ödman, O. H., 1957: Beskrivning till berggrundskarta över urberget i Norrbottens län. *Sveriges geologiska undersökning Ca 41*, 151 pp.
- Ödman, O. H., Härme, M., Mikkola, A. & Simonen, A., 1949: Den svensk-finska geologiska exkursionen i Tornedalen sommaren 1948. *Geologiska Föreningens i Stockholm Förhandlingar* 71, 113–126.
- Offerberg, J., 1967: Beskrivning till berggrundskartbladen Kiruna NV, NO, SV, SO. *Sveriges geologiska undersökning Af 1–4*, 147 pp.
- Öhlander, B. & Skiöld, T., 1994: Diversity of 1.8 Ga potassic granitoids along the edge of the Archaean craton in northern Scandinavia: a result of melt formation at various depths and from various sources. *Lithos* 33, 265–283.
- Öhlander, B., Skiöld, T., Hamilton, P.J. & Claesson, L.-Å., 1987: The western border of the Archaean province of the Baltic Shield evidence from northern Sweden. *Contributions to Mineralogy & Petrology* 95, 437–450.
- Padget, P., 1970: Beskrivning till berggrundskartbladen Tändö NV, NO, SV, SO. *Sveriges geologiska undersökning Af 5–8*, 95 pp.
- Parasnis, D.S., 1975: Temperature Phenomena and Heat Flow Estimates in Two Precambrian Ore-bearing Areas in North Sweden. *Geophysical Journal of the Royal Astronomical Society* 43, 531–554.
- Parasnis, D.S., 1981: Geothermal flow and phenomena in two Swedish localities north of the Arctic circle. *Geophysical Journal of the Royal Astronomical Society* 71, 545–554.
- Perdahl, J.-A., 1995: *Svecofennian volcanism in northernmost Sweden*. Ph.D. thesis, Luleå University of Technology, Luleå, Sweden.
- Perdahl, J.-A. & Einarsson, Ö., 1994: The marine-continental transition of the Early Proterozoic Skellefte–Arvidsjaur volcanic arc in the Bure area, northern Sweden. *GFF* 116, 133–138.
- Perdahl, J.-A. & Frietsch, R., 1993: Petrochemical and petrological characteristics of 1.9 Ga old volcanics in northern Sweden. In R. Gorbatshev (ed.): *The Baltic Shield. Precambrian Research* 64, 239–252.
- Perdahl, J.-A. & Martinsson, O., 1995: Paleoproterozoic flood basalt magmatism in the Kiruna area, northern Sweden. In J.-A. Perdahl: *Svecofennian volcanism in northern Sweden, Doctoral thesis 1995:169D, Paper V*, 1–10. Luleå University of Technology.
- Pitcairn, I. (ed.), 2013: The gold line and gold deposits in the Skellefte district. *Excursion guidebook SWE2, 12th Biennial SGA Meeting, Uppsala*, Sveriges geologiska undersökning, 46 pp.
- Pitkänen, T., 1997: *Anisotropy of magnetic susceptibility of mylonites from the Kolkonjoki and Nautanen deformation zones in Norrbotten, Sweden*. M.Sc. thesis, Luleå University of Technology, Luleå, Sweden, 64 pp.
- Pousette, J., 1988: Groundwater documentation in Sweden. *Water Quality Bulletin* 13 (4), 138–147.
- Reddy, S.M. & Evans, D.A.D., 2009: Palaeoproterozoic supercontinents and global evolution: correlations from core to atmosphere. In S.M. Reddy, R. Mazumdr, D.A.D. Evans, A.S. Collins (eds): *Paleoproterozoic supercontinents and global evolution. Geological Society, London, Special Publication* 323, 1–26.
- Rhén, I., Forsmark, T., Jackson, P., Roberts, D., Swan, D. & Gylling, B., 2008: Hydrogeological conceptualization and parameterization. Site descriptive modeling SDM-Site Laxemar. *SKB Report R-08-78*, 306 pp.
- Rodriguez-Tablante, J., Tryggvason, A., Malehmir, A., Juhlin, C. & Palm, H., 2007: Cross-profile acquisition and cross-dip analysis for extracting 3D information from 2D surveys, a case study from the western Skellefte District, northern Sweden. *Journal of Applied Geophysics* 63, 1–12.
- Romer, R.L., Martinsson, O. & Perdahl, J.-A., 1994: Geochronology of the Kiruna iron ores and hydrothermal alterations. *Economic Geology* 89, 1249–1261.
- Ros, F., 1980: Nautanenområdet. Rapport över SGU:s arbeten utförda under 1966–1979. *Sveriges geologiska undersökning Brp 81530*, 33 pp.

- Rosberg J.-E., 2006: Flow test of a perforated deep dual cased well. Proceedings, Thirty-first Workshop on Geothermal Reservoir Engineering, Stanford University, Stanford, CA, 30 January – 1 February 2006. *SGB-TR-179*, 8 pp.
- Rosberg, J.-E., 2010: *Well testing, methods and applicability*. Doctoral Thesis, Department of Engineering Geology, Lund University, 78 pp.
- Rutland, R.W.R., Kero, L., Nilsson, G. & Stølen, L.K., 2001a: Nature of a major tectonic discontinuity in the Svecofennian province of northern Sweden. *Precambrian Research* 112, 211–237.
- Rutland, R.W.R., Skiöld, T. & Page R.W., 2001b: Age of deformation episodes in the Palaeoproterozoic domain of northern Sweden, and evidence for a pre-1.9 Ga crustal layer. *Precambrian Research* 112, 239–259.
- Saarno, T., 2019. St1 Deep Heat Oy, First deep geothermal project in Scandinavia, Achievements today. IEA – Geothermal Baltic Sea Symposium, GeoTHERM, Offenburg, 13 February 2019.
- Sammelín, M., 2011. *The Nature of Gold in the Aitik Cu-Au Deposit. Implications for Mineral Processing and Mine Planning*. Licentiate thesis, Luleå University of Technology, Luleå, Sweden, 67 pp.
- Sarlus, Z., 2013: *Geology of the Salmijärvi Cu-Au deposit*. M.Sc. thesis, Luleå University of Technology, Luleå, Sweden, 75 pp.
- Sarlus, Z., 2016: *Geochemical and geochronological constraints on 1.88 and 1.80 Ga magmatic events in the Gällivare area, northern Sweden*. Licentiate thesis, Luleå University of Technology, Luleå, Sweden, 106 pp.
- Sarlus, Z., Andersson, U.B., Bauer T.E., Wanhainen, C., Martinsson, O., Nordin, R., Andersson, J.B.H., 2017: Timing of plutonism in the Gällivare area: implications for Proterozoic crustal development in the northern Norrbotten ore district, Sweden. *Geological Magazine* 154, 1–26. 148
- Schellschmidt, R. & Hurter, S., 2002: *Atlas of Geothermal Resources in Europe*, Office for Official Publications of the European Communities, Luxembourg.
- Schmelzbach, C., H. Horstmeyer, & Juhlin, C., 2007: Shallow 3D seismic reflection imaging of fracture zones in crystalline rock. *Geophysics* 72, B149–B160.
- Schwarz, G., Göransson, M., Thunholm, B. & Förster, A., 2010: Mapping thermal conductivity of the Swedish bedrock. 29th Nordic Geological Winter Meeting, Oslo. *NGF abstracts and proceedings* 1, p. 177.
- Schwarz, G. and 18 others, 2016. CHPM2030 Deliverable D 1.2, report on data availability. Publ. by the CHPM2030 project, 18 p. with 5 app.
- Skiöld, T., 1979: Zircon ages from an Archean gneiss province in northern Sweden. *Geologiska Föreningens i Stockholm Förhandlingar* 101, 169–171.
- Skiöld, T., 1986: On the age of the Kiruna Greenstones, northern Sweden. *Precambrian Research* 32, 3544.
- Skiöld, T., 1988: Implications of new U-Pb zircon chronology to early Proterozoic crustal accretion in northern Sweden. *Precambrian Research* 38, 147–164.
- Skiöld, T. & Cliff, R.A., 1984: Sm–Nd and U–Pb dating of Early Proterozoic mafic–felsic volcanism in northernmost Sweden. *Precambrian Research* 26, 1–13.
- Skiöld, T. & Öhlander, B., 1989: Chronology and geochemistry of late Svecofennian processes in northern Sweden. *Geologiska Föreningens i Stockholm Förhandlingar* 111, 347–354.
- Skiöld, T. & Page, R., 1998: SHRIMP and isotope dilution zircon ages on Archaean basement–cover rocks in northern Sweden. 23. *Nordiske geologiske vintermøde, Aarhus 13–16 January 1998*, Abstracts, 273.
- Skiöld, T. & Rutland, R.W.R., 2006: Successive ~1.94 Ga plutonism and ~1.92 Ga deformation and metamorphism south of the Skellefte district, northern Sweden: Substantiation of the marginal basin accretion hypothesis of Svecofennian evolution. *Precambrian Research* 148, 181–204.
- Skyttä, P., Hermansson, T. & Bauer, T., 2009: Three-Dimensional Structure of the VMS-hosting Palaeoproterozoic Kristineberg Area, Northern Sweden. Smart science for exploration and mining: *Proceedings of the 10th biennial SGA meeting*, Townsville, Australia, 909–911.
- Skyttä, P., Hermansson, T., Elming, S-A. & Bauer, T., 2010: Magnetic fabrics as constraints on the kinematic history of a pre-tectonic granitoid intrusion, Kristineberg, northern Sweden. *Journal of Structural Geology* 32, 1125–1136.
- Skyttä, P., Hermansson, T., Andersson, J. & Weihed, P., 2011: New zircon data supporting models of short-lived igneous activity at 1.89 Ga in the western Skellefte District, central Fennoscandian Shield. *Solid Earth* 2, 205–217.

- Skyttä, P., Bauer, T., Tavakoli, S., Hermansson, T., Andersson, J. & Weihed, P., 2012a: Evolution of early-orogenic deformation zones and their significance for the development of contrasting structural domains within the Palaeoproterozoic Skellefte District, Sweden. *Geophysical Research Abstracts* 14, EGU2012–14180, EGU General Assembly 2012.
- Skyttä, P., Bauer, T.E., Tavakoli, S., Hermansson, T., Andersson, J. & Weihed, P., 2012b: Pre-1.87 Ga development of crustal domains overprinted by 1.87 Ga transpression in the Palaeoproterozoic Skellefte district, Sweden. *Precambrian Research* 206–207, 109–136.
- Skyttä, P., Bauer, T., Hermansson, T., Dehghannejad, M., Juhlin, C., Garcia Juanatey, M., Hübner, J. & Weihed, P., 2013: Crustal 3-D deometry of the Kristineberg area (Sweden) with implications on VMS deposits. *Solid Earth* 4, 387–404.
- Smith, M., Coppard J., Herrington R. & Stein H., 2007: The geology of the Rakkurijärvi Cu–(Au) prospect, Norrbotten: A new iron-oxide–copper–gold deposit in northern Sweden. *Economic Geology* 102, 393–414.
- Smith, M.P., Storey, C.D., Jefferies, T.E. & Ryan, C., 2009: In situ U–Pb and trace element analysis of accessory minerals in the Kiruna district, Norrbotten, Sweden: New constraints on the timing and origin of mineralisation. *Journal of Petrology* 50, 2063–2094.
- Smith, M.P., Gleeson S. A. & Yardley B. W. D., 2013: Hydrothermal fluid evolution and metal transport in the Kiruna District, Sweden: Contrasting metal behaviour in aqueous and aqueous–carbonic brines. *Geochimica et Cosmochimica Acta* 102, 89–112.
- Spitz, G. & Darling, R., 1978: Major and minor element lithogeochemical anomalies surrounding the Louvem copper deposit, Val d'Or, Quebec. *Canadian Journal of Earth Sciences* 15, 1161–1169.
- St1, project website: <https://www.st1.eu/geothermal-heat>
- Stacey, J.S. & Kramers, J.D., 1975: Approximation of terrestrial lead isotope evolution by a two-stage model. *Earth and Planetary Science Letters* 26, 207–221.
- Steiger, R.H. & Jäger, E., 1977: Convention on the use of decay constants in geo- and cosmochemistry. *Earth and Planetary Science Letters* 36, 359–362.
- Stephens, M.B., Wahlgren, C.-H. & Weihed, P., 1997: Sweden. In E.M. Moores & R.W. Fairbridge (eds.) *Encyclopedia of European and Asian Regional Geology*, Chapman & Hall, 690–704.
- Stephens, M.B., Ripa, M., Lundström, I., Persson, L., Bergman, T., Ahl, M., Wahlgren, C.-H., Persson, P.-O. & Wickström, L., 2009: Synthesis of the bedrock geology in the Bergslagen region, Fennoscandian Shield, south-central Sweden. *Sveriges geologiska undersökning Ba* 58, 259 pp.
- Storey, C.D., Smith M.P. & Jefferies T.E., 2007: In situ LA-ICP-MS U–Pb dating of metavolcanics of Norrbotten, Sweden: Records of extended geological histories in complex titanite grains. *Chemical Geology* 240, 163–181.
- Sundius, N., 1912: Pebbles of magnetite-syenite-porphyry in the Kurravaara conglomerate. *Geologiska Föreningens i Stockholm Förhandlingar* 34, 703–726.
- Sundius, N., 1915: *Beiträge zur Geologie des südlichen Teils des Kirunagebiets*. Vetenskapliga och praktiska undersökningar i Lappland, arrangerade av Luossavaara–Kiirunavaara Aktiebolag, Uppsala, 237 pp.
- Svenonius, F., 1900. Öfversikt af Stora Sjöfallets och angränsande fjälltraktens geologi. *Geologiska Föreningens i Stockholm Förhandlingar* 22, 273–322.
- Tavakoli, S., Bauer, T. E., Rasmussen, T. M., Weihed, P. & Elming, S.-Å., 2016: Deep massive sulphide exploration using 2D and 3D geoelectrical and induced polarization data in Skellefte mining district, northern Sweden. *Geophysical Prospecting* 64, 1602–1619.
- Taylor, S.R., 1964: Abundance of chemical elements in the continental crust: a new table. *Geochimica et Cosmochimica Acta* 28, 1273–1285.
- Tegengren, F.R. et al. 1924: Sveriges ädlare malmer och bergverk. *Sveriges geologiska undersökning Ca* 17, 408 pp.
- Thomas, M.D., Ford, K.L. & Keating, P., 2016: Review paper: Exploration geophysics for intrusion-hosted rare metals. *Geophysical Prospecting* 64, 1275–1304
- Tollefsen, E., 2014: *Thermal and chemical variations in metamorphic rocks in Nautanen, Gällivare, Sweden*. M.Sc. thesis, Stockholm University, Stockholm, Sweden, 50 pp.

- Tryggvason, A., Malehmir, A., Rodriguez-Tablante, J., Juhlin, C. & Weihed, P., 2006: Reflection seismic investigations in the western part of the paleoproterozoic VHMS-bearing Skellefte district, northern Sweden. *Economic geology and the bulletin of the Society of Economic Geologists* 101, 1039–1054.
- Tucker, M.E., 1991: *Sedimentary petrology: An introduction to the origin of sedimentary rocks*. Blackwell Science, Oxford, 260 pp.
- Vivallo, W. & Willdén, M., 1988. Geology and geochemistry of an early Proterozoic volcanic arc sequence at Kristineberg, Skellefte district, Sweden. *Geologiska Föreningens i Stockholm Förhandlingar* 110, 1–12.
- Waara, S., 2016: *Garnet occurrence and its relationship to mineralization at the Nautanen deposit, northern Sweden*. M.Sc. thesis, Luleå University of Technology, Luleå, Sweden.
- Wanhainen, C., 2005: *On the origin and evolution of the Palaeoproterozoic Aitik Cu-Au-Ag deposit, northern Sweden*. PhD thesis, Luleå University of Technology 2005:36, 38 pp.
- Wanhainen, C., Billström, K., Stein, H., Martinsson, O. & Nordin, R., 2005: 160 Ma of magmatic/hydrothermal and metamorphic activity in the Gällivare area: Re-Os dating of molybdenite and U-Pb dating of titanite from the Aitik Cu-Au-Ag deposit, northern Sweden. *Mineralium Deposita* 40, 435–447.
- Wanhainen, C., Billström, K. & Martinsson, O., 2006: Age, petrology and geochemistry of the porphyritic Aitik intrusion, and its relation to the disseminated Aitik Cu-Au-Ag deposit, northern Sweden. *GFF* 128, 273–286.
- Wanhainen, C., Broman, C., Martinsson, O. & Magnor, B., 2012: Modification of a Palaeoproterozoic porphyry-like system: Integration of structural, geochemical, petrographic, and fluid inclusion data from the Aitik Cu-Au-Ag deposit, northern Sweden. *Ore Geology Reviews* 48, 306–331.
- Weihed, P., 2001a: A review of Palaeoproterozoic intrusive hosted Cu-Au-Fe-oxide deposits in northern Sweden. In P. Weihed (ed.): *Economic geology research, volume 1, 1999–2000. Sveriges geologiska undersökning C 833*, 4–32.
- Weihed, P., 2001b: *Economic geology research, volume 1, 1999–2000. Sveriges geologiska undersökning C 833*, 136 pp.
- Weihed, P., 2010: Palaeoproterozoic mineralised volcanic arc systems: the Skellefte district (PaMVAS). In Lorenz et al. 2010: *The Swedish Deep Drilling Program. Science and Technology Plan*. Dept. of Earth Sciences, Uppsala University, 47–50 (unpublished).
- Weihed, P.; (ed.), 2015: *3D, 4D and predictive modelling of major mineral belts in Europe*. Springer Int. publishing. 331 pp.
- Weihed, P., Isaksson, I. & Svensson, S.-Å., 1987: The Tallberg porphyry copper deposit in northern Sweden: a preliminary report. *Geologiska Föreningens i Stockholm Förhandlingar* 109, 47–53.
- Weihed, P., Bergman, J. & Bergström, U., 1992: Metallogeny and tectonic evolution of the early Proterozoic Skellefte District, northern Sweden. *Precambrian Research* 58, 143–167.
- Weihed, P., Arndt, N., Billström, K., Duchesne, J.-C., Eilu, P., Martinsson, O., Papunen, H. & Lahtinen, R., 2005: Precambrian geodynamics and ore formation: The Fennoscandian Shield. *Ore Geology Reviews* 27, 273–322.
- Westhues, A., Hanchar, J.M., Whitehouse, M.J. & Martinsson, O., 2016: New constraints on the timing of host-rock emplacement, hydrothermal alteration, and iron oxide-apatite mineralization in the Kiruna district, Norrbotten, Sweden. *Economic Geology*, 111, 1595–1618.
- White, J.D.L. & Houghton, B.F., 2006: Primary volcanoclastic rocks. *Geology* 34, 677–680.
- Whitehouse, M.J. & Kamber, B.S., 2005: Assigning dates to thin gneissic veins in high-grade metamorphic terranes: a cautionary tale from Akilia, southwest Greenland. *Journal of Petrology* 46, 291–318.
- Whitehouse, M.J., Claesson, S., Sunde, T. & Vestin, J., 1997: Ion-microprobe U–Pb zircon geochronology and correlation of Archaean gneisses from the Lewisian Complex of Gruinard Bay, north-west Scotland. *Geochimica et Cosmochimica Acta* 61, 4429–4438.
- Whitehouse, M.J., Kamber, B.S. & Moorbath, S., 1999: Age significance of U–Th–Pb zircon data from Early Archaean rocks of west Greenland: a reassessment based on combined ion-microprobe and imaging studies. *Chemical Geology* 160, 201–224.
- Wiedenbeck, M., Alle, P., Corfu, F., Griffin, W.L., Meier, M., Oberli, F., Quadt, A.V., Roddick, J.C. & Spiegel, W., 1995: Three natural zircon standards for U–Th–Pb, Lu–Hf, trace element and REE analysis. *Geostandards Newsletter* 19, 1–23.
- Wiedenbeck, M., Hanchar, J.M., Peck, W.H., Sylvester, P., Valley, J., Whitehouse, M., Kronz, A., Morishita, Y., Nasdala, L., Fiebig, J., Franchi, I., Girard, J.P., Greenwood, R.C., Hinton, R., Kita, N., Mason, P.R.D., Norman, M., Ogasawara, M.,

Piccoli, P.M., Rhede, D., Satoh, H., Schulz-Dobrick, B., Skår, O., Spicuzza, M.J., Terada, K., Tindle, A., Togashi, S., Vennemann, T., Xie, Q. & Zheng, Y.F., 2004: Further characterisation of the 91500 zircon crystal. *Geostandards and Geoanalytical Research* 28, 9–39.

Willdén, M., 1986: Geology of the western part of the Skellefte field and the Kristineberg and Horntrask sulphide deposits: In D. Rickard (ed.): The Skellefte field. *Sveriges geologiska undersökning Ca* 62, 46–52.

Williams, P.J., 2010: "Magnetite-group" IOCGs with special reference to Cloncurry (NW Queensland) and northern Sweden: settings, alteration, deposit characteristics, fluid sources, and their relationship to apatite-rich iron ores. In L. Corriveau & H. Mumin (eds.): *Exploring for iron oxide copper-gold deposits: Canada and global analogues*. Geological Association of Canada Short Course 20, 23–38.

Winchester, J.A. & Floyd, P.A., 1977: Geochemical discrimination of different magma series and their differentiation products using immobile elements. *Chemical Geology* 20, 325–343.

Witschard, F., 1970: Description of the geological maps Lainio NV, NO, SV, SO. *Sveriges geologiska undersökning Af* 9–12, 116 pp.

Witschard, F., 1975: Description of the geological maps Fjällåsen NV, NO, SV, SO. *Sveriges geologiska undersökning Af* 17–20, 125 pp.

Witschard, F., 1984: The geological and tectonic evolution of the Precambrian of northern Sweden a case for basement reactivation? *Precambrian Research* 23, 273–315.

Witschard, F., 1996: Berggrundskartan 28K Gällivare NO, NV, SO, SV. 1:50 000-scale maps. *Sveriges geologiska undersökning Ai* 98–101. (With a description in English).

Witschard, F., & Zachrisson, E., 1995: Berggrundskartan 28I Stora Sjöfallet SO, 1:50 000, *Sveriges geologiska undersökning Ai* 91.

Zweifel, H., 1976: Aitik, geological documentation of a disseminated copper deposit – A preliminary Investigation: *Sveriges geologiska undersökning C* 720, 80 pp.

APPENDIX

Abbreviations

EGS	Enhanced geothermal system
EVD	Eastern volcanosedimentary domain
GDS	Geomagnetic deep soundings
IOCG	Iron oxide-copper-gold mineral deposit
LA-ICP-MS	Laser Ablation Inductively Coupled Mass Spectrometry
MT	Magnetotellurics
NDZ	Nautanen deformation zone
VLF	Very low frequency
VMS	Volcanogenic massive sulphides
WVD	Western volcanosedimentary domain

List of databases

Table A.1. Summary of databases held by SGU and relevant for the CHPM2030 project, i.e., the two study areas in northern Sweden around the Kristineberg and the abandoned Nautanen mine.

Table A.2. Summary of data in web map services (WMS) – as from the Map Viewer (Swedish: kartvisaren), held by SGU and relevant for the two Swedish study areas of the CHPM2030 project, presented in this report. In accordance with INSPIRE access is free of charge.

Table A1: Databases at SGU	Kristineberg comments (scale, coverage, number)	Nautanen comments (scale, coverage, number)
Map area - this report	1172 km ²	202 km ²
Bedrock, ores and minerals		
Bedrock observations	Data from the outcrop database, 1779 observation points	Data from the outcrop database, 288 observation points
Bedrock samples	Numerous but not registered	128
Outcrop map	Included in Bedrock map 1:50 000 – 1:250 000	Included in Bedrock map 1:50 000 – 1:250 000
Bedrock map	1:1 000 000, entire area 1:50 000 – 1:250 000, entire area	1:1 000 000, entire area 1:50 000 – 1:250 000, entire area
Dating, isotope analysis	6 analyses	4 analyses
Drill cores	1103 cores, partly scanned	236 cores, partly scanned
Ores and minerals	Entire area	Entire area
Mineral resources	Data from 41 objects (mine to prospect)	Data from 71 objects (mine to prospect)
Mineral permits	254 km ²	119 km ²
Mineral deposits of national interest	51 km ²	21 km ²
Geophysics		
Ground geophysics, different methods, prospecting areas	Almost entire area	Almost entire area
Airborne geophysics, total magnetic field	Line spacing mostly 200 m, data points every 18 m, entire area	Line spacing mostly 200 m, data points every 18 m, entire area
Airborne geophysics, gamma radiation (K - Th - U)	One dataset each for potassium, thorium, uranium, entire area	One dataset each for potassium, thorium, uranium, entire area
Ground geophysics, gamma radiation (K - Th - U)	63 measuring sites	56 measuring sites
Ground geophysics, gravity	Bouguer anomaly field, 2512 regional and 12021 local measuring points	Bouguer anomaly field, 328 regional measuring points
Petrophysical observations	90	103
Petrophysical laboratory measurements	96	191
Magnetic susceptibility measured in laboratory	0	351
Magnetic susceptibility measured on outcrop	2020	696
VLF-profiles	0	570 measuring points
MP-profiles	0	75054 measuring points
Geochemistry		
Ground geochemistry, copper	x measuring points	x measuring points
Litho-geochemistry	Measuring points with analysed data, 511 analyses	Measuring points with analysed data, 152 analyses
Ground geochemistry, physical samples	632	157
Groundwater, well and groundwater monitoring		
Wells	137	13
Groundwater	1:1 000 000, entire area	1:1 000 000, entire area
Springs	2	2
Quaternary deposits		
Soil map	1:1 000 000, entire area 1:50 000 – 1:250 000, entire area	1:1 000 000, entire area 1:50 000 – 1:250 000, entire area
Soil map	Midnorden, 1: 750 000, entire area	Northernmost Sweden, 1:250 000, entire area
Soil thickness	Map and measuring points, entire area	Map and measuring points, entire area
Glacial striation	114 measuring points	23 measuring points
Ground stability properties	> 1:100 000, entire area	> 1:100 000, entire area
Ground permeability	> 1:100 000, entire area	> 1:100 000, entire area
Landslides and gullies	Some observation points	No observations

Table A2: Datasets in Mapviewer	Language	Kristineberg comments (scale, coverage, number)	Nautanen comments (scale, coverage, number)
Access of data	https://apps.sgu.se/kartvisare/index-en.html Remark: Data covered by INSPIRE or for scientific research are free of charge		
Map area this report		1172 km ²	202 km ²
Bedrock, ores and minerals			
Bedrock map	Swedish, English	1:1 000 000, entire area	1:1 000 000, entire area
Bedrock map	Swedish	1:50 000 – 1:250 000, entire area	1:50 000 – 1:250 000, entire area
Dating, isotope analysis	Swedish	6	4
Drill cores	Swedish, English	1103	236
Drill cores, hyperspectral scanning, IR data	Swedish, English	Yes	Yes
Ores and minerals	Swedish, English	Entire area	Entire area
Mineral resources, included in Mapviewer for ores and minerals	Swedish, English	41	71
Mineral permits	Swedish, English	254 km ²	119 km ²
Mineral deposits of national interest	Swedish, English	51 km ²	21 km ²
Geophysics			
Ground geophysics, different methods, prospecting areas	Swedish	Almost entire area	Almost entire area
Airborne geophysics, Total magnetic field	Swedish	Line spacing mostly 200 m, data points every 18 m, entire area	Line spacing mostly 200 m, data points every 18 m, entire area
Airborne geophysics, gamma radiation (uranium, potassium, thorium)	Swedish	One dataset each for uranium, potassium and thorium, entire area	One dataset each for uranium, potassium and thorium, entire area
Ground geophysics, gravity	Swedish	Bouguer anomaly field, 2512 regional and 12021 local measuring points	Bouguer anomaly field, 328 regional measuring points
Geochemistry			
Ground geochemistry, copper	Swedish, English	Measuring points with copper content	Measuring points with copper content
Lithochemochemistry	Swedish, under construction	Measuring points with analyse data	Measuring points with analyse data
Groundwater, well and groundwater monitoring			
Wells	Swedish, English	137	13
Groundwater	Swedish, English	1:1 000 000, entire area	1:1 000 000, entire area
Springs	Swedish, English	2	2
Quaternary deposits			
Soil map	Swedish	1:1 000 000, entire area	1:1 000 000, entire area
Soil map	Swedish	1:50 000 – 1:250 000, entire area	1:50 000 – 1:250 000, entire area
Soil map	Swedish	Midnorden, 1: 750 000, entire area	Northernmost Sweden, 1:250 000, entire area
Soil thickness	Swedish	Map and measuring points, entire area	Map and measuring points, entire area
Ground stability properties	Swedish	> 1:100 000, entire area	> 1:100 000, entire area
Ground permeability	Swedish	> 1:100 000, entire area	> 1:100 000, entire area
Landslides and gullies	Swedish, English	Some observation points	No observations

